Environmental Impact of Metal Nanoparticles on Growth and Development of Plants

PhD Thesis

By

Ayesha Sattar

Sulaiman Bin Abdullah Aba Al-Khail - Center for Interdisciplinary Research in Basic Sciences

(SA-CIRBS)

Faculty of Basic and Applied Sciences

International Islamic University, Islamabad.

2020

Environmental Impact of Metal Nanoparticles on Growth and Development of Plants

By

Ayesha Sattar

01-FBAS/PHDNS/F-14

Supervisor

Dr. Imran Khan

Sulaiman Bin Abdullah Aba Al-Khail - Center for Interdisciplinary Research in Basic Sciences (SA-CIRBS)

Faculty of Basic and Applied Sciences

International Islamic University, Islamabad.

2020

Environmental Impact of Metal Nanoparticles on Growth and Development of Plants

Researcher:

Ayesha Sattar

01-FBAS/PHDNS/F-14

Supervisor:

Dr. Imran Khan

Assistant Professor

Sulaiman Bin Abdullah Aba Al-Khail - Center for Interdisciplinary Research in Basic Sciences (SA-CIRBS),

Faculty of Basic and Applied Sciences,

International Islamic University, Islamabad

2020


بسم الله الرحمن الرحيم

Sulaiman Bin Abdullah Aba Al-Khail - Center for Interdisciplinary Research in Basic Sciences (SA-CIRBS),

International Islamic University Islamabad

Dated:_____

FINAL APPROVAL

It is certifying that we have read the thesis submitted by Ms. Ayesha Sattar and it is our judgement that this thesis is of sufficient standard to warrant its acceptance by the International Islamic University, Islamabad for the PhD degree in Environmental Sciences.

COMMITTEE

1. _____

External Examiner
Dr. Zia-ur-Rehman Mashwani
Assistant Professor
PMAS Arid Agriculture University
Rawalpindi

2. _____

Internal Examiner
Dr. Muhammad Arshad
Associate Professor
NUST, Islamabad

3. _____

Supervisor
Dr. Imran Khan
Assisstant Professor
SA-CIRBS, FBAS, IIUI

4. _____

Incharge SA-CIRBS
Dr. Ikram Ullah
Assisstant Professor
SA-CIRBS, FBAS, IIUI

5. _____

Co-Supervisor
Dr. Mehwish Taneez
Assisstant Professor
SA-CIRBS, FBAS, IIUI

Dean, FBAS
Prof. Dr. Muhammad Irfan Khan
International Islamic University, Islamabad, _____

A thesis is submitted to Sulaiman bin Abdullah Aba Al-Khail - Center for Interdisciplinary Research in Basic Sciences (SA-CIRBS), International Islamic University, Islamabad as a partial fulfillment of requirement for the award of the degree of PhD Environmental Sciences.

Dedicated to Dream of

My Father

Prayers of My

Affectionate Mother

&

Support of My Beloved

Husband

DECLARATION

I hereby declare that the work present in the following thesis is my own effort, except where otherwise acknowledged and that the thesis is my own composition. No part of the thesis has been previously presented for any other degree.

Date _____ _____

Ayesha Sattar

01-FBAS/PHDNS/F-14

FORWARDING SHEET BY RESEARCH SUPERVISOR

The thesis entitled "Environmental Impact of Metal Nanoparticles on Growth and Development of Plants**"** submitted by **Ayesha Sattar, registration no. 01/FBAS/PHDNS/F-14** in partial fulfillment of PhD degree in Environmental Sciences at Sulaiman Bin Abdullah Aba Al-Khail - Center for Interdisciplinary Research in Basic Sciences (SA-CIRBS), has been completed under my guidance and supervision. I am satisfied with the quality of student's research work and allow her to submit this thesis for further process to graduate with Doctor of Philosophy degree from Sulaiman Bin Abdullah Aba Al-Khail - Center for Interdisciplinary Research in Basic Sciences (SA-CIRBS), as per IIUI rules and regulations.

Dr. Imran Khan Dated: October 13, 2020

Assisstant Professor

SA-CIRBS,

International Islamic University, Islamabad

TABLE OF CONTENTS

Acknowledgement

All the virtues and praises are for ALLAH Almighty, the most Gracious, the most Merciful, who created us as a Muslim in the Sacred Ummah of the Holy Prophet Mohammad (PBUH). Lots of Salaam and gratitude to the Holy Prophet Mohammad (PBUH) whose teachings are the guiding star in the time of dark and despair.

Firstly, I would like to express my sincere gratitude to my advisor ***Dr. Imran Khan*** and co-supervisors ***Dr. Akhtar Nadhman and Dr. Mehwish Taneez*** for continuous support in my PhD study, for their patience, motivation and mentorship. Their guidance helped me in all the time of research and writing of this thesis. I could not have imagined having better advisors and mentors for my PhD study. I am truly indebted to ***Dr.Ikram Ullah*** (Inchange, SA-CIRBS, IIUI) and ***Dr. Masoom Yasinzai*** (Rector IIUI) for their support .

I would like to thank all my class fellows (Madiha, Beenish, Safia and Memona) and lab mates (specially Nazia Asghar) for their stimulating discussions and all the fun that we had in all these years. Exceptional appreciations to Dr. Lubna and Dr. Saba for their motivation and help.

Special thanks to my sisters Dr. Rabia Yasir and Dr. Laiba Sattar – you two will always be minerate of love in my life. This thesis is a tribute to my Khala (late). Last but formost to my boys Ashraf Naveed ul Haq and Amin Naveed ul Haq who granted me with honor to be a Mom and inspired me to be a better person.

Ayesha Sattar

List of Abbreviations

Acronym	Abbreviation
ABA	abscisic acid
Ana	anaphase
APX	ascorbate peroxidase
CDC	center for disease control and prevention (CDC)
CGD	chronic granulomatous disorder
Conc.	concentration
CPT	co-precipitation
CVD	chemical vapor deposition
DA	disturbed anaphase
DC	disturbed chromosome
DNA	deoxyrobise nucleic acid
DW	dry Weight
EDX	energy dispersive (x-Ray) spectroscopy
FTIR	fourier transformed infrared spectroscopy
FW	fresh weight
IM	irregular metaphase
LC	lagging chromosome
M-nu	multiple nuclei
Mat	metaphase
MI	mitotic index
NBT	nitroblue tetrazolium chloride
NODC	no. of dividing cells
NPs	nanoparticles
POD	peroxidase
Pro	prophase
PVD	physical vapor deposition

RNA	ribosenucleic acid
ROS	reaction oxygen species
SEM	scanning electron microscopy
SOD	superoxide dismutase
TaHMA	*Tritium aestivum* heavy metal ATPase
Ta*WRKY*	*Tritium aestivum* gene family for abiotic stress
TTC	2, 3, 5-triphenylte trazolium chloride
UV/Vis	ultraviolet/visible
VLS	vapor solid liquid
XAS	x-ray absorption spectroscopy
XRD	x-ray diffraction

List of Figures

List of Tables

Abstract

Zinc oxide nanoparticles (ZnO-NPs) have gained unprecedented attention and witnessed incredible growth due to its vast array of applications in cosmetics, agriculture, waste water treatment, biomedical industry, semiconductors/electronics and many more. Thus, the release of ZnO-NPs into environment as nano-pollutant has become inevitable and ecosystem can suffer from oxidative damage. This study was designed to investigate the impact of ZnO-NPs on the growth dynamics, physio-biochemical response, cytotoxicity and genetic response of *Triticum aestivum.* Two techniques were used for ZnO-NPs synthesis i.e. chemical synthesis by co-precipitation method and green synthesis using aqueous extract of orange peel along with zinc nitrate as precursor salt. Optical absorbance properties of ZnO-NPs were determined by ultraviolet-visible (UV-Vis) spectroscopy and showed sharp absorbance peak at 373 nm and 377 nm for chemical and green synthesized ZnO-NPs, respectively. Presence of Zn-O bond was confirmed by the Fourier transformed infrared (FT-IR) spectroscopy which displayed peaks in finger print region of 450-590 for metal oxide. Surface chemistry of ZnO-NPs were studied by X-ray diffraction (XRD) spectroscopy. XRD patterns witnessed the hexagonal wurtzite crystalline structure and particle size of 15±5 nm and 20±5 nm as calculated by the Debye–Scherrer equation. Chemically synthesized ZnO-NPs possessed flower like structure and green synthesized ZnO-NPs have needle like structure as illustrated by scanning electron (SEM) microscopy. Elemental composition of ZnO-NPs was confirmed by energy dispersive spectroscopy (EDS) which presented pure phase of ZnO.

Physiochemical response of *T. aestivum* seedlings towards ZnO-NPs stress showed a decrease in germination index up to 43 % and 69 % along with significant decrease in seedlings growth and biomass. Membrane stability index was dropped and electrolyte leakage kept on increasing in a dose dependent manner. Photosynthetic pigments (chlorophyll and carotenoids) were adversely effected while estimation of plants stress markers (proline, lipid peroxidation and sugar content) showed steady increase in concentration along with increase in amount of ZnO-NPs stress. Amount of soluble proteins in *T. aestivum* seedlings remained unaffected by ZnO-NPs stress. Oxidative damage to antioxidant defence mechanism of *T. aestivum* seedlings by ZnO-NPs was estimated in terms of phenols, flavonoids, superoxide dismutase (SOD), catalase (CAT) and ascorbate peroxidase (APX). Antioxidant defence mechanism {non-enzymatic (phenols &

flavonoids), enzymatic (SOD, CAT, APX)} showed endurance to oxidative stress till 400 mg/L and then their concentrations were dropped exponentially for chemically synthesized ZnO-NPs. However, these parameters showed a steady increase for biologically synthesized ZnO-NPs. Mitotic index (MI) and chromosomal aberration helped to determine the cytological damage to *T.aestivum* root tips by ZnO-NPs. For chemically and green synthesized ZnO-NPs, MI was plunged from 59.35 % to 28.60 % and 60 % to 43 %, respectively. Percent aberrations were raised up to 81.83 % and 54.60 %. Chromosomal aberrations were recorded in form of disturbed anaphase, irregular metaphase, disturbed chromosomes, multiple nuclei, fragmentation, uncoiling, stickiness, legging chromosomes and ghost cells. Chemically synthesized ZnO-NPs imparted more aberration as compared to green synthesized ZnO-NPs. Genetic response of *T.aestivum* seedling was quantified by quantitative reverse transcriptase – polymerase chain reaction (qRT-PCR). Heavy metal *ATPase* gene i.e. *TaHMA2* and growth related genes i.e. *TaWRKY10* were chosen for this purpose. Results have shown that *TaHMA2* was upregulated for both chemically and biologically synthesized ZnO-NPs conferring high metal tolerance to *T.aestivum* seedlings. However, maximum expression level of *TaWRKY10* gene was observed till 400 mg/L and it was dropped down for chemically synthesized ZnO-NPs. Although, it was upregulated in case of biologically synthesized ZnO-NPs. Results have clearly shown that green synthesized ZnO-NPs were more biocompatible being non-toxic to seedlings at high concentrations as compared to the chemically synthesized ZnO-NPs. However, there is a dire need to regulate the release of nano pollutants into the environment due to their potential harmful impacts on the ecosystem.

CHAPTER 1

INTRODUCTION

1.1. Brief History of ZnO-NPs

Nanoparticles (NPs) are surprisingly neither exclusively man-made nor result of the modern research practices. These occur in nature as organic molecules (such as proteins, viruses, polysaccharides and others) and inorganic molecules (such as aluminosilicates, metals, iron oxy hydroxides etc). NPs have continuously being used as color pigments and in glass industry (Heiligtag & Niederberger, 2013). Next big leap in nano sciences remained the Michael Faraday's systematic study of light and matter interactions. Which is being marked as beginning of nanotechnology and colloidal chemistry. Richard Zsigmondy – a noble prize laureate in chemistry, devised the term nanometer and measured the size of gold colloids by microscope in this range. Richard Feynman in 1959 introduced the concept to manipulate atoms at atomic level. Norio Taniguchi – a Japanese scientist described the semiconductor processes at nanoscale. Gold era of nanotechnology started with the discovery of fullerenes. Whereas, from the beginning of the 21st century nanotechnology and nanoscience's has become center of the science (Marcovich & Shinn, 2014, Fonash & Van de Voorde, 2018).

From the last decade of previous century, NPs and nanomaterials have been manufactured in large quantities. Net global market of nanocomposites have reached to 1.6 billion US dollars and an annual growth rate of 26.7 % is estimated from 2016 to 2021 (Bhushan, 2017). Among these nanomaterials, ZnO-NPs hold its unique position due to extraordinary properties. Owning to its practical applications, these are most studied NPs, so far. Thus, ZnO-NPs are being synthesized on industrial scale and their exhaust to the environment is inevitable. ZnO-NPs keep entering into the environment throughout their life cycle from synthesis to discarded waste material (Sun *et al.*, 2014). These NPs are known for its extraordinary strength and stability. These are found in surface water in large amounts and their toxicity has been reported in aquatic algae, zebra fish and other marine animals (Zhu *et al.*, 2008, Aravantinou *et al.*, 2015, Suman *et al.*, 2015, Bhuvaneshwari *et al.*, 2016). Toxicity of ZnO-NPs has reviewed by the Vandebriel and Jong (Vandebriel & De Jong, 2012). However, presence and toxicity of ZnO-NPs in air and soil has not yet been investigated.

Plants are the producers in this universe and all other creatures are dependent on them for food and raw materials. Heavy metals/metal oxide levels beyond threshold levels results in numerous harmful effects such as leaf chlorosis, photosynthesis inhibition and altered homeostasis

of nutrition as evident by numerous previous studies (Munzuroglu & Geckil, 2002, Prakash & Chung, 2016). Several scientific studies have reported the phytotoxicity of the ZnO-NPs (Du *et al.*, 2011, Mukherjee *et al.*, 2016, Subbaiah *et al.*, 2016, Wang *et al.*, 2016, Tripathi *et al.*, 2017). Major mechanism of toxicity is oxidative stress while others include genotoxicity and cytotoxicity in plants that comprise of lipid peroxidation, falloffs in mitotic index (MI) and increased occurrences of chromosomal anomalies (Ghosh *et al.*, 2016, Ahmed *et al.*, 2017).

1.2. Industrial Applications of ZnO-NPs

Estimated global market of ZnO-NPs in 2015 was $ 2,099 million. Which is expected to grow upto $ 7,677 million till 2022. ZnO-NPs are available both in powder form and suspensions. It reveals unique physiochemical, anti-corrosive, anti-fungal, anti-bacterial properties. ZnO-NPs also work as catalyst and UV filters. These are employed in household products, cosmetics, surface coatings paints, textile industry, medical dressings and electronics (Jaiswal *et al.*, 2019). Some of these utilities are discussed below:

Ultraviolet radiations (both A & B) from sun can cause injury to skin cell through free radicals formation. ZnO-NPs smaller than 200 nm in size have proven their effectiveness to scatter light and imparts preferred whitening and texture to skin. It is also used in ointments and foot care products (Naveed Ul Haq *et al.*, 2017). Assumed risks to human health posed by these NPs is unexplored yet.

ZnO-NPs produces green luminescence due to its oxygen vacancies and makes it superfit for bio-imaging. This property can further be augmented by the dopping of transition elements such as cobalt, nickle and copper. Scientists are seeing ZnO-NPs as cure to cancer and exploring its anticencerial properties through cell apoptosis, autophagy and anticancer drug delivery. ZnO-NPs is a potential medicine for diabetes and its anti-inflamatory properties have gained a lot of attention (Jiang *et al.*, 2018, Jiang *et al.*, 2018, Wiesmann *et al.*, 2020)

ZnO-NPs have accomplished much consideration of the academics for the management of diseases like severe chronic granulomatous disorder (CGD), hemophilia, combined immune deficiency (ADA-SCID), on genital blindness, neurodegenerative diseases, viral infections, heart disease, diabete, lysosomal storage disease and muscular dystrophy (Gao *et al.*, 2006, Zhao *et al.*, 2013).

ZnO is a semiconductor and its characteristics can be upgraded in many ways that makes it an exhilarating contender for the sensor investigation. These sensors have played a crucial role from detecting epidemic ailments outbreaks to environmental pollutants (Dimapilis *et al.*, 2018). Engineers have developed ZnO-NPs sensors for detecting biochemistry of enzymes, sensing cholesterol and other chemicals such as ethanol and n-butanol with good response, high stability and short recovery time (Kazeminezhad *et al.*, 2013, Liu & Lal, 2015, Kim *et al.*, 2017).

ZnO-NPs have been extensively explored for fertilizers, soil improvments, water purifier, plant protectors and many other agricultural applications (Taheri *et al.*, 2015). Center for disease control and prevention (CDC) has reported more than three thousand deaths due to food born diseases in 2011. Thus, these diseases have become a major concern around the globe and packaging materials with microbial resistant properties have become highly desirable (Espitia *et al*., 2012). Sawai and co-workers discorved the antimicrobial properties of ZnO-NPs in 1995 and now there are packing materials in which ZnO-NPs layer is incorporated in polymeric materials (Espitia *et al.*, 2012). ZnO-NPs protects the food by three processes; i.e. by releasing antimicrobial ions ii. damaging the cell wall of microbes iii. by generation of ROS through light activation (Elmer & White, 2016). Scientists have testified the pest control properties of ZnO-NPs and demonstrated that it reduces the occurance of disease by 28 %. Due to its greater solubility, ZnO-NPs are readily available to plants as compared to traditional fertilizers. Therefore, it can also be an alternate to traditional plant nourishments chemicals (Milani *et al.*, 2012).

1.3. Physiochemical Characteristics of ZnO-NPs in Reference to Toxicity

ZnO-NPs due to smaller size can easily be taken or enter into bodies of organisms including plants, planktons, micro flora and fauna through ingestion, respiration or any route of environmental exposure. Therefore, positive or negative impact of ZnO-NPs on living system may result majorly due to extrinsic (smaller size) properties rather than intrinsic properties (exceptional nanoscale properties) (Auffan *et al.*, 2009). Despite colloidal chemistry, basic theories of Physics may not be applicable to describe the behaviour of such particles. Although, properties of ZnO-NPs such as reactivity and unusual surface arrangement may have enhanced by the phenomenon such as redox reactions, formation of ROS species or dissolution (Billinge & Levin, 2007). Thus,

ecotoxicological studies should deal or address the toxicity of NPs in environment at these two scales.

1.3.1. Extrinsic Properties

Size dependent thermodynamics, crystallinity, band gap and thermal properties are discussed here with reference to toxicity of ZnO-NPs.

NPs having size below 20-30 nm possess extra energy on its surface and are unstable thermodynamically. In order to stabilize them, crystallographic changes such as lattice deformation or contraction, rearrangement of surface atom, morphological changes or defect appearance is required (Auffan *et al.*, 2009). ZnO-NPs show a large variety of structure entirely dependent upon synthesis techniques and reaction conditions. It can form nanorods, nanowires, nano-belts and also complex morphologies. However, pure ZnO-NPs are hexagonal wutzrite. Thus, the lattice deformation, defect appearance, rearrangement of morphology or change in shapes may become not only more frequent but also unpredictable in most of cases. However, for most of commercially prepared NPs such detailed studies are not in practice (Zhang *et al.*, 2015).

Difference of energy between the electron of conduction band and valance band in known as “band gap”. This energy decreases abruptly as the diameter of nanomaterial decreases from 6 nm to 8 nm. This phenomenon is known as lattice contraction. It helps the electronic confinement and creates the discrete electronic spaces that are absent in bulk materials. ZnO-NPs possess a band gap of 3.34 ev while of micron ZnO is 3.19 ev. Which makes the nano ZnO a semiconductor and is responsible for its depart in properties from bulk material (Chernyshev, 2009). Exploration of this hypothesis considers the band gap of metal oxide NPs in relationship to the energy levels of biological environment. As a result, similarity in energy state of materials and cellular environment may lead to electron transfer. Consequently, redox reaction and ROS production may increase unpredictably (Zhang *et al.*, 2012).

Thermal characteristic of NPs is also size dependent. Effect on melting temperature of ZnO-NPs is very pronounced with the size below 20 nm. Same is the case for normalized heat of fusion. Which is otherwise considered to be constant according to classical thermodynamics. Electric and magnetic properties of the NPs are also size and crystal dependent (Dormann *et al.*, 2007).

1.3.2. Interfacial or Intrinsic Properties

Size dependent properties of ZnO-NPs affects the exposure as well as hazardness of these materials. Enhanced reactivity may have resulted from greater electron affinity and their transfer to the solution. These properties are also responsible for aggregation of nanomaterials, naturally befalling macromolecules and adsorption of pollutants (Murdock *et al.*, 2008). These phenomena are considered to be responsible for ROS production, transfer of chemical species and exhaust of toxic species in solutions – major sources of NPs toxicity (Auffan *et al.*, 2009).

ZnO-NPs possess active sites on their surfaces that are responsible for ROS generation due to difference in electronic and atomic structures (Gupta & Bahadur, 2018). This postulate strengthens the size dependent toxicity of NPs. Other factors that may stimulate the generation of ROS are oxidation state, surface coating, bounded materials, degree of agglomeration, aggregation and solubility (Latha & Kumari, 2016).

Chemical stabilities of the metal/metal oxide NPs are responsible for its toxicities in biological systems. Less soluble NPs are proved to be less hazardous and vice versa (Braydich-Stolle *et al.*, 2009). ZnO-NPs shows higher solubility thus, poses a higher toxicity in mammalian model than other metal NPs. In vitro studies have revealed that dissolution of ZnO-NPs releases Zn^{2+} and $Zn(OH)^{-}$ ions and imparts noxiousness to fresh as well as marine flora and fauna (Liu *et al.*, 2018). Dissolution is also a size dependent phenomenon and is observed to increase as the size decreases. Research have shown that there is a good relationship between intracellular free zinc and ZnO-NPs induced cytotoxicity (Shen *et al.*, 2013).

NPs tend to attract each other through physical interactive forces and chemical bondings. NPs attract each other to reduce their surface energies and form larger units. This phenomenon is known as aggregation (Cao, 2004). Studies have revealed that ZnO-NPs demonstrate an affinity to produce concentration dependent aggregates. However, smaller secondary aggregates were observed to produce more ROS and hence increased toxicity than larger primary aggregates (Tripathy *et al.*, 2014).

ZnO-NPs are semiconductors and get activated by the light. Their reactivity increases dramatically when get exposed to UV or visible light. When ZnO-NPs are excited by the light electrons are excited and move from valance band to conduction band and generates an electron

pair hole. That can either breakdown to no net chemical transformations or combines with surface bound molecules (like Oxygen) to form superoxide anion radicals. These hole are powerful antioxidants and can produce radicals. Intermediate steps of this process may generate singlet oxygen and other ROS (Wang *et al.*, 2013).

1.4. Uptake, Translocation and Internalization of ZnO-NPs in Plant Body

ZnO-NPs industry have grown intensively in the recent years and is expected to increase 58,000 tons by the year 2020 (Ma *et al.*, 2013). Plants get exposed to ZnO-NPs pollution from soil, water and air. Among these factors, soil and water remain the major contributors. ZnO-NPs may enter in the plant body through roots as well as aerial parts. Size of the NPs appears to be largest hurdle in ZnO-NPs uptake by the plants. 40-50 nm is the size limit for all NPs absorbance in plants (Taylor *et al.*, 2014). Plant species belong to different botanical families and differ in physiology and vary in their response towards NPs. Other factors that alter the ZnO-NPs characterization in soil are the humic acid and organic matter that plays a crucial role in coating, solubilisation, dissolution, aggregation and ultimately uptake by the plants (Pérez-de-Luque, 2017). Role of micro-organism in natural environment can never be ignored. Studies have shown that symbiotic micro-environment of the *Arbascular mycorrhiza* fungi offer resistance to heavy metal NPs uptake by the plant. Thus, plant uptake of NPs reduces significantly. Whereas, another soil bacterium *Pseudomonas chlororaphis* O6 augments the bioavailability and uptake of heavy metal NPs (nano CuO and nano ZnO) (Feng *et al.*, 2013, McNear Jr, 2015). However, as a rule of thumb NPs pass from cell wall as well as cell membrane through complex series of events. Plant cell membrane is composed of lipid bilayer with hydrophilic head and hydrophobic tails that serve as barrier which must be crossed to enter into the plant cell by three possible pathways:

i. Diffusion: attributed by the size, charge, composition and shape, ZnO-NPs may diffuse through the plasma membrane in certain conditions (Verma *et al.*, 2008).
ii. Endocytosis: cells take up ZnO-NPs through endocytosis either in the fluid or solid phase or it can be receptor mediated. ZnO-NPs may form a vesicle in fluid phase and enter by the mass action. ZnO-NPs can get attached to membrane lipids or proteins in solid phase. Which are internalized later on. However, endocytosis depends upon

mechanical parameters and potential difference across the membrane (Rejman *et al.*, 2004).

iii. Channels and membrane transporter proteins: ZnO-NPs are translocated within the plant cell through membrane transporters and channels. However, low probability and high selectivity are the limiting factors (Ho *et al.*, 2010).

ZnO-NPs can enter into the seed coat through parenchymatous intercellular spaces. These spaces help the movement of solutions into the cotyledon. Once inside the plant cell ZnO-NPs are transported symplastically or apoplastically. They can be transported from cell to cell by plasmodesmata (Rico *et al.*, 2011). ZnO-NPs passes through apoplast of the endodermis before reaching the stele of the plant. The whole phenomenon is integrated passively. Xylem acts as significant tool in transportation and translocation of NPs and serves as vehicle (Judy, 2013, Aslani *et al.*, 2014). Researchers have demonstrated that transport of ZnO-NPs takes place through xylem and phloem, back and forth in roots and shoots. This whole mechanism is supposed to be carried by active transport accompanied by cellular signalling, plasma membrane regulations and recycling (Tripathi *et al.*, 2017).

1.5. Toxicity of ZnO-NPs in Plant Model

ZnO-NPs can be hazardous to plants by following three possible mechanisms:

i. Release of toxic ions on solubilisation which may initiate Fenton like reactions to generate ROS (Kruszewski *et al.*, 2011).
ii. ROS by surface interactions (Yang *et al.*, 2009).
iii. Direct physical interaction with biological targets (Brayner, 2008).

1.5.1.1. Biochemical Basis of ZnO-NPs Phytotoxicity

Plants use oxygen during photosynthesis for production of energy. ROS i.e. hydroxyl radical ($^{\cdot}OH$), singlet oxygen ($^1O_2$), superoxide anion redical ($O_2^{\cdot-}$), hydrogen peroxide (H_2O_2) and water are produced by the reduction of ground state oxygen. To measure the oxidative stress researcher's employee different assays such as propidium iodide fluorescence assays, electrolyte leakage test and lipid peroxidation assays. ROS is generated via two mechanisms; (i) energy transfer mechanism of oxygen. (ii) cascade of electron transfers reactions. Toxic effect of ROS

varies with its type, mechanism of production and interaction with the plant cell. Different type of ROS reacts with specific type of compound hence varies in consequences (Rico *et al.*, 2015).

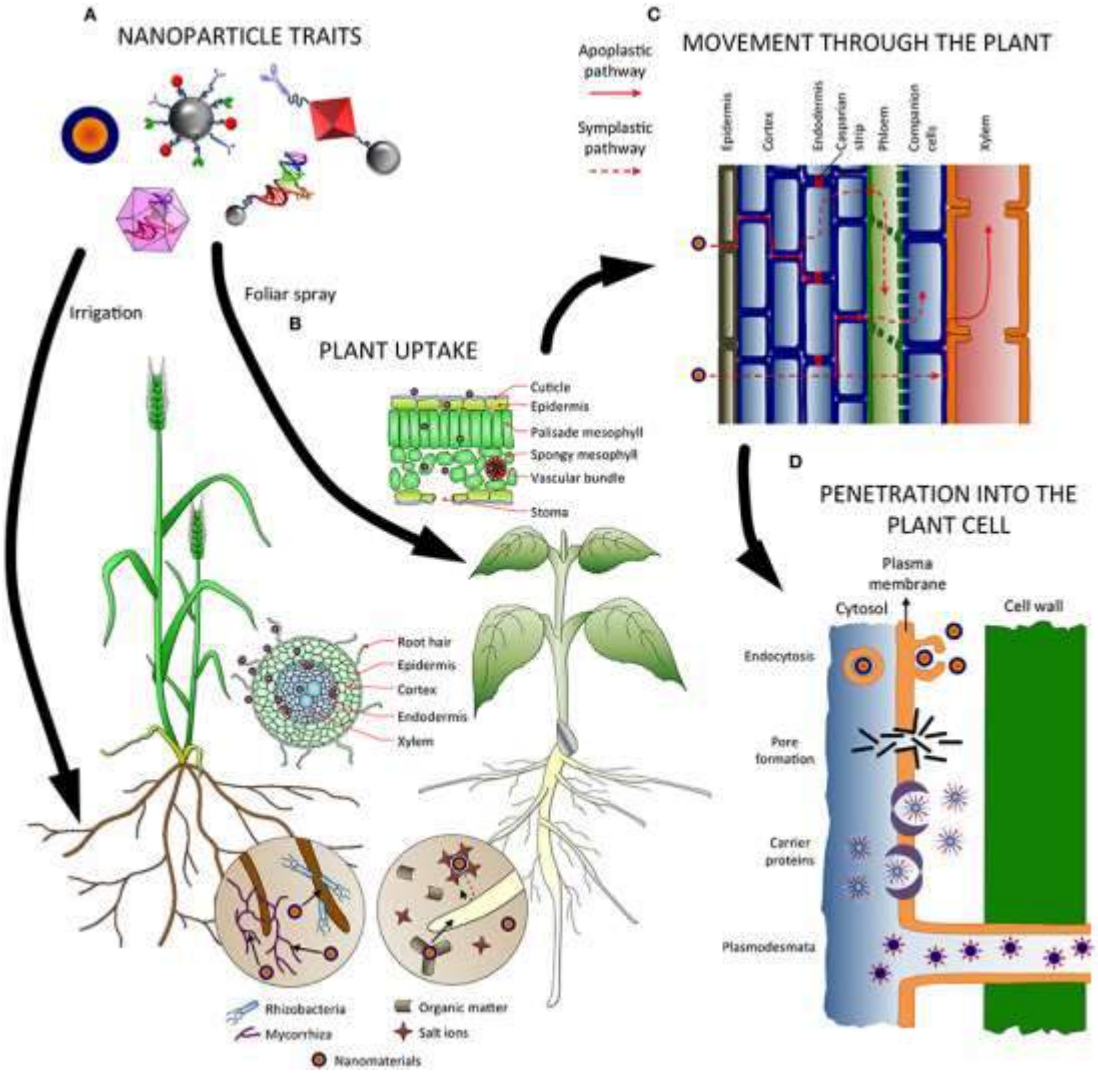

Figure 1:1:Translocation of ZnO-NPs within the plant body

Adopted from: (Pérez-de-Luque, 2017)

1.5.1.2.Singlet Oxygen ($^1O_2$)

Electrons in biradical oxygen have parallel spin. When it absorbs adequate amount of energy, singlet oxygen is formed by reversing spin of an unpaired electron. Now, this singlet activated oxygen can take part in divalent reduction by transporting two electrons (Apel & Hirt,

2004). In a photosystem triplet chlorophyll is produced in antenna system by scarce volume of energy. In a reaction center singlet oxygen is produced from recombination of charges induced by light. Triplet form of chlorophyll (Chl) reacts with $^3O_2$ to formulate very caustic singlet oxygen.

$$Chl \xrightarrow{light} {}^3Chl$$

$$^3Chl + {}^3O_2 \longrightarrow Chl + {}^1O_2$$

Most probably $^1O_2$ can persist for only 3 µs in cell, 4 µs in H_2O and 100 µs in non-polar environment and is only able to diffuse several hundred nanometres within biological systems. However, it reacts with all biological molecules present in its vicinity. It reacts with DNA, unsaturated fatty acids and proteins. Nucleic acid undergoes alterations by selective reaction of deoxyguanosine in presence of $^1O_2$. It is considered to be responsible for the destruction of photosystem II that may transformed to cell death (Hackbarth *et al.*, 2010). $^1O_2$ is appeased by alpha-tocopherols, beta carotene or in photosystem II with a D1 protein (Krieger-Liszkay *et al.*, 2008).

1.5.1.3.Superoxide Anion Redical ($O_2^{\cdot -}$)

$O_2^{\cdot -}$ is a primary ROS that initiates a series of reaction for production of secondary ROS. These reactions are either metal catalysed or enzyme catalysed subject to type of cell. Superoxide anion redical has modest reactivity with half-life of 1 µs. It has both reducing and oxidizing characteristics. Electrophilic activity of $O_2^{\cdot -}$ towards electron rich molecules is inhibited by anionic charge. $O_2^{\cdot -}$ reduces cytochrome C and oxidizes clusters of [4Fe-4S] (dehydratase or aconitase) (Halliwell & Gutteridge, 1984).

1.5.1.4.Hydrogen Peroxide (H_2O_2)

$O_2^{\cdot -}$ is easily dimutised either enzymatically by SOD or non-enzymatically by accepting two protons. It is formed in the cell in normal state, in addition to number of stress conditions.

$$2\ O_2^{\cdot -} + 2H^+ \longrightarrow H_2O_2 + O_2$$

$$2\ O_2^{\cdot -} + 2H^+ - S{-}O \longrightarrow D\ H_2O_2 + O_2$$ (Bienert *et al.*, 2007)

H_2O_2 is relatively long lived but moderately reactive chemical species (half-life – 1 ms). It easily crosses the biological barriers due to absence of unpaired electrons and covers larger distances within the cell. It is an important signalling molecule of stress conditions. At higher

concentrations it can react with amino acids such as methionine residues (–SCH3) or cysteine (SH). It can oxidize the thiol group of enzymes and make them inactive. Even at greater concentrations it can interrupt programmed cell death (Bienert *et al.*, 2007, Halliwell & Gutteridge, 2015).

1.5.1.5.Hydroxyl Redical (.OH)

H_2O_2 and $O_2^{\cdot -}$ are required for the formation of. OH. It follows a metal catalysed Haber-Weiss mechanism as follows:

$$Fe^{3+} + O_2.- \longrightarrow Fe^{2+} + O_2$$

$$Fe^{2+} + H_2O_2 \longrightarrow Fe^{3+} + {}^{\cdot}OH + OH^-$$

$$O_2^{\cdot -} + H_2O_2 \longrightarrow {}^{\cdot}OH + OH^- + O_2.$$

Due to an unpaired electron hydroxyl anion is the utmost reactive species amongst all ROS. That can react with all cellular organelles and cause them damage leading to cell death as cell have no defence mechanism against it. It is also produced by the Fenton reaction under light mode and causes chloroplast fragmentation.

1.6. Sites of Formation of ROS in Plant Cell

Major ROS producing organelles in plant cell are as follows.

1.6.1. Chloroplast

ROS are produced in chloroplast in both photosynthetic system (PS) I and II through electron transport chain (ETC). However, in stress conditions (like salt stress, drought, NP stress or any other biotic or abiotic stress) this production is enhanced. In normal conditions, PS reduces NADP to NAPH through supply of electron. Nicotinamide adenine diphosphate (NADPH) enters in Calvin cycle causing reduction to final electron receptor. In stressed state, NADP supply is reduced causing ETC to be overloaded. Thus, electrons are leaked from ferredoxin and give rise to Mahler's reaction to generate $O_2^{\cdot -}$. Which triggers the formation of secondary ROS (Elstner, 1991).

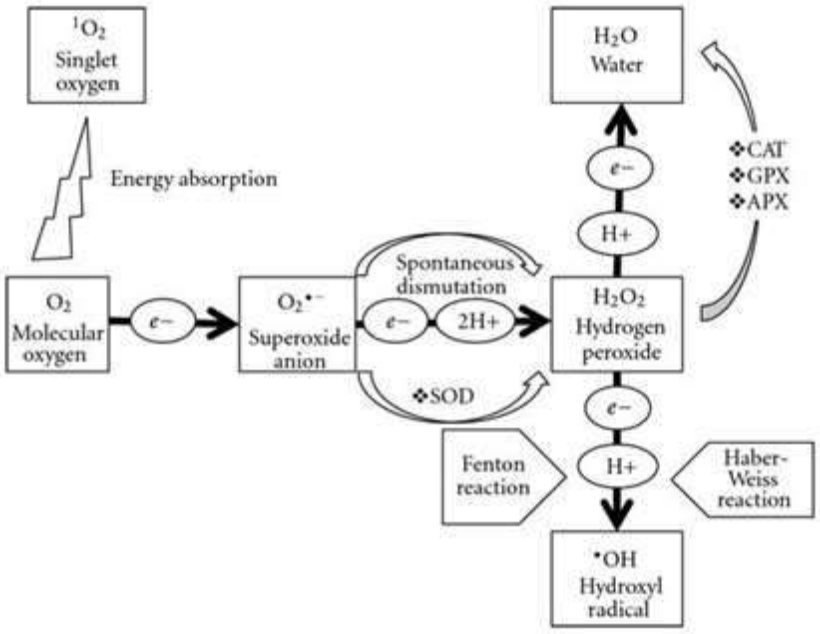

Figure 1:2:ROS production in plants

Adopted From (Sharma *et al.*, 2012)

1.6.2. Mitochondria

ROS production can occur at multiple sites of mitochondria.

i. Reverse flow of electrons occurs (from complex II to complex I in ETC) when there is limited supply of NAD^+ substrate that enhances production of ROS in flavoprotein portion of NADPH. In this state ROS is also produced in complex I controlled by hydrolysis of ATP.

ii. ETC complex III can also produce $O_2^{\cdot-}$. Ubisemiquinone is a highly unstable radical. Which is quite favourable for leakage of electrons for ROS synthesis.

iii. ATP synthesis and ETC are highly linked in mitochondria in normal aerobic conditions. However, under stress state components of both systems get modified and likely to produce ROS.

iv. Enzyme mediated ROS also takes place in mitochondria. Some enzymes like (aconitase) directly generates ROS while others such as GAL (1-galactono-γ lactone

dehydrogenase) are capable to forage electron to ETC for indirect production of ROS (Huang *et al.*, 2016).

1.6.3. Endoplasmic reticulum

Cyst $P_{450}R-$ is produced as an intermediate when Cyst P_{450} reacts with RH- an organic substrate, reacts with flavoproteins. This radical reacts with triplet oxygen due to presence of an unpaired electron. Oxygenated complex i.e. Cyst P450-ROO− may reduce to either cytochromes or decomposes by releasing $O_2^{\cdot -}$ (Mittler, 2002).

1.6.4. Peroxisome

Due to oxidative type of mechanism it is prime site for H_2O_2 production. Gylcolate oxidase, oxidizes the glycolate for production of H_2O_2 in photorespiration where, $O_2^{\cdot -}$ is also produced. Three essential peroxisomal membrane polypeptides (PMPs) with different molecular weights (18, 29, and 32 kDa) were establish to be involved in fabrication of $O_2^{\bullet -}$. Here, NADH serves as an electron donor for $O_2^{\bullet -}$ production in 18 & 32 kDa (PMP). While in 29 kDa NADPH serves as electron donor (Noctor *et al.*, 2002).

1.6.5. Plasma Membrane

Spin-trapping techniques have provided the evidence for production of ROS in plasma membrane. $O_2^{\cdot -}$ is produced from NAD(P)H facilitated by two enzymes NADPH oxidases and quinone reductases. These enzymes provide electron from NAD(P)H to O_2 to form $O_2^{\cdot -}$. Which is further dimutised by SOD to form H_2O_2 (Apel & Hirt, 2004).

1.6.6. Cell Wall

Peroxidases present in cell wall catalyses the H_2O_2 production from NADPH. The reactions are facilitated by conifer alcohol (a monophenol). Malate dehydrogenase is considered to provide NADPH for the reaction. Scientists have shown that ROS is produced in cell wall during K-deficiency stress and as hypersensitive response by some bacterial strains (Kim *et al.*, 2010).

Germin – an oxalate oxidase in cell wall generates CO_2 and H_2O_2 from cell wall. Enzymes like amine oxidase triggers the deamination phenomenon of polyamines and produces H_2O_2 during abiotic stress (Cona *et al.*, 2006).

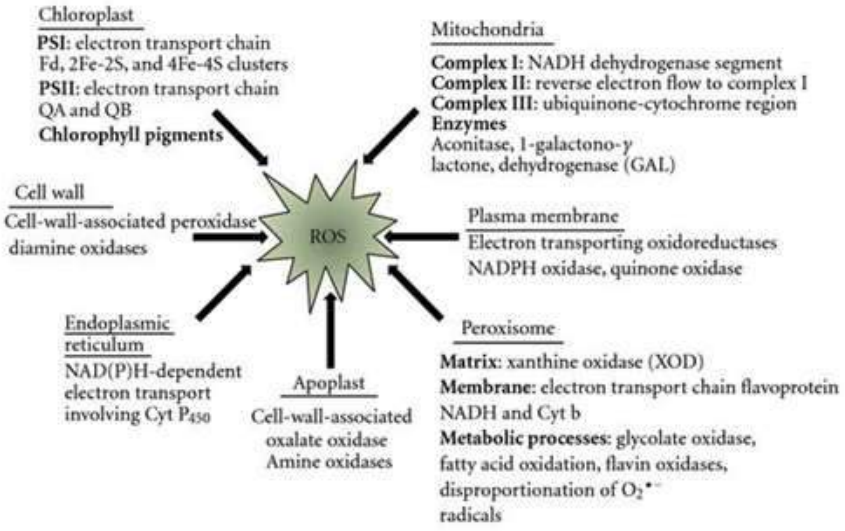

Figure 1:3: ROS Production in Different Cell Organelles

Adopted From:(Sharma *et al.*, 2012)

1.7. Chromosomal Aberrations Induced by ZnO-NPs

"Changes in the genetic material which causes phenotypic abnormality involve duplication, deletion, DNA rearrangement or mutation. Degree of these modifications may differs from loss or gain of a nucleotide (point mutation) to loss or gain of a chromosome. Among these changes, those can be viewed by a light microscope are termed as "chromosomal aberrations". Therefore, a chromosomal abnormality to be identified under microscope should involve more than 4 x 10^6 bp and a source of dividing cells (Schröck *et al.*, 1996). Chromosomal aberrations are known as confirmatory biomarker of stress genotoxicity and ionization to living cells (Natarajan, 2002). Cytotoxicity and genotoxicity induced by ZnO-NPs in plant cell is very poorly studied. Only few studies performed on model plants like *Allium cepa L.* and *Vicia faba* can be found in literature. These plants have proven to be excellent experimental material to study clastogenicity. As of the available studies agree that ROS induces oxidative damage to chloroplast, mitochondria, and DNA (nuclear). A number of modifications can occur in organic bases due to oxidative stress. Modifications in one strands causes mismatch to other strands leading to genetic mutations. Both base moieties and sugars are prone to oxidation by ROS. Enhanced degradation of RNA can also

occur as oxidative stress intensifies. Usually, DNA bases are damaged by addition of ·OH at double bond and sugars are denatured by removal of hydrogen from deoxyribose. All pyrimidine, purine bases as well as deoxyribose backbone are vulnerable to attack by ·OH. $^1O_2$ reacts with guanine only, whereas, O_2•− and H_2O_2 do not react with bases at all (Jain *et al.*, 2018). Chromosomal anomalies are divided into two categories a) numerical aberrations., b) structural aberrations;

a. Numerical Aberrations - these abnormalities are triggered by failure in chromosomal detachments. Thus, daughter cells may have either greater number of chromosomes or chromosome deficient. Examples are down syndrome (47 chromosomes) and turner's syndrome (45 chromosomes). In plants these aberrations are not much emphasized.
b. Structural Aberrations - changes in parts of chromosome give rise to structure related abnormalities. It comprises loss, gain or reallocation of chromosomal parts. That leaves a section with little genomic material while other part has too much of it. Majorly, four types of structural aberrations are known i.e inversion, translocation, duplication and deletion (Preston, 2014).

Genotoxicity or more specifically abnormalities in genetic material take place by following three mechanisms:

i. Direct genotoxicity - ZnO-NPs of size 8-10 nm can directly reach and interact with DNA. ZnO-NPs of size greater than 10 nm can get access to DNA during cell division. Direct interaction of ZnO-NPs with genetic material causes direct genotoxicity. It can harm genetic information through adduct formation, phosphorylation, altering stacking forces between bases or changing the gene expression. Charge and hydrophobic surface of the ZnO-NPs play crucial role is all these interactions.
ii. Indirect Toxicity - Despite of attacking DNA directly, ZnO-NPs can coalesce with mitotic spindle or nuclear proteins (proteins that are involved in transcription, replication or repair). ROS generated by ZnO-NPs can target antioxidant enzymes and inhibit proteins by binding either mechanically or chemically resulting in disruption of cell cycle checkpoints.
iii. 3rd mechanism governs through in vitro antioxidant inhibition and accumulation of ROS which ultimately leads to DNA damage (Barillet *et al.*, 2010).

1.8. Gene Expression as Influenced by Abiotic Stress in Plants

Abiotic stresses are important cause of damage to plants in general and responsible for up to 50% reduction in crops yield, in particular. Plants are continuously exposed to environmental changes. These changes when extreme and rapid are identified as stress by the plants. plants are sessile, thus they have developed a variety of mechanisms to fight against abiotic and biotic stresses. In present study our major focus is on environmental factors conferring threat to plant's growth and vigor. These mechanisms majorly consist of stress recognizing indicators, transduction of these cues to active response and control of stress relevant genes are essential components of plant stress management and forbearance. Plants combat against abiotic stresses operates by regulating the transcriptional factors. Scientists have developed significant understanding of how genes respond of environmental stresses and number of cis-regulatory and transcriptional factor have been reported (Ciarmiello *et al.*, 2011). In current study two families of stress related genes were selected as follows:

Among those *WRKY* family is one of ten largest respondents to abiotic stress. Different *WRKY* genes show different expression level to various environmental factors. However, Wang and co-workers have reported that Ta*WRKY10* genes play role in decreasing ROS levels caused by abiotic factors (Bai *et al.*, 2018).

Heavy metals pollution from industry particularly transition elements have lethal effects on environment as well as on human health. These elements cause oxidative damage and protein dysfunctioning. Plants have developed regulatory mechanisms against metal toxicity and to ensure adequate supply of nutrients. Thus, *HMAs* genes belong to this regulatory mechanisms of plants. HMAs belong to P_{1B} – type ATPases. These are heavy metal ATPases that are substrate specific and are allocated into two groups Cu/Ag pumps and Cd/Pb/Co/Zn transporters (Deshpande *et al.*, 2018).

It is a standardized lab technique for recognition and quantification of target mRNA. It can be used for relative as well as absolute quantification of the target gene. In this method complementory DNA (cDNA) is synthesized by total or mRNA through reverse transcriptase. cDNA is used as PCR template. Two techniques are used for quantification of PCR product, i) non-specific DNA binding fluorescent dyes – that intercalate within DNA (double stranded), ii)

oligonucleotide probes that are sequence specific and labelled with fluorescent dyes (Ciarmiello *et al.*, 2011).

1.9. Importance of Trophic Levels and Triticum aestivum as Food Grain

Autotrophs produces food by using water, carbon dioxide, minerals from the soil and heat from sun as source of energy. They have vital role in creation and maintaining life on earth. All animals cannot prepare food for themselves. Thus, plants are basics of food chain, feeding primary (herbivores), secondary (carnivores) and tertiary consumers (omnivores). Also they provide raw materials for shelter, clothing and all other products being prepared in modern industry and act as sink for all waste created through anthropogenic means.

Triticum aestvum (*T. aestivum*) is member of family Poaceae with third largest produced cereal grain on earth with production of 713 million tons. *T. aestivum* is most important agricultural crop in Pakistan. Where eighty percent of farmers grow it over forty percent of country's cultivatable land. As estimated, 3.04 % of world's *Triticum aestivum* is produced in Pakistan as reported by FAO. World's population is increasing immensely particularly in developing countries like Pakistan. In 2009, FAO projected that world-wide grain supply is essential to increase 70% to meet the demand for food supply. Arable land is limited and use of fertilizers has increased many folds to fulfill the food requirements. Nanofertilizers have emerged as a sustainable solution and have demonstrated promising perspective of development and application (Khot *et al.*, 2012). However, the accumulation, deposition and interaction of these NPs in plant tissues either as environmental contaminant or nanofertilizer is poorly understood. Understanding the importance of trophic routes is essential in eco toxicology because organisms living in contaminated ecosystems are likely to feed on contaminated food (Ruus *et al.*, 2005). Few notions concerning NP accumulation in different trophic levels is as follows:

Bioaccumulation: Accumulation of contaminant in an organism by all routes of exposure.

Bioconcentration: Amassing of a contaminant in an organism solely from its environment.

Biomagnification: Concentration of a contaminant in an organism at a trophic level is higher than the contaminants concentration at lower trophic level.

A number of studies have been reported so far that addresses the interaction of plants with heavy metals. However, we are still lacking in our knowledge about the interaction of NPs with

ecosystems and organisms. It is reported there is a higher accumulation in some plant tissues that has a direct effect on its growth, vigor and development. Deposition and interaction of the NPs with plant tissues depends upon its size and characteristics and availability in the media. Major toxicity posed by the NPs is due to ROS. Which comprises free radicals, superoxides, peroxides and hydroxyl ions. Metal/metal oxide NPs increase amount of ROS in plant cell that disrupts the normal cellular function and alters enzymatic pathways (Sabo-Attwood *et al.*, 2012).

1.10. Statement of the research problem/thesis statement

Environmental consequences of the indusrial pollution has yet to dealt with. However, scientists are finally comprehending the environmental effects of anthropogenic activities created from traditional pollutants. Although understanding a phenomenon never means what we have found a solution also. Now, with growing scientific knowledge we have entered in an era of nano-materials. The nano-materials are working wonders and have rendered unlimited services because of their distinctive size and surface to volume ratio. They are being synthesized on industrial scale and environmental toxicties of the nano-materials is not fully understood yet. Scientists are studying the distribution and fate of NPs at initial stage in mammalian models. Whereas, question remains about the negative/positive impacts on plant kingdom. Scientific studies published so far presents contradictory results. Also, there is a lack of rules and regulation for industrial scale synthesis, handling, utilities and disposal disposal of engineered NPs and as a result these NPs in the environment are being accumulated.

1.11. Hypothesis

i. Anthropogenic addition of nano-pollutants into environment is resulting in negative impacts on plant growth and development.

ii. Green synthesized NPs are less toxic than chemically synthesized NPs.

1.12. Aim and objectives of research

1.12.1. Aim

The aim of this research study is to investigate the interactive mechanism/impact of metal/metal oxide NPs with plant tissue that creates toxicity.

1.12.2. Objectives

Following are the specific objectives of the research;

- To synthesis and characterize chemically and green ZnO-NPs.

- To characterize both types of ZnO-NPs by UV-Vis spectroscopy, FTIR spectroscopy, XRD spectroscopy, SEM and EDX.
- To analyze the impact of both types of ZnO-NPs on physiological parameters of *T.aestivum.*
- Quantitative analysis of primary and secondary metabolities of *T.aestivum* as effected by chemically and green synthesized ZnO-NPs.
- Cytotoxiclogical study of *T.aestivum* root tips to confirm the ZnO-NPs toxicity.
- To study stress and growth related genes in *T.aestivum.*

1.13. Scope

Widespread and varied use of ZnO-NPs in industry has made it inevitable to undersand their whole life cycle – starting from raw material to industrial application and then to dumping of waste material. These spectacle particles have completely different properties from their parental bulk materials. Inspite of their confirmed utilities and profits, still, there are misgivings about their environmental impacts. Most of the times synthetic ZnO-NPs are smaller than the size of biological cell. Which may increase their absorbance in the biological systems. However, ultimate effects particularly negative impacts of ZnO-NPs on living cell is not yet clear And we could not fully understand the. Most of the studies performed so far to gauge the ZnO-NPs hazard are on mammalian models. Ecological systems are complex and interconnected. It requires a lot of effort and research to understand the fate and destination of NPs in an ecological system. The work under consideration will be an important contribution in this regard as there is no previous study reported yet that comprehends the impacts of ZnO-NPs on *T.aestivum* and addressing the expression of genes controlling the stress conditions created by the ZnO-NPs.

CHAPTER 2

LITERATURE REVIEW

Studies/researches related to co precipitation synthesis, green fabrication by plant extract, toxicity mechanism and toxicity of ZnO-NPs in plant models are enlisted and documented is this chapter.

2.1. Synthesis of ZnO-NPs

Most employed synthetic techniques to prepare ZnO-NPs are reviewed below**.**

2.1.1. Liquid phase synthesis

This method of NP preparation have many advantages over solid or gas phase procedures such as control over shape and size can by achieved at relatively low temperature within short time limit. It is a cost effective method as compared to other techniques. Simpler experimental techniques are used in liquid phase than solid or gas phases. Surface functionalization can be obtained with respect to the field of application. Liquid phase production gives a liberty to control size and shape of the nano-materials (Mantzaris, 2005). There are two approaches namely i.top down – in which bulk material is etched up into nanopartciles in a liquid phase, ii bottom up – in which molecules/atoms gives rise to NPs and forms a colloidal solution (Karatutlu *et al.*, 2018). Since antiquity, colloidal methods are well established and simplest ones first reported in 1857 by Faraday. Sol gel methods also depends upon same principal. Sols are colloidal solutions in which solid particles having a diameter of few hundred nano-meters is suspended. Gels are produced by poly esterification or poly condensation folloed by Ostwald ripening. Sol gels are advantageous to obtain uniform structures with high purities.(Khan *et al.*, 2016). Khan and companions have reported the materialization of thron like ZnO-NPs by this method. They have employed sodium hydroxide (NaOH), Zinc acetate dihydrate [$Zn(CH_3COO)_2 \cdot 2H_2O$] and CTAB as precursor chemicals. NPs had an average size of less than 50 nm and possessed antimicrobial properties (Khan *et al.*, 2016).

In hydrothermal and solvolthermal processes, initiators are dissolved in hot aqueous or non-aqueous solvants at moderate to high temperatures(100-1000^{o}C) and considerably high pressures(1-10,000 atm) both of these methods are known to form variety of structures such as bulk powders, thin films, wires(1D), rods (2D) and spheres (3D). Also, thermodynamically stable ZnO-NPs can be formed by altering reaction conditions.(Gersten, 2005). Rai and companions has documented the single layred ZnO-NPs through solvothermal process by alterting the precursor

Zn-salt.ZnO-NPs in variety of sizes (20nm,25nm,100nm,150nm) were obtained. Synthesized rod like ZnO-NPs were sensitive to NO_2 (Rai *et al.*, 2013).

2.1.2. Gas phase synthesis

There is a going concern in well-developed nanometrials as they are acting as building blocks for other maerials and commodities. Gas phase techniques allows the formation of comples nano-materials with tunable and controllable chemical properties. All modifications in this method are based upon atomization of matter followed by precise amalgamation of aoms into NPs (Huttel *et al.*, 2018).

For ZnO-NPs, spray pyrolysis is a widely used technique in which precursor Zn sakt in converting into aerosol droplets through flame heating. size of these droplets is reducind through dehydration. Last step of the technique consist of sintering and decomposition to acquire required material (Iskandar, 2009).

Inert vapor condensation method is sub-divided into chemical (with catalyst) and physical (without catalyst) vapor deposition. Inside a chamber resistive heat vaporizes the Zn-source. Radio frequencies, laser or electron beams are used as heart sources. Vapors migrates from a heat chamber to cooler chamber that have inert gas. From cooler chamber bapors are collected. Agglomeration and coalesces are major disadvantages of with procedure (Uhm *et al.*, 2007).

2.1.3. Physical methods

Physical methods for NPs synthesis consist of, physical vapor deposition, laser ablation, high energy ball milling, sputter deposition, melt mixing, ion implantation and electric arc deposition. Rate of NP production is very high in majority of procedures. That is why majority of industrial procedures employess physical method. Benjamin and companions developed high energy ball milling in 1961 as an non-equilibrium procedure. Powdered materials are subjected to collion by high energy ball inside a ball mill (Salah *et al.*, 2011). Amir khan with co-scientists conveyed that high energy ball milling practices are very cost effective, simple and efficient. For preparation of ZnO-NPs, they used 15 ball of average diameter of 20mm curbed in a 500 ml bowl. FESEM and XRD studies confirm the formation of ZnO-NPs having size 60nm (Uhm *et al.*, 2007). Salah et.al., reported the similar methodology and investigated its antimicrobial properties as well (Salah *et al.*, 2011).

A laser beam is used to confiscate particles from liquid or a solid surface is laser ablation technique. Pulsed laser ablation was used by Ismail in double distilled water to produce ZnO-NPs of 35 nm in diameter and spherical in shape (Ismail *et al.*, 2011).

Materials can be converted into plasma at high refluxes. While at low refluxes, materials absorb energy from vapors or laser. Other most studied and frequently used methods are chemical vapor deposition (CVD), physical vapor deposition (PVD) and vapor solid liquid (VLS) (Tigli & Juhala, 2011). For surface coating of the (PVD) materials physical vapor depositions are used. Two types of techniques are used in PVD known as sputtering and evaporation. In sputtering, particles escape from surface after collion of high energy particle. These highly energized particles are supplied by plasma (Espitia *et al.*, 2012).

2.1.4. Phyto-Fabrication of ZnO-NPs

Green/bio synthesis techniques provides a promising alternative to the tradition synthesis method. It employees minimum amount of chemicals thus posing least burden on environment in the form of pollutants. Scientists are experimenting on a number of green techniques some of them are discussed below:

a. Green Synthesis of ZnO-NPs by Plant Extract

Green routes are used for the synthesis of ZnO-NPs because of the least possible number of chemicals utilized that produces minimum probable pollutants. These techniques are energy efficient and cheaper. Scientists are looking at plants, algea, fungus, virsuses and bacteria to use them as vehicle for NP synthesis. In this regard plants have proved to be fascinating tools by eliminiating the utility of hazardous chemical and tedious culuring and downstraming processes. However, plant extracts are more preferable for the scientists due to simplicity of mehods and remain the most explored biological phenomenon so far.(Khan *et al.*, 2015, Khan *et al.*, 2016). Plant are capable to synthesis NPs both by in vitro and in vivo techniques.

In vivo methodologies exploities the plant’s ability to uptake metals from soil or water, hyper accumulates and reducing them to recoverable NPs. Phytomining and phytoremediations are well established example of this phenomenon. However, the focus mainly remained on silver and gold NPs. Hardly a couple of studies can be found addressing green synthesis of ZnO-NPs by these routes.

In vitro pathways make use of plant's extract most often aqueous extracts. These extracts are rich in phytochemicals that bio-reduce the metal to their respective NPs from their precursor salts. Phenols, flavonoids, polypeptides, tannins, saponins terpenoids and starches are chemicals that play key role in bio-reduction. These phytochemicals serve as capping agents as well (Ingale & Chaudhari, 2013, Makarov *et al.*, 2014, Mohamad *et al.*, 2014).

b. Microorganisms facilitated synthesis of NPs

Microbes are known as ecofriendly mechines for NP synthesis. Bio-mineralization, bioaugmentation, erosion and bioleaching techques are already relying on interactions between microbes and metals (Klaus *et al.*, 2001). Despite of its certain limitations it is most environmental friendly method for metal oxide synthesis either extracellular and intracellular.

Myconanotechnology is a new term coined to describe the synthesis of nano-maerials by fungi. It offers many advantages over other micro-organisms as it is easy to isolate and downstreaming processes are much simpler (Jain & Mehata, 2017, Nayantara & Kaur, 2018). For intracellular production, fungal biomasses are incubated with zinc precursor salt for a certain period of time in dark. Whereas, extra-cellular methodology involves the treat of fungal filterate with metal salt solution (Kon *et al.*, 2015, Yadav *et al.*, 2015).

Studies are available addressing ZnO-NPs production using fungal biomass. Nineteen fungal cultures were isolated from rhizopheric soil by Jain and co-workers. Among these cultures *Aspergillus aeneus* isolate NJP12 showed maximum potential for production of ZnO-NPs extracellularly at ambient conditions. Protein coating acted as stabilizer for resultants NPs (Jain *et al.*, 2013).

Jacob and companions utilized *Aspergillus niger* filterate and synthesized spherical ZnO-NPs with an average size of 39.4-114.6 nm (Jacob *et al.*, 2014).

Basker and cohort reported extracellular formation of ZnO-NPs using filterate of *Aspergillus terreus.* Resulted NPs were 54.8 to 82.6 nm in size with spherical shapes (Baskar *et al.*, 2013). Commercial biotechnology is using bacteria for bioleaching, genetic engineering and bioremediation. Bacteria can reduce metal providing themselves a prospective candidate for NP production. Scientific literature can be found addressing synthesis of ZnO-NPs via bacteria

pathways. Jayaseelan documented formation of metal oxide NPs by *Aeromonas hydrophila* strain. Resultant ZnO-NPs were oval and spherical in shape having size of 57.72 nm(Jayaseelan *et al.*, 2012). Microbial pathways of NP synthesis operates through integration of many mechanisms such as; transportation of metal ions across the cell, cellular biochemistry, microbial resistance for hazardous metals, nucleation of metal oxide, intracellular accumulation of metal ions,deposition of metal ions within the cells,and stimulated metal binding locations (Hussein *et al.*, 2009).

Lactobacillus sporogens strain produced ZnO-NPs having a diameter of 5-15nm. Investigators also explain the mechanism of formation of NPs. Precursor salt was reduced by oxido-reductase enzymes. These enzymes were activated by nutritional media, variation of pH (Chakra *et al.*, 2015).

Actinomycetes are interesting creatures that can be considered as becteria as well as fungi. These are also potential candidates for NP synthesis. Scientists have attempted to develop cost effective and friendly methods using *Sargassum muticum*- a macroalga found in oceans. NPs had hexagonal wurtzite structure and had a size of 30-57 nm (Azizi *et al.*, 2014).

c. Other green synthesis methods

Other than microbes, plant extracts and plants, scientist are also using other greener techniques to synthesize NPs e.g. Intestinal waste of slaughtered goat was reported to be used in NP synthesis by Jha and co-scientists. They obtained agglomerates of NP of 3-11 nm in size. This work should be considered an important step in waste disposal that would otherwise spread diseases (Jha & Prasad, 2016). Researchers are also using peels of vegetables and fruits to prepare NPs. Mishra and cor-workers using peels of Punica granatum. They used zinc nitrate as precursor salt (Davar et al., 2015). In another study scientists used extract from peels of Musa balbisiana to synthesize ZnO-NPs. Obtained NPs were less than 20 nm in size that srved as catalyst for preparation of chalcone derivatives (Dobrucka & Długaszewska, 2016).

2.2. Co – Precipitation Method

Term Co-precipitation or Coprecipitation (CPT) states a process of simultaneous precipitation of a component i.e normally soluble with a micro component from a solution by forming mixed

crystals (Patnaik, 2004). CPT is largely used for NPs synthesis, nowadays (Lu *et al.*, 2007). Mechanism of CPT includes three processes namely as:

i. Inclusion: crystallographic effect occurs when an impurity resides in a lattice site in crystal structure of carrier. This happens when charges and ionic radius of carrier and impurities are same (Coomber, 2012).
ii. Occlusion: as the crystal grows adsorbed impurity inside it, grow along crystal (Congress, 2016).
iii. Adsorption: an impurity adsorbate, bounds at precipitates surface (Kolthoff, 1932, Harvey, 2000, Lu *et al.*, 2007).

2.2.1. Process of ZnO-NPs Synthesis by Co-Precipitation (CPT) Method

Fractional precipitation of the target ion along with ions existing in solution, occurs (Chauhan *et al.*, 2010). Substances that are widely used during CPT are hydroxides, carbonates, chlorides, and oxalates. In following example $ZnSO_4$ was used as precursor salt. Carbonate buffer solution of pH 4.6 (alkaline solution) was added drop wise to salt solution. Which produced precipitates of $Zn_4(CO_3^{2-})_3(OH)_2$.

$$4(Zn^{2+} + SO_4^{2-}) + 4(Na^+CO_3^-)\ HOH \longrightarrow Zn_4(CO_3^{2-})_3(OH)_2 + 4(Na^{+2} + SO_4^{2-}) \quad (1)$$

$$Zn_4(CO_3^{2+})_3(OH)_2 \longrightarrow 4ZnO + H_2O + 3CO_2 \quad (2)$$

Reaction mixture has to be stirred for couple of hours at room temperature after addition of buffer solution. Then, precipitates were filter and washed several times with double distilled water. The Precipitates were dried at 110 ºC for two hours and then calcinated at 300-1100 in a muffle furnace. This method has proved to be an excellent technique to control size, shape, yield and purity of the nanoparticle (Singh, 2015, Dhas *et al.*, 2018). Recently a number of authors have used it in synthesis of ZnO nanoparticle.

2.3. Synthesis of ZnO-NPs from orange Peel Extract

In 2010-2011 global production of citrus was 115 million tons. 81 % of which was all varieties of orange (Berk, 2016). Orange industry majorly comprises of edible parts of the fruit. Fruit's by-products generated from fruit consumption and industrial processing contributes 50% of fresh fruit weight and a substantial amount of it is discarded as waste. Thus, there is a growing

concern about utilization of peels and to extract natural chemicals from it (Ibrahim *et al.*, 2015, Farouk *et al.*, 2016). These peels serve as cheap source of priceless phytochemicals such as tannins, flavonoids, essential oils and polyphenols. There is a dire need to develop such methodologies and strategies that are environmental friendly, cost effective and giving better yields. Major types of flavonoids in orange peels are apigenin, naringenin, hespertin, naringin, hesperidine and neohesperidin. Main constituent of phenolic content is P-coumaric acid, hydroxycinnamic acids, ferulic acid, and caffic acid (Tripoli *et al.*, 2007). Another significant component is essential oils which comprise citral, n-decanal, linalyl acetate, α-Pinene, citronella and D-limonene (Espina *et al.*, 2011). These phyto chemicals have anti-microbial, anti-carcinogenic, anti-atherogenic and anit-oxidant properties (Lagha-Benamrouche & Madani, 2013). Thus, these can be used as chelating, reducing and stabilizers for synthesis of NPs in order to develop greener and cheaper methodologies. Synthesis of NPs have been reported in literature employing phyto chemicals extracted from orange waste.

2.3.1. Synthesis of Ag NPs from orange peel

Most recently Barros (2018) synthesized Ag-NPs from orange peel extract. These Ag-NPs were 48.1±20.5 nm in size with −19.0±0.4 mV zeta potential (de Barros *et al.*, 2018). Kahrilas and co-workers (2014) synthesized one pot, micro-wave assisted Ag-NPs with the help of orange peel extract. These NPs had diameter of 7.36 ± 8.06 nm. GC-MS was used for analysis of orange peel extract. Most active compound which played vital role is Ag-NP synthesis was found to be aldehydes that also acted as capping agent (Kahrilas *et al.*, 2014). Konwarh and co-scientists (2011) synthesized Ag-NPs from orange peel extract in basic conditions and reported that abundance of ascorbic acid, carotenoids, sugars and pectins played key role in reductive properties of the extract. These green synthesized Ag-NPs were tested for ctyo-compatibility with THP-1 cell line in humans and also against *Bacillus subtilis* MTCC 736 (Konwarh *et al.*, 2011). Kaviya and companions (2011) employed Ag-NPs at two different temperatures (room temperature and 40 ºC. NPs synthesis was established by UV/Vis spectra, TEM images, EDS,and FTIR. Biological activity of NPs was tested against gram positive and negative becteria (Kaviya *et al.*, 2011). Awad and his co-workers (2014) biogenically synthesized Ag-NPs employing orange peel extract. NPs formed had an average diameter of 91.89 nm. Active ingredients found in formation of NPs was flavonoids as detected by the thin layer chromatography (TLC). These NPs exhibited antibectrial

properties against both bacteria (gram positive and gram negative strains) (Awad *et al.*, 2014). Omran (2018) bio reduced silver nitrate with the help of orange peel extract having particle size around 15nm (Omran *et al.*, 2018).

Balashanmugam and companions (2013) adopted the eco-friendly approach to synthesized Ag from extract of orange peel. Formation of NPs was confirmed by EDAX, TEM and FTIR while biological activity was tested against four fruit pathogenic bacteria (Balashanmugam *et al.*, 2013). Castero and co-scientists (2013) fouced on controlling shape and size of Ag-NPs by changing initial pH of the orange peel solution. Antimicrobial effect was also tested by scientists (Castro *et al.*, 2015). Vinay (2018)used Soxhlet apparatus to prepare ethanolic extract of orange peels which was further used to synthesize Ag-NPs of size 178.8 nm to 191.6 nm (Vinay *et al.*, 2018).

2.3.2. Hydrothermal Synthesis of Quantum Dots Using Orange Peel.

Quantum dots have also been prepared and reported by the scientists earlier in Taiwan. They obtained wasted orange peels from local market. Orange peels were dried followed by carbonization at 150 °C in an oven for 10 hours. Orange peels were washed with H_2SO_4 (0.1M) with a subsequent aqueous rinse. Peels were filtered and oven dried at 150 °C (2-hours). Then, sodium hypochlorite (60 mL) was added to peel and left for four hours at room temperature. The oxidized materials was autoclaved (Teflon lines) for 2 hours at 180 °C by adding 25 mL of water. After natural cooling of autoclave, acquired brown solution was rinsed with dichloromethane in order to remove organic material. Solution was centrifuged for 15 min at 5000 rpm. Solvent layer was discarded and remaining was dried for 2 hours at 100°C. C-dots yield was calculated by raw material's weight and of products weight (Prasannan & Imae, 2013, Chen *et al.*, 2016).

2.3.3. Synthesis of TiO_2-NPs from Orange Peel

Rao and co-workers (2015) have synthesized TiO_2 from orange peel. A brief of their work is discussed here. Left overs from oranges eaten in scientist's lab were collected and shredded into small pieces. 50 g of orange peels were extracted with 150 mL of water at 90 ºC for two hours. The extract was filtered. Titanium tetra-iso-propoxide (1.5 N aq. soln.) was used as precursor salt. The mixture was subjected to constant stirring for 3 hours continuously at room temperature. Mixture was kept on stirring for couple of hours at room temperature. Formation of crytsline NPs with tetragonal structure and 19 nm in size was confirmed by the XRD (Rao *et al.*, 2015).

2.3.4. ZnO-NPs from Orange Peel (OP) Extract

Few attempts have been reported in literature to synthesize ZnO-NPs from orange peel/waste. Most significant of which so far seems to be made by Rehan and co-workers (Rehan *et al.*, 2018).

Nava and co-workers (2017) have reported the synthesis of ZnO-NPs from orange peel extract. Orange fruits were bought from local market, washed and peeled off. Peels were dried in an food drier, until complete dry. Peels were ground to fine powder. Then, 1 g of powder was placed in a flask with 30 mL of water. Stirred for 3 hours and placed at 60 ºC for 60 min. Solution was filtered and stored in argon atmosphere. Zinc nitrate was used as precursor salt. 2 g of the salt was added to 45.2 mL of orange peel extract and kept on stirring for 60 min. Reaction mixure was placed in a water bath (60 ºC) until glassy caramel appeared. Lastly, it was heated at 400 ºC for an hour. Resulted material was grounded to fine powder with the help of amorter. NPs characterization using XRD, FTIR and SEM showed the hexagonal wurtzite structure (Nava *et al.*, 2017)

2.4. Phytotoxicity of ZnO-NPs

Potentially three types of mechanisms are responsible for toxicity of ZnO-NPs (Balážová *et al.*, 2018).

i. Leakage of ions particularly of Zn(II) can disrupt the cell homeostasis.
ii. Surface interactions of NPs may generate ROS and chemical radicals.
iii. NPs interactions with biological systems may inhibit photosynthesis, block water transport channels and disrupt nutrient cycles (Brunner *et al.*, 2006, Xia *et al.*, 2006, Lin & Xing, 2008, Ma *et al.*, 2013).

2.5. ZnO-NPs Toxicity in Onion *Allium cepa L*

Ahmad and companions (2017) reported toxicity of ZnO-NPs in *Allium cepa L.* Commercially synthesized ZnO-NPs of size 25.5 nm and hexagonal in shape were used in study. They tested a concentration range of 50, 100, 200, 500 and 1000 µg/mL. Mitotic index of *A. Cepa* bulbs was significantly decreased (23 ± 8.7 %) on 12 hrs exposure to ZnO-NPs whereas, chromosomal aberrations (18 ± 7.6 %) were increased following a dose dependent pattern. Internalization, surface attachmen and biomolecular intervention of ZnO-NPs were confirmed by

FTIR and TEM images. Asymmetrical and symmetrical stretching of P=O was confirmed by FTIR spectra expressing nuclear demages. Concentration of antioxidant enzymes were significantly higher in ZnO-NPs stressed roots as compared to control ones. Furthermore, upsurge in ROS alterations and production were detected in roots by ΔΨm (Ahmed *et al.*, 2017).

ZnO-NPs of size less than 20 nm were bought commercially from Rasker and companions and tested on *Allium Cepa* at a concentration ranging from 0 to 40 mg/L. Declined Mitotic Index (MI) and intensification in chromosomal irregularities were witnessed in greater treatments of ZnO-NP. Seed germination was elevated in lesser concentrations, however showed decrease in values at higher concentrations (Raskar & Laware, 2014).

Gosh reported toxicity of ZnO-NPs in *Allium cepa*, *Nicotiana tabacum*, and *Vicia faba*. NPs were bought commercially having size of 85 nm. They used concentration of 0.2, 0.4, and 0.8 g/L. Results showed aberrations in root cells of *Allium cepa*, augmented chromosome aberrations, cell-cycle arrest and loss of membrane integrity. In *Nicotiana tabacum* and *Vicia faba* increased concentration of lipid peroxidation, antioxidant enzymes, ROS production were noted. Morphological internalization and alterations were revealed by TEM images in plant tissue (Ghosh *et al.*, 2016).

Demir and Kaya have studied the genotoxicity of ZnO-NPs in *Allium cepa* roots. ZnO-NPs were bought commercially and had average diameter around 35-50 nm and spherical in shape. The researchers used concentration range of 10, 100, and 1000 µg/mL. For the comet assay, outcomes presented dose-dependent augmentation in DNA injury of cells treated with 100 and 1000 µg/mL of ZnO-NPs (≤35 and 50 nm) for proportion of DNA tail (% DNA tail) was obvious. Analysis showed 71.25 % DNA tail rate and 79.3 µm tail moment for ≤35 nm ZnO-NPs and 40.68 % DNA tail rate and 44.1 µm tail moment for 50-80 nm ZnO-NPs (DEMİR *et al.*, 2014).

Phytotoxicity of ZnO in *Allium cepa* was also reported by Ghodake and companions. The NPs used in study were bought commercially and had size of 50-100 nm and were shaped spherical, or hexagonal. They used concentrations gradient of 5-20 g/mL. Root elongation was adversely effected in dose dependent way. ZnO-NPs severely demeged chromosomal and cellular modules processing its hazardous phytotoxic nature (Ghodake *et al.*, 2011).

2.5.1. ZnO-NPs Toxicity in Rice (*Oryza Sativa)*

Mahajn and co-scientists reported reduction in root length at germination stage. ZnO-NPs used were bought commercially and tested a concentration rage of 10-1000 mg/L. There test experiments were carried out on *Cicer arietinum* and *Vigna radiata*. Agar was used as plant growth medium and also to avoid precipitation of insoluble NPs. Seeds germination development was observed as affected by the NP stress. Growth of mung was strengthening till 20 ppm and of gram till 1 ppm. Beyond that conc. growth was negatively affected by ZnO-NP conc. Uptake of NP was also conc. dependent in both crops (Mahajan *et al.*, 2011).

Boonyamitipong and Kositsup studied three parameters namely: i. seed germination percentage, ii. root length, iii. number of roots in Rice (*Oryza sativa L*.) at concentration of 10, 100, 500, and 1000 mg/L and found that Nano-ZnO is found to stunt roots length and reduce number of roots. They used commercially synthesized ZnO-NPs with average size less than 100 nm in this study (Boonyanitipong *et al.*, 2011).

Lin and Xing established hydroponic culture systems to study the internalization and translocation of ZnO-NPs in ryegrass (*Lolium perenne*) with the help of light, transmission electron and scanning electron microscopes. They bought NPs from Hongchen Material Sci & Tech co., Zhejing, China having surface area of 50 ± 10 m^2/g and size of 20 ± 5 nm. It was confirmed by the scientists that toxicity of ZnO-NPs is due to dissolution as well as adherence of NPs on roots. Individual ZnO-NPs were found in protoplast and apoplast of root stele and endodermis. Consequently, ryegrass biomass reduced significantly, root tips were shrunk, cortical and epidermal cell were either highly vacuolated or collapsed (Lin & Xing, 2008).

Chen and co-scientists also focused on toxicity evaluation of ZnO-NPs choosing rice as model plant. Hydroponic conditions were employed. Physiological parameters, biomass, chlorophyll pigments were analyzed. They also quantified the photosynthesis and antioxidant enzymes related genes. ZnO-NPs were also found in cytoplasm and intercellular spaces of plant as observed by the transmission electron microscopy and ultra-thin slicing. NPs presence in aerial parts of plant was also confirmed by inductivity coupled plasma. Activities of selected parameters were regulated confirmed by the down regulation of relevant genes (Chen *et al.*, 2018).

Yang and co-workers reported ZnO-NPs toxicity in five crops. They reported that ZnO-NPs were not found harmful till a concentration of 2000 mg/L and beyond that root length inhibition was recorded. They also concluded that ZnO-NPs impose toxicity in a dose dependent manner (Yang *et al.*, 2015).

Salat and co-workers prepared ZnO nano-rods from commercially available nano-powder. These nano-rods were 0.25 nm in diameter and 117 µm in length. The scientists choosed *Oryza sativa, L.* as experimental plant and used a concentration range of 0, 250, 500 and 750 mg/L. Plant growth parameters were significantly increased under ZnO-NPs stress. Activities of antioxidant enzymes [superoxide dismutase (SOD), catalase (CAT), malondialdehyde (MDA) and peroxidase (POD)] were significantly reduced. Ultrastructural analysis depicted significant damage to root cells and mesophyll. Gene expression of APXa, APXb, CATa, CATb, CATc, SOD1, SOD2 and SOD3 were down regulated (Salah *et al.*, 2015).

2.5.2. ZnO-NPs Toxicity in Maze (*Zea mays*)

Most recently Balazova have reported phyto-toxicity of ZnO-NPs in halophyte from genus Salicornia. NPs were bought commercially and had average size of 50 nm. Results showed that shoot length was decreased more than 50 % in conc. dependent manner. ROS was found in shoot of plants which reduced the amount and toxicity of enzymes such as PER, SOD, GR, ESC, and APX. iii. Lipid peroxidation level was three folds high in treated plants than in untreated ones. iv. Imbalance in Zn(II) ion disturbed the cell homeostatic resulting in loss of mitochondrial potential, increased selenium ion conc. and programmed cell death (Balážová *et al.*, 2018)

Corn seedlings were tested for toxicity of commercially purchased ZnO-NPs having particles size of 21-27 nm and conc. range of 0-1600 mg/L. At 400 mg/L ZnO-NPs significantly abridged the germination (40 and 53% respectively). At 20 °C and ZnO-NPs conc. of 50, 400, and 1600 mg/L reduced root growth by 18, 47 and 26 % respectively. At 30 °C and 100 mg/L ZnO-NPs conc., root growth was reduced by 42 %. At any temperature the XAS analyses showed presence on ZnO-NPs in roots. Protein band with molecular weight of 85 kDa decreased its expression at 30 °C, while a protein of 75 kDa increased its expression at 30 °C (López-Moreno *et al.*, 2017).

Industrial scale production of ZnO-NPs have increased manifold resulting an increase in exhaust of environmental nano-pollutants. Plants serves as a back bone in ecosystems and key component of raw material and food supply chains. Thus, proper understanding of plant-NP's interaction is very crucial. Scientists have sought the help of stereospecific and microscopic techniques to comprehend the interactions of Zn^{2+} and Zn NPs with maize. Results interpreted that ZnO-NPs increase the concentration of zinc ion in plant tissues that is stored as zinc phosphate. Majority of the NPs were present in epidermis tissues, while small amount was also observed in vascular system, cortex and root cells. ZnO-NPs could not reach to shoots, most probably due to dissolution. Although zinc phosphate was found in both organic and inorganic forms (Lv *et al.*, 2015).

Corn (*Zea mays L.*) and cucumber (*Cucumis sativus L*) were chosen as test plants for commercially synthesized ZnO-NPs of size 30 nm. Role of seed coat in reducing toxicity was evaluated through a concentration range of 0-1000 mg/L. Root length of both plants were reduced however, germination rate remained unaffected. Zn uptake by the corn was much higher than the cucumber and was related to the presence of Zn^{+2} in the ZnO suspension. TEM results confirmed the presence of Zn ions in seed coat which acted as barrier to mitigate the nano-toxicity (Zhang *et al.*, 2015).

In this study, cucumber plants were grown to full maturity in soil amended with either ZnO-NPs at concentrations of 0, 400, and 800 mg/kg. NPs were obtained from University of California Center for Environmental Implications of Nanotechnology (UC-CEIN) and had average diameter of 10 nm. Chlorophyll and gas exchange were monitored and physiological markers were recorded. ZnO-NPs were reported to release Zn(II) ions in soil. Yet, it was not found to disturb gas exchange or chlorophyll content. ICP-MS results showed the bioaccumulation of ZnO-NPs into the fruit at a conc. of 110 mg/Kg of dry weight. Whereas, XRF studies evidenced its presence in vascular bundle of the plant (Zhao *et al.*, 2013).

Zhao and co-workers studied the toxicity of ZnO-NPs on corn (*Zea Mays*) at very low concentration in soil condition. Soil was modified by adding 0, 400, and 800 mg/kg ZnO-NPs. They monitored gas exchange at every 10 days. ICP-OES/MS was used to determine Zn concentration in biomass after harvest. While, nutrient composition was determined by µ-XRF. Results depicted that photosynthesis was inhibited by 12 %, stomatal conductance by 15%, and

relative chlorophyll content by 10 % at day 20 at ZnO-NPs conc. of 800 mg/Kg. Crop yield was reduced by 49 %. Nutrient composition was altered significantly and overall crop health was suffered (Zhao *et al.*, 2015).

Zhao and co-scientists worked on the concept that metal oxide NPs can interact with nutrients and soil matrix and can alter it. Thus, significantly affecting the growth and nutrition on the cultivated plants. Study was carried out in two steps: in 1st step soil was amended with ZnO-NPs (0-800 mg/Kg), and in 2nd step soil was added with ZnO-NPs 400 mg/kg and alginate 0, 10, 50 and 100 mg/Kg. NP used were bought commercially, had an average diameter of 10 nm and were spheroids in shape. Dynamics of ZnO-NPs were determined by ICP-OES. Observed data showed that plant biomass was significantly reduced with an increased activity of antioxidant enzymes. However, in soil amended with ZnO-NPs and alginate showed normal trends in all studied parameters. Thus, alginate can be used as solution of ZnO-NPs pollution (Zhao *et al.*, 2013).

Pokhrel and Dubey reported potential anomalies in the morphology and anatomy of crop plants-*Zea Mays* as induced by the ZnO-NPs. They were commercially prepared NPs and had an average diameter of 11±0.7 nm. Analyses involve histology of the primary root morphology and anatomy using light microscopy, metal bio uptake, moisture content, rate of germination, and root elongation. Structural changes in maize primary root cells were uncovered as a result of NP stress. Microscopic evidence reveals 'tunneling-like effect' with ZnO-NPs treatment (Pokhrel & Dubey, 2013).

2.5.3. Phyto-Toxicity imposed by ZnO-NPs in Tomato (*Solanum lycopersicum L.*)

Doğaroğlu and Köleli has studied effect of commercially synthesized ZnO-NPs at a concentration range of Tomato 0, 200, 400 or 800 mg/dm^3. They concluded that (*Solanum lycopersicum L.*) plant growth, photosynthetic characteristics, chlorophyll fluorescence parameters and activities of antioxidative enzymes were inhibited in dose dependent manner (Doğaroğlu & Köleli, 2017).

Wang and co-workers have reported toxicity of ZnO-NPs in tomato (*Solanum lycopersicum L.*) bought commercially and check at 200, 400 and 800 mg/dm^3. Analysis was performed at 35th day and results showed that ZnO-NPs treatments significantly inhibited tomato

root and shoot growth, decreased the content of chlorophylls a and b reduced photosynthetic efficiency and some other chlorophyll fluorescence parameters in a concentration-dependent manner. Supernatant of ZnO-NPs was also tested for toxicity and was found harmless. Thus, it was argued that toxicity of ZnO-NPs is not due to Zn^{+2} ions but damaged photochemical systems and chlorophyll were cause of decreased biomass. They also reported enhanced activity of antioxidant enzymes and transcription factors related to antioxidant systems. Results were contradictory to previously reported results by Doğaroğlu and Köleli (Wang *et al.*, 2018).

Adverse reduction in tuber biomass was observed by the Bradfield when he was testing commercially synthesized ZnO-NPs on sweet potatoes (*Ipomoea balatas*) at a concentration array of 100-1000 mg/Kg DW. Zn was accumulated in both flesh and peels of sweet potatoes. 70 % of accumulated volume of metal was found in flesh. Which was considerably high than permissible limit of daily metal intake for a seven years old kid. Results suggested that NPs released its counterpart metallic ion before deposition into biological tissues (Bradfield *et al.*, 2017).

Raliya and Nair compared the toxicity of TiO_2 and ZnO-NPs in tomato (*Solanum lycopersicum L.*). ZnO-NPs were prepared from sol-gel method and obtained spherical NPs of an average diameter 22-28 nm. They tested conc. range of 0-1000 mg/Kg. and reported that threshold concentration for tomato plant is 700 mg/Kg plant growth is promoted and beyond that limit plant biomass and fruit nutritional value was negatively affected. NPs were distributed through vascular system as elevated concentrations were found in plant's parts (Raliya *et al.*, 2015).

2.5.4. ZnO-NPs Toxicity in Beans

Cruz, Savassa along with their co-workers studied phyto-toxicity of ZnO-NPs in common beans at three different particle size i.e. 20 nm, 40 nm,60 nm by following the fact that by choosing size and medium of NPs toxicity can be controlled. They tested concentration from 100 to 1000 mg/Kg. X-ray spectra showed that uptake velocities are related to the solubility. μ-XRF images confirmed the crucial role of cortex in movement of NPs to vascular bundle. In vivo XAS exhibited that NP were not transported as ZnO rather as organic macro molecules were formed (da Cruz *et al.*, 2017).

García-Gómez and co-scientists choosed to study long term toxicity of ZnO-NPs in two plants i.e. bean (*Phaseolus vulgaris*), Tomato (*Solanum lycopersicon*) in natural soil under

greenhouse conditions. ZnO-NPs had particle size of 100 nm and bought commercially. pH was found to be a driving factor in ZnO-NPs toxicity. Oxidative stress parameters, carotenoids and chlorophyll was measured and significant reduction was found. NP toxicity was found to be higher in acidic soil as compared to the calcareous for beans and reverse was true for tomato. Also NP toxicity was more related to intrinsic properties of ZnO-NPs. (García-Gómez *et al.*, 2017).

Phaseolus vulgaris (beans) were grown either on natural soil or organic matter enriched soil which was stressed by ZnO-NPs. Seed nutrient composition was assessed on harvest. NPs were bought commercially with 10-300 nm in size and hexagonal in shape. ZnO-NPs were found to augment growth at all concentration used. However, other nutritional parameters were negatively affected in dose dependent manners. Other contributing factors remained soil composition and environmental conditions (Medina-Velo *et al.*, 2017).

Green Pea (*Pisum sativum L.*) are highly consumed legumes on earth. Lattice or surface modification effect of ZnO-NPs was studied on it after 6 days of growth period. NPs of size 10 nm were bought commercially and selected dosage consist of 250 and 1000 mg/Kg of soil inside a green house. Higher conc. of ZnO was found in all parts of plant on harvesting. Plant biomass, chlorophyll content, proteins and elements (Al, Si) remained unaffected with an exception of 1000 mg/Kg. However, significantly higher concentrations of Zn were found in plant tissues. Higher, concentration of sucrose was analyzed in plant which is an important stress marker and indicator of higher amounts of ROS. Thus, confirming the phyto-toxicity of ZnO-NPs on soil grown crops (Kaviya *et al.*, 2011).

Hossain and friends tried to elaborate the mechanism behind the ZnO-NPs toxicity in plants. Soybean was used as model plant and NPs having an average diameter of 50 nm were bought commercially. Dark blue spots were appeared on leaves after histochemical staining with NBT. Which were evident of oxidative burst due to NPs. Root uptake of Evans blue was much higher in ZnO-NPs treated plants than the controlled ones showing higher rate of cell viability. Oxidation-reduction cascade related genes, such as GDSL motif lipase 5, SKU5 similar, galactose oxidase and quinone reductase were down regulated. Results of gel free proteomic analysis showed that 104 commonly found proteins found in roots were significantly changed. These proteins were related to secondary metabolism, cell organization and hormone metabolism. In leaves, 16 proteins

related to protein degradation and chlorophyll synthesis were found having altered compositions (Hossain *et al.*, 2016).

In this study nutrient elements of soybean plants grown in a soil containing 0-500 mg/L of ZnO-NPs were analyzed. The NPs used were bought commercially and had an average diameter of 10 nm. The samples were digested and analyzed through ICP-OES/MS. Results depicted that at max. conc. of ZnO-NPs plant had more Cu, Mn and Zn. Significant correlation was found in P and S in roots to NP dosage (Peralta-Videa *et al.*, 2014).

Another study by Yoom and co-workers has also reported the long term toxicity of ZnO-NPs on growth, development and reproduction of soybean evaluated in a standard soil microcosm. ZnO-NPs of average diameter 50 nm were bought commercially. The soil was treated with 0, 50, or 500 mg/Kg (dry weight) of ZnO-NPs. Observed data showed that soybean development was damaged in both treatment groups, particularly in the group that received 500 mg/Kg ZnO-NPs. Plant biomass was effected in terms of length, weight and surface. Plants in the 500 mg/Kg treatment group did not form seeds (Yoon *et al.*, 2014).

Soybean (*Glycine max*) was germinated and grown till full maturity in soil amended with ZnO-NPs at concentration 500 mg/Kg. At maturity plant were harvested and plant tissue including pod was analysed by synchrotron μ-XRF and μ-XANES. Exploration of μ-XANES data showed O-bound Zn, in a form resembling Zn-citrate, which could be an important Zn-complex in the soybean grains. On the other hand, the synchrotron μ-XRF results showed that Ce remained mostly as CeO_2 NPs within the plant (Hernandez-Viezcas *et al.*, 2013).

Stevia rebaudiana Bertoni belonged to sun flower family and was used in toxicity studies by Javed and Usman. ZnO-NPs of particle size 34 nm were synthesized by the precipitation method and used at concentration 0.1-1000 mg/Kg. 1 mg/Kg was found to be threshold concentration at which ZnO-NPs had positive impact on plant. Beyond that conc. there was a sharp decline in 2,2-diphenyl-1-picryl hydrazyl (DPPH) scavenging activity, total antioxidant capacity, total reducing power, total flavonoid content and total phenolic content in a conc. dependent manner (Javed *et al.*, 2017).

Doğaroğlu and Köleli used Barley (*Hordeum vulgare L.*) plant as model to study the negative effect of ZnO-NPs on plants. NPs were synthesized by wet chemical synthesis and had

an average diameter of 30 nm. They used a concentration range of 0, 5, 10, 20, 40, and 80 mg/Kg. Studied parameters include seed germination, root elongation, chlorophyll content and the activities of antioxidant enzymes. Physiological parameters were studied at day 7 and there was no proven toxicity of ZnO-NPs on germination. While chlorophyll content and antioxidant levels (superoxide dismutase, catalase, ascorbate peroxidase, glutathione, and proline) were adversely effected at maximum conc. (Doğaroğlu & Köleli, 2017).

Liu, Zhang and Rattan experimented the toxicity of ZnO-NPs at very low concentrations at 0.05 ppm. ZnO-NPs were synthesized by co-precipitation techniques. Agglomerates of NPs having an average size of 10-100 nm were formed. Their observations showed that toxicity of NP was comparable to the Zn ions. Also it was found to be growth stimulant at germination stage as growth of Lettuce seedlings were enhanced by 12-45 %. Thus, metal oxide NPs can be used as fertilizer in very low concentrations (Liu *et al.*, 2016).

Zhang and co-scientists studied the toxicity of ZnO on aquatic plant mesocosmes. ZnO-NPs were purchased from Sigma-Aldrich with particle size of 35±5 nm having 99.8 % purity. They used a concentration of 10, 100 & 1000 mg/L. NP suspensions were formed by sonicator. Experiment was carried out in hydroponic culture. Growth of *S. tabernaemontani* was significantly inhibited at 1000 mg/L as compared to control plants. Levels of Zn in the plant roots for the ZnO-NPs treatment ranged from 402 to 36513 µg/g, while values ranged from 256 to 9429 µg/g (dry weight) for Zn^{2+} treatment, implying that the uptake of Zn from ZnO-NPs was substantially greater than that for Zn^{2+}. The root uptake (of the initial mass of Zn in the solution) for ZnO-NPs treatment ranged from 8.6 % to 43.5 % while for Zn^{2+} treatment they were 1.66 % to 17.44 %. Presence of ZnO-NPs was confirmed by the transmission electron microscopy and proved that NP can pass through plant cell wall (Zhang *et al.*, 2015).

Bandyopadhyay and co scientists used alfalfa as a model plant to study the phyto-toxicity of ZnO-NPs and to compare it with its bulk counterpart. They bought commercially available ZnO-NPs of average diameter of 10 nm. ZnO-NPs was exposed to the symbiotic alfalfa (Medicago *sativa L*)–Sinorhizobium meliloti association at concentrations ranging from 0 to 750 mg/Kg soil. Plant growth, Zn bioaccumulation, dry biomass, leaf area, total protein and catalase (CAT) activity were measured in 30 day old plants. At 750 mg/Kg NP reduced the plant biomass, shoot, root

length and germination by 80 %. STEM-EDX showed reduction in CAT activity, protein amount, leaves, root, stem nodules tissues in a conc. dependent manner (Bandyopadhyay *et al.*, 2015).

Rosa and co-workers investigated the biotransformation of ZnO-NPs using alfalfa (Medicago sativa), cucumber (Cucumis sativus), and tomato (Solanum lycopersicum) as a model plants. ZnO-NPs of size 10 nm were bought commercially and tested at a concentration range of 0–1600 mg/L. At 1600 mg/L ZnO-NPs, germination in cucumber increased by 10 %, alfalfa and tomato germination were reduced by 40 % and 20 %, respectively. The highest Zn content was of 4700 and 3500 mg/Kg dry weight (DW), for alfalfa seedlings germinated in 1600 mg/L ZnO-NPs and 250 mg/L Zn^{2+}, respectively. Bulk X-ray absorption spectroscopy (XAS) results indicated that ZnO-NPs were probably bio transformed by plants (de la Rosa *et al.*, 2013).

2.5.5. ZnO-NPs Toxicity in *Brassica*

Xiang and co-scientists tested the toxicity of four different types of ZnO-NPs i.e ZnO-30, spherical ZnO-50, columnar ZnO-90, and hexagon rod-like ZnO-150 on germination of *Brassica pekinensis L* (Chinese cabbage) at a concentration range of 0-80 mg/L. Scientists observed that inhibition was evident mainly during seed incubation rather than the seed soaking process. Both the production of free hydroxyl groups (·OH) and the Zn bioaccumulation in roots or shoots resulted in toxicity of nano-ZnOs to chinese cabbage seedlings. The toxicity of nano-ZnOs was affected significantly by their primary particle sizes in the minimum dimensionality, but large columnar ZnO-90 and small spherical ZnO-50 had comparable toxicities (Xiang *et al.*, 2015).

Rao and Shekhawat used Brassica *juncea* as test plant to study the toxicity of ZnO-NPs in hydroponic settings. NP used were bought commercially with an average diameter of 50 nm and were cube and rod shaped. Tested concentration of ZnO-NPs were 0, 200, 500, 1000, 1500 mg/L for 96 h. Plant biomass was decreased significantly with an elevated concentrations of stress markers such as proline and lipid peroxidation. Antioxidant enzymes like CAT, APX, SOD and GR kept on increasing in a concentration dependent manner. Aggregates on NP were observed on roots surface (Rao & Shekhawat, 2014).

Mousavi and co-workers bought ZnO-NPs from Sigma-Aldrich which were 97 % pure and particle size was less than 50 nm. Nano-suspensions were prepared in deionized water. NPs were cube and rod in shape as tested by SEM and TEM. They choosed *Brassica napus* as study plant.

Release of Zn^{2+} from NP suspension was determined by atomic absorption spectroscopy and germination assay was performed. Results showed that germination was inhibited in a concentration dependent manner (Mousavi Kouhi *et al.*, 2014).

Salvinia natans (L.) is an aquatic plant and was chosen as test plant to study the ZnO-NPs at a concentration range of 1-50 mg/L. NPs were bought commercially and had an average diameter of 25 nm. Photosynthetic pigments were decreased significantly and antioxidant enzymes like SOD and CAT were increased as observed by the Hu and co-workers. Aquatic plant was exposed to NP stress for 7 days.Plant parts (roots and leaves) were investigated for Zn^{2+} ion accumulation. However, observations showed that plant growth was not significantly affected. ZnO-NPs at a concentration of 50 mg/L can adversely effect *S. natans*, and their stress is affected by their aggregation and dissolution (Hu *et al.*, 2014).

Cowpea roots were studied for ZnO-NPs toxicity. NPs were bought commercially and had an average diameter of 65-67 nm. ZnO-NPs were testified at a concentration of 500 mg/Kg. Results showed that ZnO-NPs were sticked to roots and transported upward as Zn(II) ion. However, no significant toxicity was observed (Wang *et al.*, 2013).

Corn plants were experimented for ZnO-NPs toxicity at a concentration gradient of 100 to 800 mg/Kg. The uptake (mg/Kg) of Zn by one-month old corn plants varied from 69 to 409 in roots and from 100 to 350 in shoots, respectively, in soils contaminated with different concentrations of ZnO-NPs. Confocal microscopic images showed that aggregates of NPs had moved to cortex and epidermis by apoplastic pathway. NPs were also found in vascular bundle by passing through endodermis through symplastic pathway (Zhao *et al.*, 2012).

2.5.6. Toxicity of ZnO in Wheat (*Triticum aestivum*)

Watson and companions experimented with Buck *Triticum aestivum* to examine the toxicity of ZnO-NPs. ZnO-NPs were bought commercially and had average diameter of 50 nm and spherical in shape. High concentration range i.e 0-4000 ppm was used in experiment. There was a considerable decrease in root growth at 2000-4000 ppm dosage of NP. Morphological features and epidermal cells showed altogether different patterns due to NP dosage. DNA polymorphism was evident at a conc. of 2000-4000 ppm (Lee *et al.*, 2013).

Zn in an essential nutrient in soil for plant growth. Scientists have studied the bioavailability of Zn ions in soil amended with ZnO-NPs. Used NPs were bought commercially with an average diameter of less than 100 nm, rhomboid in shape and tested on *Triticum aestivum*. They used a test concentration of 0.01 mg/Kg. In the acidic soil, the ZnO-NPs caused dose-dependent phytotoxicity, observed as inhibition of elongation of roots of *Triticum aestivum*. Soluble Zn in the acid soil was 200-fold higher and shoot levels were tenfold higher than from the alkaline soil correlating with phytotoxicity (Watson *et al.*, 2015).

Phytotoxicity of 100 nm rhomboid NPs bought commercially was test on *T. aestivum* by Dimka and Mclean. They selected a 500 mg/Kg dosage and reported that Zn was accumulated in *T. aestivum* shoots as Zinc phosphate. Which was found 24 folds greater in treated plants as compared to non-treated ones. Oxidative stress in plants caused decreased chlorophyll in shoots and increased concentration of stress markers like lipid peroxidation, oxidized glutathione in roots. Also, elevated activities of peroxidase and catalase were observed (Dimkpa *et al.*, 2012).

Du and Sun choosed to investigate the *T. aestivum* growth and soil enzyme activities as effected by the ZnO-NPs at a concentration of 5 g. ZnO-NPs were commercially and had slab like structure. Observations showed that *Triticum aestivum* biomass was reduced significantly. NPs were dissolved in soil, thus, enhanced uptake of ZnO-NPs by *Triticum aestivum* was observed. Soil enzymes like catalase, peroxidase and protease were reduced. Consequently, soil health was effected (Du *et al.*, 2011).

Shaymurat and friends synthesized spherical ZnO-NPs of 50 nm in size by sol-gel method and experimented its toxicity on Garlic (*Allium sativum L.*). Their observations showed that root length was inhibited in a conc. dependent manner which was completely ceased at 50 mg/L. Root cell viability was performed using 2, 3, 5-triphenylte trazolium chloride (TTC) as histological stain. Cell viability was lost after 8 hr stress 30, 40 and 50 mg/L. Mitotic index was also reduced in time and conc. dependent manner. NPs induced chromosomal and mitotic aberration such as chromosomal bridging, lagging, breakages and stickness (Shaymurat *et al.*, 2012).

ZnO nanopowder (particle size < 100 nm; surface area 15–25 m^2/g) were synthesized by Kratschmer–Huffman arc method and tested on *Arabidopsis thaliana*. A full concentration of 100 mg/L was used for a time of 7 days. Micro-array experiment was performed and results depicted

that 660 up- and 826 down-regulated genes ZnO stress. The down-regulated genes upon ZnO-NPs exposure were involved in cell organization and biogenesis, including translation, nucleosome assembly and microtubule based processes (Landa *et al.*, 2012).

Hernandaz *et al.,* bought commercially prepared ZnO-NPs (10 nm) to study its toxic effect on desert plant Prosopis juliflora-velutina (velvet mesquite) at very high concentrations (500-4000 mg/L). ICP-OES results showed presence of ZnO-NPs in roots, stems and leaves at level of 2102 ± 87, 1135 ± 56, and 628 ± 130 mg/Kg. CAT activity was increased in leaves, roots, and stem. APOX was increased only in leaves and stem. XANES showed presence of NP in plant tissues. XRE analysis established the presence of NPs in vascular bundle (Hernandez-Viezcas *et al.*, 2011).

Prosopis juliflora-velutina, Salsola tragus and Parkinsonia florida are desert plants and chosen for testing ZnO-NPs toxicity at a wide concentration range of 0-4000 mg/L. X-ray absorption spectroscopic (XAS) studies showed elevated amounts of Zn^{2+} as compared to the controlled ones and provided information about potential biotransformation of ZnO-NPs in biological system. Germination of all three plants was not significantly affected ($P < 0.05$). Root lengths were reduced by 14 %, 16 % and 14 % respectively at 4000 mg/L (de la Rosa *et al.*, 2013).

In this study, the toxicity on soil enzyme activity and growth of *Cucumis sativus* treated with Zn or ZnO-NPs was evaluated in pot soils for eight weeks. NPs were bought commercially with 50 nm in diameter and spherical in shape. Which were administrated at a concentration of 2000 mg/Kg. Activities of soil β-glucosidase, phosphatase and dehydrogenase were decreased. Roots length was decreased where shoot length and biomass underwent a slight increase (Kim *et al.*, 2011).

2.6. Response of *TaHMA2* and *TaWRKY10* to Abiotic Stress

TaHMA2 plays a crucial role in regulating metal ion uptake in root while *WRKY10* is an important stress fighter against abiotic factors:

2.6.1. TaHMA2

TaHMA2 gene was isolated by the Scientists Tan and co-workers. They also, characterized it to comprehensively describe its function in *Triticum aestivum*. Results showed that *TaHMA2* is

localized in plasma membrane. *TaHMA2* was over-expressed in moderate Zn-stress but Zn resistance decreased under high levels of Zn and Cd stress, respectively (Tan *et al.*, 2013).

Qiao and other scientists confirmed that *TaHMA2* is involved in Zn^{2+} transportation across the membrane. They studied the binding mechanism of *TaHMA2* is Arabidopsis and showed that over-expression of *TaHMA2* and its derivatives increase fresh weight, root length and Cd^{2+}/Zn^{2+} translocation from roots to shoots in Arabidopsis, as compared to the control experiments. Transport activity and tolerance of *TaHMA2* is reported to be reduced by Cys mutagenesis. While mutagenesis of Cys in the N-MBD reduced the tolerance and transport activity of *TaHMA2*, suggesting the involvement of Cys in Zn^{2+}/Cd^{2+} binding and translocation in *Arabidopsis*. This study therefore provides a theoretical possibility for the application of *TaHMA2* in transgenic breeding to regulate metal element balance in crop plants (Qiao *et al.*, 2018).

Nano-carrier-mediated foliar zinc fertilization was used by Deshpande and co-workers to study the effect on homeostasis of metal related genes as well as on gluten content of *Triticum aestivum*. Zn ions are transported from chloroplast to cytoplasm by *HMA* transportes. These transporters are present in chloroplast of leaf tissues. Later on, these ion are tranlocated to emerging grains. Form and concentration of Zn ion in intracellular spaces largely altered these transports (Qiao *et al.*, 2018).

2.6.2. Ta*WRKY10*

There are a number of evidences that depicts that *WRKY* family is involved in response to abiotic stress specially ROS stress (Yan *et al.*, 2014). 1st *WRKY* gene was cloned in sweet potato and since then it has been identified in more than twenty crops (Wang *et al.*, 2019). A study has reported 40 *WRKY* genes in *Triticum aestivum*. Among these 40 genes, expression of Ta*WRKY*2 and 19 are confirmed to increase by salt stress, drought and exogenous ABA application (NIU *et al.*, 2012). Almost all *WRKY* transcription factors show specificity to bind preferentially to the W-box [TTGAC(C/T)] of promoters of their target genes, and thus regulate the expression of the downstream genes (Ciolkowski *et al.*, 2008)

CHAPTER 3

MATERIALS & METHODS

3.1. Chemicals and Reagents

Zinc nitrate hexahydrate (Zn(NO3)2.6 H2O; ≥99.0 %), bovine serum albumin (lyophilized powder essentially fatty acid free), Tris HCl (99.0 %), hydrogen peroxide (35 %), TritonTM X-100 (laboratory grade), ninhydrin (ACS reagent), acetic acid (ACS grade), phosphoric acid (≥98 %), L-proline (≥99 %), 5-Sulfosalicylic acid dehydrate (ACS reagent), Quercetin (HPLC grade) and ethanol (ACS spectrophotometric grade) were purchased from Sigma-Aldrich (St. Louis, MO, USA). Gallic acid (98 %), trichloroacetic acid (99 %), malondialdehyde bis (diethyl acetal) (≥96 %), L-methionine (reagent grade; ≥98 %), ascorbate (≥98 %), KBr (FTIR-grade; ≥99 %) Acetone (ACS reagent), Folin & Ciocalteu's phenol reagent (suitable for determination of total protein by Lowry method, 2 M), sodium hypochlorite (reagent grade), potassium-phosphate monobasic buffer (≥98 %) and colchicine (≥95%, HPLC, powder), hydroxychloroquine sulfate (≥98%, HPLC powder), dimethyl sulfoxide (ACS reagent, ≥99.9%), xylene (reagent grade)were obtained from Merck (Darmstadt, Germany). Aluminium chloride (98.5 %), nitro blue tetrazolium chloride (analytical grade), aceto-Orcein Solution (2 %) and permount^{TM} (slide mounting medium) were bought from Fisher Scientific (Loughborough, UK). Sodium-phosphate buffer (1 mol/L, pH 7.4) was bought from Oxoid (Basingstoke, Hampshire, UK). Deionized water was used. All chemicals were employed without further purification.

3.2. Synthesis of ZnO-NPs by Co-Precipitation Method

For chemical synthesis of NPs, a large number of techniques have been reported in literature so far. Among these techniques co-precipitation method is relatively simple and an efficient one for lab synthesis of NPs. Zinc sulphate hepta hydrate [$ZnSO_4$:$7H_2O$] and sodium hydroxide (NaOH) were used as starting materials. $ZnSO_4$:$7H_2O$ and NaOH were separately dissolved in deionized water to form clear solution of molarity 1 M and 0.5 M respectively. Then, NaOH solution was added dropwise to $ZnSO_4$:$7H_2O$ solution with constant stirring at room temperature. White precipitates were formed which were stirred for 2 hrs.. Precipitates were allowed to settle down for 2 hrs. Precipitates were separated by centrifugation (10,000 rpm. 15 min, room temperature) (Himac CT 15RE, Hitachi, Düsseldorf, Germany) and washed thoroughly with distilled water several times and then with ethanol. Finally, the precipitates were oven dried at 75 °C to obtain white powder of ZnO-NPs .

3.3. Green Synthesis of ZnO-NPs from Orange (Citrus Sinensis) Peels

Following steps were carried out for synthesis of green ZnO-NPs:

3.3.1 Plant Material

Fresh oranges (*Citrus X sinensis*) were bought from local market in Islamabad and taken to central lab facility at SA-CIRBS, IIUI. Fruits were thoroughly washed under running tap water to remove dirt, pesticide residues and micro flora. Fruits were peeled using a stainless steel knife and peels were further cut into smaller pieces. These small pieces were washed with sterile distilled water. Orange (Citrus Sinensis) Peels were oven dried (Horizontal Forced Air Drier, Proctor and Schwartz Inc., Philadelphia PA) at 50 ˚C for 48 hours in hot air oven, until moisture content was dropped under 10%. Dried leaves were pulverized to fine powder in a sterilize cyclotec sample mill and passed through 0.5 mm sieve. The powder was kept in air tight glass jars and stored in refrigerator.

3.3.2 Preparation of Orange Peel Extract Extract

Antioxidants from orange peel powder were extracted as reported by Zia (2006), with minor modifications. Ten grams of grounded peels were extracted with 100 mL of double distilled water overnight in an orbital shaker at 40 rpm (JSSI-100T, JSR, Korea) at room temperature. The extract was filtered through cheese cloth and the residue was re-extracted under the same conditions twice. Filterate was stored in an air tight container and stored at 4ºC (Zia ur, 2006).

3.3.3 Synthesis of Green ZnO-NPs

Zinc nitrate hexa hydrate [$Zn(NO_3)_2.6H_2O$)] was used as precursor salt. 10 mM aqueous salt solution was prepared. 10 mL of aqueous extract of orange peels was taken in a beaker and heated upto 60 ºC. To aqueous extract of orange peel was added salt solution drop wise with constant stirring. The mixture was observed for color change. The reaction was stopped by putting the reaction mixture in ice bath as soon as the white precipitates of ZnO-NPs were appeared. Reaction mixture was filtered and centrifuged at 10,000 rpm for 10 mins. Filtrate was washed several time with distilled water (each washing was followed by centrifugation at 10,000 rpm for 10 min) to remove any foreign substances. Obtained material was calcined to 400 ºC.

3.4. Characterization of ZnO-NPs

There isn't any single method that can be used to characterize the NPs. There is a combination of the techniques that is used to characterize NPs. In the present study following techniques were used to characterize the ZnO-NPs. Optical absorption properties of ZnO-NPs were determined by using ultraviolet visible double beam spectrophotometer (T70/T80 series, pg Instruments, UK). Spectra was recorded in the range 200-500 nm using quartz cuvettes against deionized water as blank.

Fourier transform infrared (FT-IR) (Tracer-100, Shimadzu Europa, Duisburg, Germany) spectrophotometry was used to determine surface chemistry or more specifically Zn-O bond nature, functional groups involved in reduction and capping of ZnO-NPs. Spectra were recorded using an IR Tracer-100 spectrophotometer. FTIR analysis was performed by KBr pellet method in a 1:30 (ZnO-NPs: KBr) ratio. Transmittance mode was used at a resolution of 4 cm^{-1} over a range of 400-4000 cm^{-1}. Peaks were plotted as transmittance on y-axis and wave number (cm^{-1}) on x-axis.

Phase and crystal size of the synthesized ZnO-NPs was analyzed by powder X-ray diffraction using a high-speed energy-dispersive Lynx-eyed Xe-T detector on a D8 instrument, Advance, Burker, USA. Diffraction was recorded as a function of 2θ over a range of 10-80º with a step rate of 0.01º and step size of 0.02º. Monochromatized X-ray beam with Ni-filtered Cu Kα radiation ((λ=0.15406 nm) was used. Instrument was operated at current of 40 kA and voltage of 40 kV Crystal size of ZnO-NPs was determined by Debye–Scherrer equation (equation I):

$$D = (k\lambda) (\beta \cos\theta) \ldots \text{Eq (I)}$$

where k = proportionality constant and bears a value of 0.9; λ = wavelength of X-ray emitting from Cu Kα; β = value of full width at half maxima (FWHM) and θ = Bragg's angle in degrees.

Surface structure of ZnO-NPs was determined under JSM 6610LV scanning electron microscope (JEOL, Sanyu Denshi Co. Tokyo, Japan). Finely powdered ZnO-NPs were coated on carbon tape by adhering thin layer on a grid. Excess sample material was removed by a blotting paper and allowed to dry under a mercury lamp for 5 min. Same sample was used for energy dispersive spectra (ED-XRF instrument, model 41-XMX0002, Oxford). EDX spectra reflected the elemental composition, chemical purity and stoichiometry of synthesized ZnO-NPs.

3.5. Seed pre-Treatment and Sowing

Good quality *T. aestivum* seeds with high germination rate were obtained from the National Agricultural Research Council, Islamabad. Seeds were surface-disinfected by soaking in 5 % (w/v) NaOCl solution for 15 min and washed thoroughly with double distilled water. Seeds were sowed on two layers of sterilized Whatman filter papers, thoroughly soaked in 5 mL of dispersions of ZnO-NPs prepared by sonication as described by Au-Kaur et al. (2017) in a US-4120 ultrasonicator (Shenzen, China) at concentrations of 200, 400, 600, 800, and 1000 mg/L in Petri dishes. Seeds were gently placed in the Petri dishes with a sterile forceps, six replicates of five seeds per dish were used. The Petri dishes were placed in the dark for 48 h to break seed dormancy and were observed for germination rate every 24 h for a period of 6 days continuously (Thrane *et al.*, 2015, Au - Kaur *et al.*, 2017).

3.6. Determination of Physiological Analysis of Wheat (*Triticum aestivum*) Seedlings

Seeds were placed in dark for 48 hours at stable room temperature in growth chamber in order to break seed dormancy. Rate of germination was recorded and kept an eye for contamination. Later on, 12 hr, light and darh cycle at 25 ºC was provided. Number of germinating seeds were counted daily. Germination index was calculated on 5^{th} day from the following formula:

$$GI= (Sg/St) x100$$

Where, GI is germination index, Sg indicates number of seeds germinated after five days and St represents the total number of seeds. For the measurement of seedling parameters, Triticum seedling were harvested on 6^{th} day. Ten plants per treatment were selected randomly and length of roots and shoots were measured manually. For measuring fresh weight, ten seedlings were selected randomly and weighted immediately after harvesting. Then, these seedlings were oven dried at 65 ºC for 24 hrs and weighted until weight becomes stable. Index of tolerance and stress tolerance index was calculated by following formula:

$$IT = (Le / Lc) x 100$$

Where IT is index of tolerance, Le is length of roots or shoots in experimental group and Lc is length of root or shoot in control group

$$STI = (FWe/FWc) x 100$$

Where STI is stress tolerance index, FWe is fresh weight of either roots or shoots in experimental group and FWc is fresh weight of either roots or shoots in control group (Manmathan & Lapitan, 2013).

For determination of membrane stability index (MSI) 0.1 g of *T. Aestivum* shoots were cut into segments of approximately 1 cm in length. These segments were placed in a test tube having 10 mL of deionized water. These test tubes were kept into pre-heated water bath at 40 ºC for 30 min. Conductivity meter (HI 2300 EC/TDS/NaCl meter, HANNA instruments) was used to measure electrical conductivity (C1). Then, samples were boiled for 10 min in a water bath at 100 °C and conductivity (C2) was measured again. Membrane stability index was calculated by following formula (Hajra & Mondal, 2017):

$$MSI = [1-(C1/C2)] *100$$

For the measurement of ion leakage from roots, 0.3 g of roots were washed thoroughly with double distilled water. Roots from individual concentration and control groups were incubated in separate test tubes each containing 10 mL deionized water at 25 °C. Electrical conductivity (EC_0) was measured with conductivity meter (HI 2300 EC/TDS/NaCl meter, HANNA instruments, USA). These test tubes were incubated for 12 hrs and electrical conductivity (EC_1) was measured. Then, these test tubes were placed in boiling water bath and electrical conductivity (EC_2) was measured again. Ion leakage from the roots was determined by relative conductivity using the following formula:

$$\text{Ion Leakage} = [(EC_1 - EC_0)/EC_2] *100$$

3.7. Biochemical Analysis

Detailed biochemical analysis was performed in order to get the complete biochemical profile of the subject plant.

3.7.1 Chlorophyll/Pigment Estimation

For the extraction of chlorophyll we followed the method as described by the Thrane and his co-workers (Thrane *et al.*, 2015, Sudhakar *et al.*, 2016). Plant pigments were extracted with the help of 96 % ethanol. About 0.5 g of fresh plant material was homogenized in 96 % ethanol with the help of pestle and mortor. The homogenize was centrifuged at 10,000 rpm for 15 min at

4 °C. The supernatant contained the plant pigments. The pellet was discarded. OD was determined at 663 nm, 645 nm and 470 nm with the help of UV/visible spectrophotometer by using 96 % ethanol as blank.

Chlorophyll a (Ca) = 13.95 A665 − 6.88 A649

Chlorophyll b (Cb) = 24.96 A649 − 7.32 A665

Carotenoids (Cx+c) = (1000 A470 − 2.05 Ca − 104 Cb)/245

Total chlorophyll content = Ca +Cb

3.7.2 Proline Content – Proline

20 mg of frozen plant material (either shoots or roots) were homogenized using 0.75 mL of sulfosalicylic acid (3 %). Homogenized material was centrifuged for 10 min at 14000 rpm at 4 ºC. Ninhydrin buffer (2.5 M phosphoric acid, 2.5 % ninhydrin & 60 % acetic acid in ratio 1:1:1, v/v/v) was added in 0.4 mL of supernatant. Reaction mixture was allowed to stand at 60 ºC in a water bath for 95 min. After that it was allowed to cool down at room temperaturewas and 0.8 mL of Toluene was added. Two phases were separated. Optical density of organic layer was recorded at 520 nm. L-proline was used as standard (Bates *et al.*, 1973, Zegaoui *et al.*, 2017).

3.7.3 Total/Crude Protein

In order to estimate proteins in *Triticum aestivum*, fresh plant material was grounded in 3 mL of 0.1 N, NaOH by using pestle mortar. Samples were agitated on vortex (Robus Technologies RTV-100) for 3 sec and allowed to stand at room temperature for 30 min. The samples were centrifuged and supernatant was decanted. Aliquots of three replicates per sample were mixed to which was added 100 µL of 0.1 N NaOH. To each sample was added 5 mL of diluted Bradford dye reagent (Bio-Rad Laboratories). Absorbance was recorded at 595 nm against NaOH as blank. For proteins estimation standard curve was drawn using bovine serum albumin and amount of protein was represented as mg/g of fresh weight (FW) (Denno *et al.*, 1986, Jones *et al.*, 1989)

3.7.4 Lipids (Lipid Peroxidation Assay)

Assay used for this purpose was reported by (Du & Bramlage, 1992). Frozen plant material was homogenized in cold acetone and filtered using Whatman filter paper no. 4 paper. Original (thiobutaric acid) TBA procedure was followed by reported by (Heath & Packer, 1968).

20 % percent aqueous solution of tricholoacetic acid (TCA) (2 mL) and 0.67 % aqueous solution of thiobutaric acid (TBA) (1 mL) were mixed with 2 mL of plant extract. Mixture was allowed to stand for 15 min in a boiling water bath. Reaction was stopped instantly, under tap water and centrifuged for 15 min at 15000 rpm. Clear supernatant was separated and diluated with distilled water upto 10 mL. Absorbance was taken at 532 nm of clear solution and of non-specific turbidity was taken at 600 nm. Distilled water was used as blank.

3.7.5 Carbohydrates (total soluble sugars, non-reducing and reducing sugars)

Total sugars were extracted by the method described by Mukherjee. (Mukherjee *et al.*, 2016). Plant material was oven dried at 68 °C for 24 hrs, grounded to fine powder in pastel and mortar and passed through 40 mesh and stored in airtight container in dark at room temperature. 100 mg of dried sample was homogenized in 2 mL of 80 % ethanol and heated in a water bath at 80 ºC for 30 minutes. After cooling to the room temperature extract was centrifuged for 30 min at 14,000 rpm – a process that was repeated twice. The supernatents were combined and total soluble sugars were estimated specrophotometerically (absorbance = 490 nm). Glucose was used to draw standard calibration curve. For reducing sugars absorbance was taken at 620 nm and non-reducing sugars were determined by subtracting reducing sugars from total sugars.

3.7.6 Estimation of Total Phenols

Methodology employed to determine total phenolic contents was reported by (Ainsworth & Gillespie, 2007). Harvested plant material (20 mg approximately) was immediately freezed by liquid nitrogen and stored at -80 °C. 2 mL of ice-cold methanol (95% v/v) was added to each sample and homogenized in an ice-cold pestle and mortar. After homogenization, samples were incubated in dark at room temperature for 48 hrs. Then, samples were centrifuged at 13,000 g for 5 min at room temperature. Supernatant was collected in 2 mL microtubes. 100 µL of 95 % (v/v) methanol was added to each supernatant. Added 200 µL of 10 % (v/v) Folins-ciocalteu reagent and vortexed thoroughly. Into each sample tube was added 800 µL of 700 mM sodium carbonate Na_2CO_3 and incubated at room temperature for two hours. 200 µL of sample or standard was taken into a cuvette and absorbance was measured at 765 nm.

Standard curve was drawn using gallic acid as standard and absorbance was taken at 765 nm. Total phenolic content was estimated as gallic acid equivalents from regression equation.

3.7.7 Estimation of Flavonoids

For the estimation of flavonoid content, 0.5 mL of an aqueous solution of $AlCl_3$ (2 %) was added to 0.5 mL of ethanolic plant extract, and OD was recorded at 420 nm. Total flavonoids were calculated using a quercetin standard curve (Woisky & Salatino, 1998, Ordonez *et al.*, 2006).

3.7.8 Estimation of Anti-Oxidant Enzymes

For preparation of plant extract, 0.5 g of fresh shoots or roots were ground in 5 mL of 100 mM sodium potassium buffer under ice cold conditions, followed by the addition of 4 % PVP-40, β-mercapto ethanol (5 mM) and EDTA (2 mM). The mixture was centrifuged at 20,000 rpm (4 C˚) for 10 minutes and supernatant was called enzyme extract and used for analysis of antioxidant enzymes. Enzyme activity assays were performed for both roots and shoots.

a. Superoxide Dismutase (SOD)(EC- 1.15.1.1)

the enzyme assay mixture comprised 27 mL sodium-phosphate buffer (50 mmol/L, pH 7.8), 1 mL aqueous nitro blue tetrazolium chloride (NBT) solution, 1.5 mL methionine (20 nmol/L), and 1 mL of a 1 % Triton-X 100 solution. To 1 mL of enzyme assay mixture, 0.3 mL of riboflavin solution (3 µmol/L) and 0.1 mL enzyme extract was added. The tubes were incubated for 10 min in a light box providing a uniform light intensity of 40 W. A complete reaction mixture without enzyme extract was used as blank. Absorbance was taken at 560 nm. One unit of SOD corresponded to the amount of enzyme causing inhibition of photo-reduction of NBT by 50 % (Stewart and Bewley 1980).

b. Catalase (CAT) (EC. 1.11.1.6)

Catalase (CAT) activity was assayed by mixing 2.8 mL phosphate buffer (50 mmol/L, pH 7.0) and 0.1 mL enzyme extract. The reaction was started by addition of 0.1 mL H2O2 (0.4 %) and the absorbance was recorded at 240 nm. Enzymatic activity was calculated in terms of l mol/L H2O2 consumed per minute per milligram protein at 25 ± 2 °C (García-Limones et al. 2002).

c. Ascorbate Peroxidase (APOX) (EC. 1.11.1.11)

The reaction mixture was prepared by mixing 300 µL ascorbate (0.25 mmol/L), 1.5 mL sodium-phosphate buffer (50 mmol/L, pH 7.8) and 600 µL H2O2 (0.4 %), to which 600 µL of the

enzyme extract was added. Absorbance was recorded at 290 nm. One unit of enzyme activity refers to the amount of enzyme required to oxidize 10 µL of ascorbate/min/g fresh weight (Nakano and Asada 1981).

3.8. Cytotoxicology Study – Chromosomal Aberrations

Determination of Chromosomal aberrations is a classical method for the confirmation that a substance is causing toxicity to biological system of plant

3.8.1. Preparation of Solutions -Colchicine Pre-Treatment

For studying chromosomal aberrations roots were pre-treated with 0.05 % colchicine solution. Which was prepared by mixing 0.01 g of colchicine powder, 0.05 g of 8-hydroxy quinolone and 10 drops of dimethyl sulfoxide. 20 mL volume was made by adding distilled water.

3.8.2. Aceto-orcein Stain [2% (w/v)]

Aceto-orcein stain was used for studying chromosomal aberrations in *Triticum aestivum* root. Stain was prepared by adding 10 g of orcein in 225 mL of absolute acetic acid and solution was made 500 ml by adding distilled water. Both colchicine and aceto-orcein were kept in air tight container at 4 ºC.

Roots tips were analyzed for mitotic index. Healthy grains were placed on a filter paper moistened with 3 mL of ZnO-NPs suspension from 0, 200, 400, 600, 800 and 1000 mg/L in a petri dish at room temperature. Seeds were placed in correct direction i.e. seed crease was touching the paper. Tests were performed at comparatively constant temperature 25 ± 2 ºC until roots attained the length of 2-3 cm. It was made sure that root physiology of the germinating seedlings may not be disturbed by the light thus minimizing the interruption of cell cycle. Roots were nipped off with tweezers around 10 a.m. Root tips were placed on labelled filter paper moistened with colchicine pre-treatment solution. Petri dishes were covered with sheet of paper and left at room temperature for 3.5 hrs. Root tips were laid flat so that remained in contact with colchicine solution. Labelled glass vials were stood in a plastic tray with plastic strip in between each row. Added the aceto-orcein solution in each vial ¼ way up such that it may cover the root tip. Root tips were incubated for 3.5 hrs in vials such that one vial stands for one concentration used.

3.8.3. Preparing the Squash

Root tips were aborted from stain using tweezers and placed in a small vial containing 45 % acetic acid. The vial was heated for a few seconds over a lamp flame and brought to slow boil. Acetic acid was bubbled once and hold away from flame and shaken slowly. This step was repeated once again. Acetic acid along with root tip was poured into an evaporating dish. One root was taken out and placed on a filter paper. Filter paper absorbed the excess acetic acid and root tip was placed on a microscope slide. Slide was placed under stereoscopic microscope at 2x magnification. 2-2.5 mm apical root tip was cut off and discarded. Surface cells were scraped to take out dividing cells out. Slide was removed from the microscope and added one drop of 45 % acetic acid. A cover slip was placed gently over macerated area. Edge of the cover slip was held with a tip of a folded filter paper. Cover slip was tapped down with the help of an arrowhead needle. The filter paper absorbed the excess acetic acid and firm pressure stopped the cover slip from moving. Cover slip was slightly warmed over the flame. Covered with a piece of filter paper and pressure applied with help of thumb. Then observed under 40x or 100x magnification.

3.8.4. Making Slides Permanent

Cover slip from each slide was freezed and removed. Slides were dried at room temperature and treated with xylene for 10 min. then dried again at room temperature and mounted in permount. Cover glass was allowed to dry in mounting medium, stored, observed and photographed.

Mitotic index was calculated for each concentration of NPs by observing ~ 2000 cell. Mitotic index was calculated from formula

Mitotic Index (MI) = cells in diving phase / total number of cells

The occurrences of chromosomal anomalies, such as fragmentation uncoiling, nucleotide deletion, stickiness, c-metaphase, distributed anaphase, bridges, lagging chromosomes, multi nuclei, elongation, gaps, erosion and multipolar anaphase were also recorded (Abdelsalam *et al.*, 2018)

3.9. Quantitative Reverse Transcription-Polymerase Chain Reaction (qRT-PCR) Analysis

Quantification of gene expression under abotic/biotic stress can give us valuable information about gene function or plant's response to stress. There are also other methods to

quantify this expression such as RNase protection assay and northern plot. But those are time intensive and some time it become nearly impossible to generate precisely accurate results. Scientists have developed a technique that overcome this barrier. qRT-PCR requires very small amount of sample, reproduces fast and accurate data and have ability to analyse more than one gene at a time.

A real time polymerase chain reaction or quantitative-PCR is powerful lab technique that give liberty to detect amplicon (PCR product) at early state of reaction (real time mode). Thus PCR product is measured when PCR cycle is in exponential mode. Most important step in development of qRT-PCR remains the ability to convert an RNA or mRNA into copy DNA (cDNA). Very 1st copies of DNA from template RNA were generated for retroviral derived RNA-dependent, DNA polymerase (Temin, 1995). Real time PCR follows the same principle as of conventional PCR. In which short copies of DNA should be doubled theoretically at each cycle. Which is practically not possible. As in the start of the reaction, reaction substracte are enough in amount and the above narrated principle is followed. But as the reaction proceeds concentration of reactants goes down resulting gradual decrease in DNA copies. As result progress in PCR can be fragmented into three phases; i. exponential, ii. linear and iii. plateau. In conventional PCR, compound differences in the linear phase can vary amount of product to a greater extent and acuuracy for quantification remains no longer reliable. Whereas, in case of real time, amount of amplicon can b quantified at each cyle with the help of a fluorescent dye. This method has many advantages such as high speed due to reduced number of cycle, eleminition of need to run a gel for product detection and off course greater sensitivity. There are two type of dye; i. an interclating dye- it intercelates with double stranded DNA can more PCR product is produced and gives fluorescence at its own, ii. Fluorescently labelled oligonucleotides are known as hydrolysis probles. These probes are designed in such a day to get attach with one of the primer during downstream cycle of PCR and produces fluorescent during reaction.

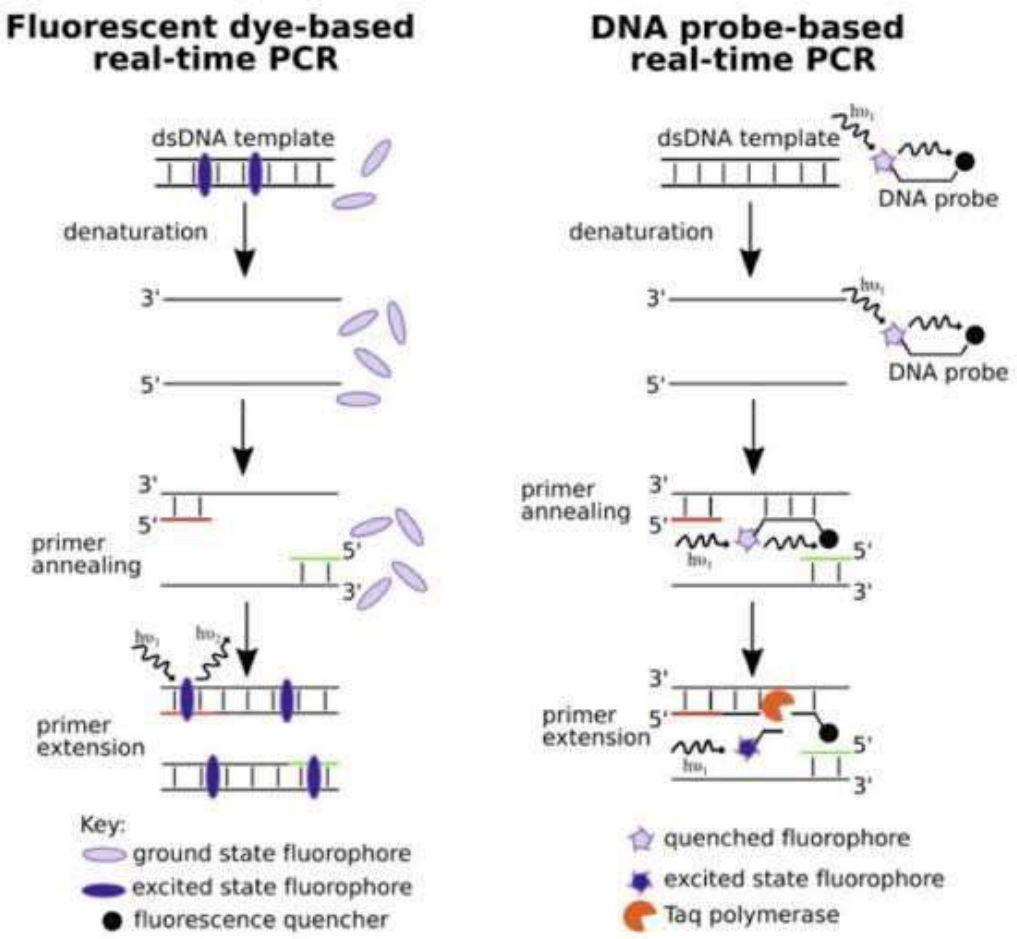

Figure 3:1:Steps and Process of quantitative real time polymerase chain reaction

3.9.1. Relative Quantification of qRT-PCR Product

Here, question arises what is best qRT-PCR quantification technique to determine the correct amount of mRNA in a sample. Generally, two types of quantification techniques are used to greater extent known as relative or comparative quantification and absolute quantification. The later one make use of calibration curve for analysis. These calibration curves are derived from diluted PCR product, RNA or DNA recombinant, spiked samples of tissues or linearisd plasmids. Units becomes irrelevant to express relative quantities. As a practice, constant expressed genes are taken as reference and are co-amplified as an exogenous control (amplified in a separate tube) or endogeneous control (multiplex assay).

The relative expression of gene of interest (GOI) is calculated on the basis of "delta delta CT method. The so-called 'delta Ct' or 'delta-delta Ct' method without efficiency adjustment. Here an optimum doubling of the target DNA during each accomplished real-time PCR cycle is presumed (Temin, 1995)

3.9.2. RNA Extraction From Plant Tissue

To generate reliable data from qRT-PCR most important consideration is quality and quantity of extracted DNA. RNA os ubiquitous in nature which makes it less stable than DNA. Moreove, DNase are less stable than RNase making RNA more susceptible to degradation and conatimantion, if not dealt with care.

Plant materials are full of secondary metabolities and phytochemicals, that may harm both quantity and quality of extract RNA. Befor extraction work station was swaped with 70% ethanol. All glassware was autoclaved with pestle mortar, that was further dried and prechilled at -20°C. centrifuge was preset at 4 °C

Plant materials are saturated with secondary metabolities and phyto-chemicals, which may effect the nucleic acid extraction both in terms of quality and quantity. It's crucial to take extra care, in case of RNA extraction from plant tissue. The half life of RNA is very low,t is readily converted into cDNA because RNA is vulnerable to RNases present in environment or store it at -80 °C. Before starting the extraction, TRIzol method was used for mRNA extraction. Precisely, 200 mg of frozen dry plant material was crush in liquid nitrogen to fine paste with the help of pestle mortar and allowed to thaw at room temperature. I ml of TRIzol was added to homogenate and transferred to 1.5mL centrifyge tubes. Tubes were shaken gently and incubated at room temperature for 5 min. 400µL of chloroform was added and again incubated at RT for 3 minutes. Then, micritubes were centrifuged at 12,000 rpm for 10 min at 4 °C for phase separation. Upper aqueous layer was transferred to new pre-cooled tube and placed in ice box. Chilled iso-propanol was added to each tube in a 1:1 ratio. Tubes were incubated on ice for 10 min and again centrifuged at 12,000 for 10 min at 4 °C. supernatant was discarded. Pallet was washed twice with 70% ethanol. And air dried completely. 40 µL of RNase free water or DEPC water was added. RNA was stored at -80°C until downsteam application.

3.9.3. cDNA Synthesis

To convert RNA to cDNA, EasyScript ™ Reverse Transcriptase & cDNA Synthesis kit (Applied Biological Materials Inc. G32 & G34) was used.

a. Reagents

Template (RNA), Primers oligod(T), dNTPs, EasyScript ™ Rtase, RT Buffer, RNaseOFF Ribonuclease Inhibitor, Nuclease free water (NF H_20)

b. Protocol

All the reagents were mixed well and tubes were centrifuged briefly:

RNA-primer mixture was prepared as below:

Table 3.1: RNA Primer Mixture

Reagents	Stock Conc.	Working Conc.	Vol/reaction
Total RNA			7 µL*
Primers	40 µM	4 µM	1 µL
dNTPs	10 mM	1 Mm	1 µL
NF H20			1 µL
Final Volume			10 µL

"n" is the number of reactions for which you are making MasterMix. Depending upon concentration of RNA the mixture was incubated at $65^{O}C$ for 5 minutes and chilled on ice bath for 2 minutes. Briefly spinned down the mixture. cDNA Synthesis Mix was prepared as indicated:

Table 3.2: Reagent's ratio for cDNA Synthesis

Reagents	Stock Conc.	Working Conc.	Vol/reaction
EasyScript TM Rtase	200U/ µL	200 U	1 µL

RT buffer	5X	1X	2 µL
RNaseOFF Ribonuclease Inhibitor	40U/ µL	20U	0.5
NF H20			6.5µL
Final Volume			10 µL

"n" is the number of reactions for which you are making MasterMix.

Added 10µl of the cDNA Synthesis Mix into each RNA-primer mixture and was mixed gently and centrifuged briefly. Tubes were incubated at 42 ºC for 60 min. Reaction was terminated by incubating the tubes at 85OC for 5 min. Tubes were chilled on ice bath and centrifuge the tube briefly. The synthesized cDNA can be directly used for downstream application or stored at -20OC.

3.9.4. Polymerase Chain Reaction (PCR)

Techniques in molecular biology were revolutionized with the development of PCR by an American nobel laureate Kary Mullis in 1983s. It is used to make several copies of a specified DNA segment and has become a common clinical and medical laboratory tool. Four primers were used to optimize the annealing temperature (Ta). Sequences of forward and reverse primers used in this study are:

Table 3.3: List of qRT-PCR Primers

Primers	**Tm**	**Sequence**
Triticum aestivum Beta Actin –R	57°C	GAACCTCCAACTGAGAACAACATTACC
Triticum aestivum Beta Actin –F	55°C	GTTCCAATCTATGAGGGATACACGC

Triticum aestivum GAPDH –R	58°C	CCAGTGCTGCTTGGAATGATG
Triticum aestivum GAPDH –F	55°C	TGTCCATGCCATGACTGCAA
Ta*WRKY10*-R	58°C	CATGTTCATCGTCTCGCCT
Ta*WRKY10*-F	53°C	TGTACAATTTCGAAGCCGGT
TaHMA2-R	57°C	TTCCACTGCCTTTCTCCCTC
TaHMA2-F	56°C	GGGCATCCGCTTATTTGG

Following chemicals were used and in table all the used and available concentrations are mentioned: Template cDNA, Forward & reverse Primer,Taq polymerse enzyme 5U/ µL Thermoscientific, PCR buffer, dNTPs, $MgCl_2$, PCR water:

Table 3.4: Recipie of PCR master mix

PCR Reagents	**Stock Conc.**	**Working Conc.**	**Vol/Rec**
cDNA template	-	-	1 µL
P_F	10 µM	0.2 µM	0.4 µL
P_R	10 µM	0.2 µM	0.4 µL
dNTPs	10 mM	0.2 Mm	0.4 µL
Buffer	10X	1X	2 µL
$MgCl_2$	25 mM	2.5 Mm	2 µL
taq Polymerase	5U/ µL	1.5 U	0.3 µL
PCR H_2O			13.5 µL
Final Volume			20 µL

"n" would be any number for which you are making master mix. Polymerase chain reactions were performed on a Galaxy XP Thermal Cycler (BIOER, PRC). Optimized PCR conditions were shown in table.

Table 3.5: Optimized PCR conditions

Steps	Sub-cycles	Conditions	PCR cycles
Initial Denaturation		95 °C, 10 min	1
PCR Cycles	Denaturation	95 °C, 1 min	40
	Primer annealing	---1 min	
	Primer extension	72 °C, 1 min	
Final extension		72 °C, 10 min	1
Hold		°C, ∞	1

3.9.5. Quantitative Real Time - PCR

qRT-PCR is a frequently used technique in molecular biology. It is performed in a thermal cycler that has ability to irradiate sample by a light beam on a definite wavelength. Excited fluorophores emit the light and fluorecence is detected by the sensors. Following chemicals were used in this experiment: Template cDNA, Forward & reverse Primer, 2X SYBR Green/ROX qPCR Master Mix (Thermoscientific) (K0221), Nuclease free water. All of the optimized concentrations are shown in table:

Table 3.6: Optimized qRT- PCR conditions

PCR Reagents	Stock Conc.	Working Conc.	Vol/Rec
cDNA template	-	1:10	2.6 µL

P_F	10 µM	0.2 µM	0.2 µL
P_R	10 µM	0.2 µM	0.2 µL
SYBR Green	2X	1X	5 µL
PCR H_2O			2 µL
Final Volume			10 µL

3.10. Statistical Analysis

All the values were presented as mean ± SD of triplicate of every individual experiment. One way Anova along with Tukey studentized Range (HSD) Test at level of probability test level of 0.05 was performed using IBM SPSS STATISTICS 20.

CHAPTER 4

RESULT AND DISCUSSION

4.1. Characterization of ZnO-NPs

Physical and chemical properties of chemically and green synthesized ZnO-NPs were characterized by following techniques;

4.1.1. UV/Vis Spectra

UV/Vis spectra of the ZnO-NPs prepared through co-precipitation method and green method is given below. Spectra was recorded at wave length range of 200-500 nm. ZnO-NPs synthesised through co-precipitation method showed a characteristic sharp peak around 373 nm at room temperature as depicted in figure 4.1 i.e. evident for purity of NPs. Similar absorption was observed by the Ahmad (Ahmed *et al.*, 2017).

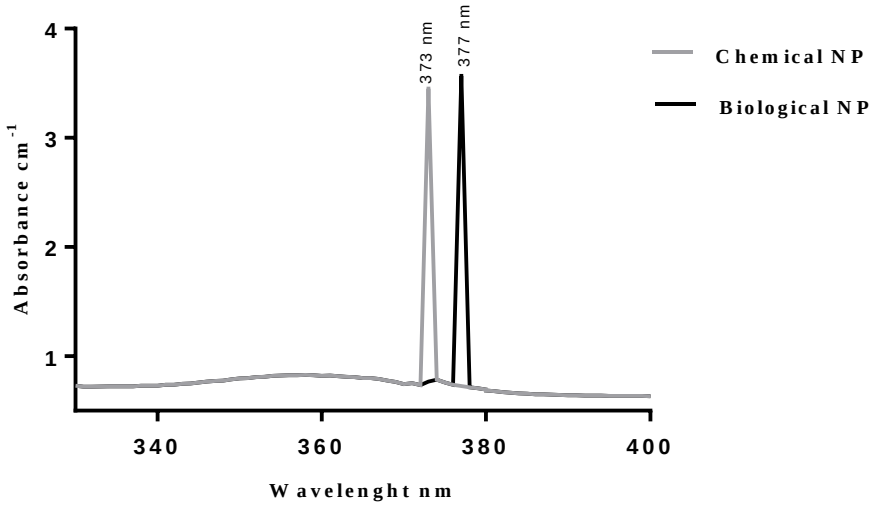

Figure 4:1: UV-Vis Spectra of ZnO-NPs prepared from co-precipitation and green Method

UV/Vis spectra (Figure 4.1) of the green synthesized ZnO-NPs was found at 377 nm and exhibits the characteristic peak of the pure ZnO-NPs (Bala *et al.*, 2015). This distinguishing absorption peak of ZnO-NPs points towards intrinsic band gap as a result of electronic transitions from valance band to conduction band ($O_{2p} \rightarrow ZnO_{3d}$). Sharp peak is also evident of particle being in nano size having a narrow size distribution (Zak *et al.*, 2011). UV spectra exhibits large excitation binding energies of ZnO-NPs at room temperature. In an absorption spectra decrease in particle size leads to increased band gap.

While there is an opposite ratio between band gap and absorption wavelength (Bhuyan *et al.*, 2015).

4.1.2. Fourier Informed Infrared (FTIR) Spectroscopy

Infrared (IR) spectra was recorded over a range of 400-4000 cm^{-1}. Metal oxides generally show absorption band below 1000 cm^{-1} due to inter-atomic vibrations. Absorption band of Zinc oxide lies between 450 to 590 cm^{-1}. At ambient pressure and temperature ZnO-NPs crystallizes in the wurtzite structure, a hexagonal lattice characterized by two interpenetrating sub-lattices of Zn2+ and O2- ions, such that each Zn ion is surrounded by a tetrahedron of oxygen ions and vice versa. This arrangement gives rise to polar symmetry along the hexagonal vertical axis. The wurtzite structure of ZnO crystal has C6v symmetry. There are 4 atoms in the hexagonal unit cell leading to 12 phonon branches, 9 optical and 3 acoustic, classified according to the following irreducible representations: Γ= 2A1 + 2B1 + 2E1 +2E2, where A and B modes present one-fold degeneracy and E modes are twofold. One A1 mode and one E1 pair are the acoustic phonons. The 9 optical phonons are divided into one A1 branch (both Raman and IR active), one doubly degenerate E1 branch (both Raman and IR active), two doubly degenerate E2 branches (Raman active only) and two inactive B1 branches. Results depicted up strongly conincides with Yoshikawa (2008) (Yoshikawa *et al.*, 2008). Who further explained the crystalline structure of ZnO-NPs by Raman spectra and explained that the two most intense peaks are associated to the E2 modes, the first at 99 cm-1 (named E2 low), dominated by the vibrations of the heavy Zn sub-lattice, the second at 437 cm-1 (named E2 high) which involves mostly the oxygen atoms. Thus, crystalline structure of ZnO-NPs corresponds to E2 form of hexagonal wurtzite crystal lattice (Babu et al., 2013, Shoeb et al., 2013). In the present work strong absorption was found at 409, 443, and 490 cm^{-1} as evident from the figure 4.2 (a). IR bands shown in 1700-600 cm^{-1} relates to C–O, C=O, and C–H are expected due to ethanol wash. Remaining peaks are most expectedly due to H-O bending modes and stretching vibrations of the adsorbed water (Mayo *et al.*, 2004, Abdolmaleki *et al.*, 2011).

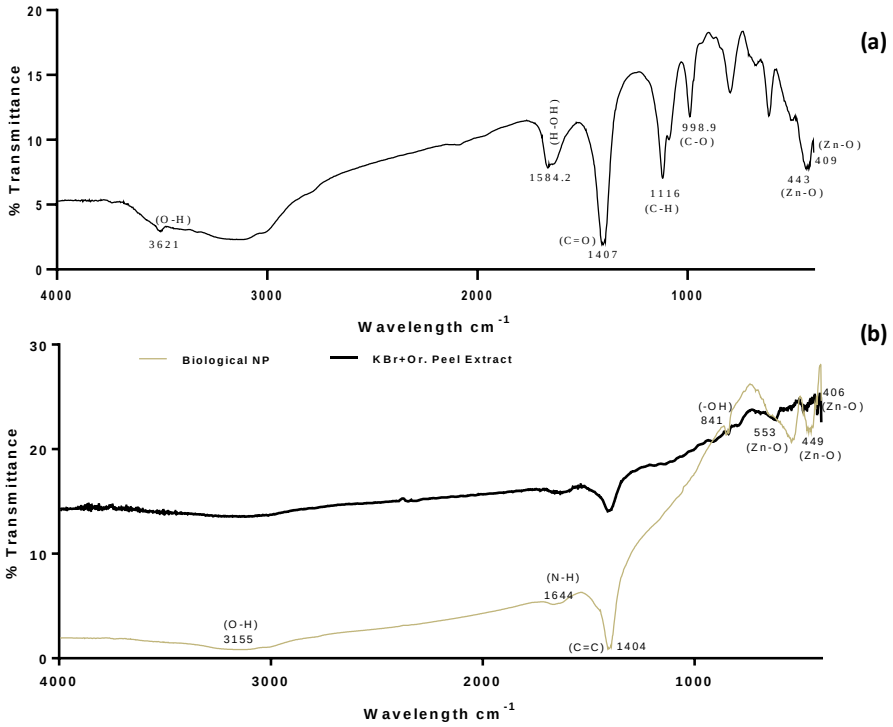

Figure 4:2: Fourier Transformed Infrared Spectra of; (a) Chemically Synthesized ZnO-NPs, (b) Biologically Synthesized ZnO-NPs from aqueous extract of orange peels.

Chemical structure of the ZnO-NPs synthesized from aqueous extract of orange peels was also confirmed by the FTIR spectra (Figure 4.2 (b)). Presence of Zn-O bond is evident from four bands i.e 406, 449, 538 and 841 cm^{-1}. Absorption band at 538 cm^{-1} is a characteristic band of the ZnO-NPs and corresponds to the E_2 plan of the hexagonal wurtzite plan of ZnO crystal structure. While in case of KBr and orange peel extract peaks there are some characteristics peaks for biomolecules such as polyphenols 841 cm^{-1}, 1404 cm^{-1}(c=c) and 1644 cm^{-1} (N-H). All these functional groups served as reducing as well as capping agents for the synthesis of green synthesized ZnO-NPs (Koupaei *et al.*, 2016).

4.1.3. X-Ray Diffraction (XRD) Spectroscopy

XRD is a non-detrimental technique that is used to extract information about crystallographic structure and chemical composition of the natural and man-made materials. Figure 4.3(a) shows the XRD pattern of chemically synthesized ZnO-NPs. In

depth analysis was performed to obtain x-ray diffraction data of synthesized ZnO-NPs in order to determine crystal and phase parameters. Highest intensity peak was obtained at 2θ=36.3º. ZnO-NPs sample was well crystallized as depicted by the strong intensity and sharpness of the peaks. Obtained peaks in accordance to crystal lattice is given below in the table:

2θ	31.8º	34.4º	36.3º	47.6º	56.6º	62.6º	68º	69.1º
Crystal Lattice	100	002	101	102	110	103	112	201

According to Debye– Scherrer equation average crystal size found was 50±5 nm by the FWHM (full width half maxima) of most dominant peak (101). Peaks obtained at (100), (002) and (101) confirmed the hexagonal wurtzite crystalline structure of the ZnO-NPs and relates to $P6_3$ mc of Hermann–Mauguin notation and C46v of Schoenflies notation. The hkl values were in complete harmony with standard card of ZnO powder samples (The International Centre for Diffraction Data, PA, USA; ICDD card No: 080-0075). These results were in complete agreement with previously reported by number of authors (Dinesh *et al.*, 2014, Kumari *et al.*, 2015, Khan *et al.*, 2016).

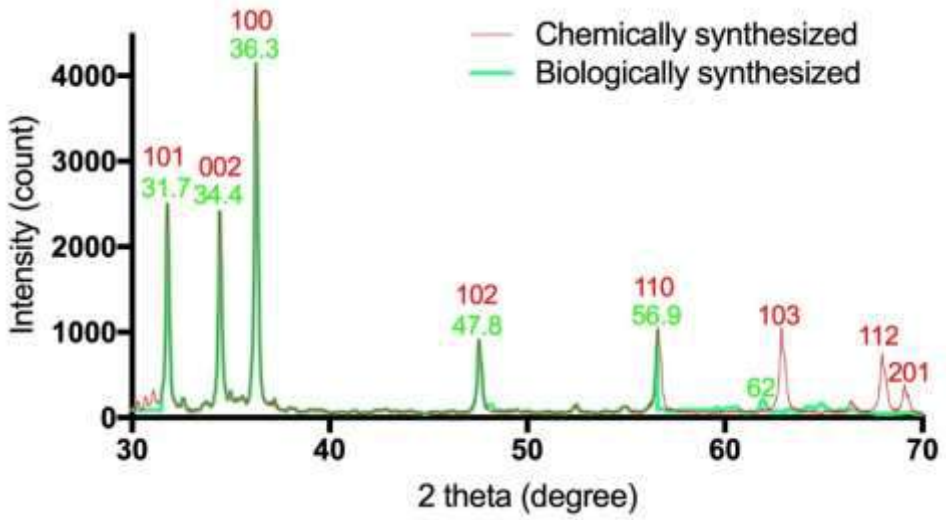

Figure 4:3: X-Ray Diffraction Patterns of Chemically and green synthesized ZnO-NPs

Obtained XRD pattern of green synthesized ZnO-NPs is shown in figure 4.3. Intense peeks were observed at 2θ=31.7º, 34.4º, 36.3º, 47.8º, 56.9º and 62º. These values can be indexed to (100), (002), (101), (102), (110) and (103). These XRD patterns were found to be in agreement with (JCPDS card no. 89–7102) (Ebadi *et al.*, 2019). Peaks obtained at (100), (002) and (101) confirmed the hexagonal wurtzite crystalline structure of the ZnO-NPs. Maximum intensity peak was found to be at 2θ=36.3º and average crystalline size calculated by Debye– Scherrer was 90±5 nm.

Chemically synthesized ZnO-NPs exhibited relatively small size which were coagulated in large clusters on a matrix of residual organic material from the reducing agents. However, green synthesized ZnO-NPs were annealed at 400 ºC which significantly increased the particles size. According to previous reports crystal size and shape depends upon annealing temperature and particles size tend to increase and larger particles are formed due to crystal growth. These larger crystals are attributed to fact that during annealing process thermal energy re-orients the particles and reduces the number of defects in grain boundries (Zapata *et al.*, 2009, Bala *et al.*, 2015, Thi *et al.*, 2020).

4.1.4. Scanning Transmission Electroscopy (SEM) and Energy Dispersive (X-ray) Spectra (EDX)

SEM was used to analyze the structure of ZnO-NPs. Figure 4.4 (a) has shown individual ZnO-NPs as well as NPs aggregates. It shows visible branched flower like structure and coincides the previously reported results (Kou *et al.*, 2012, Kazeminezhad *et al.*, 2013, Paino *et al.*, 2016). EDX spectra (figure 4.4 (b)) is tremendously dominated by ZnO peaks andgives detailed information of O 1s and Zn 2p.

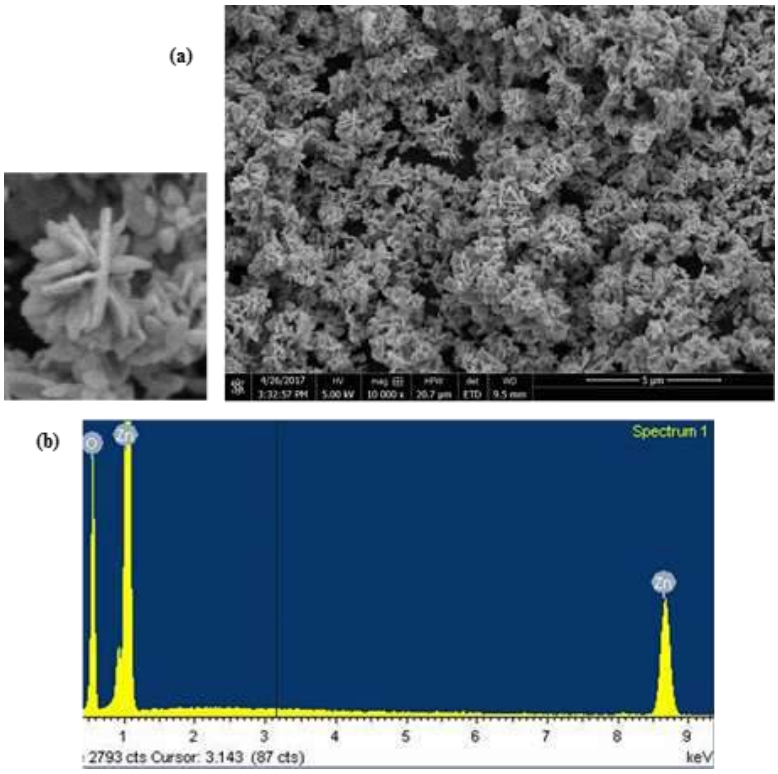

Figure 4:4: (a)Scanning Electron Micrograph of ZnO-NPs Showing Clear Flower Like Structure; (b) Energy dispersive (x-ray) Spectra of ZnO-NPs Showing Elemental Composition

Surface morphology of green synthesized ZnO-NPs was revealed by SEM as illustrated in figure 4.5 (a). It shows homogenous nature and equal distribution of the ZnO-NPs over the surface. Scanning electron micrograph has shown that ZnO-NPs synthesized by aqueous solution of orange peel have needle like structure.

Formation and chemical composition of green synthesized ZnO-NPs was confirmed by EDX spectra (figure 4.5(b)) that clearly confirmed the formation of ZnO-NPs. EDX spectra confirmed the chemical constituents of ZnO-NPs i.e Zn (57.15%) and O (42.85%). An extra peak was of carbon due to use of organic material that served as reducing and capping agent. Narrow width and strong intensity of ZnO peaks depicts the high crystallinity of ZnO-NPs. These findings were in close agreement with previously reported results with slight changes in chemical composition (Bala *et al.*, 2015).

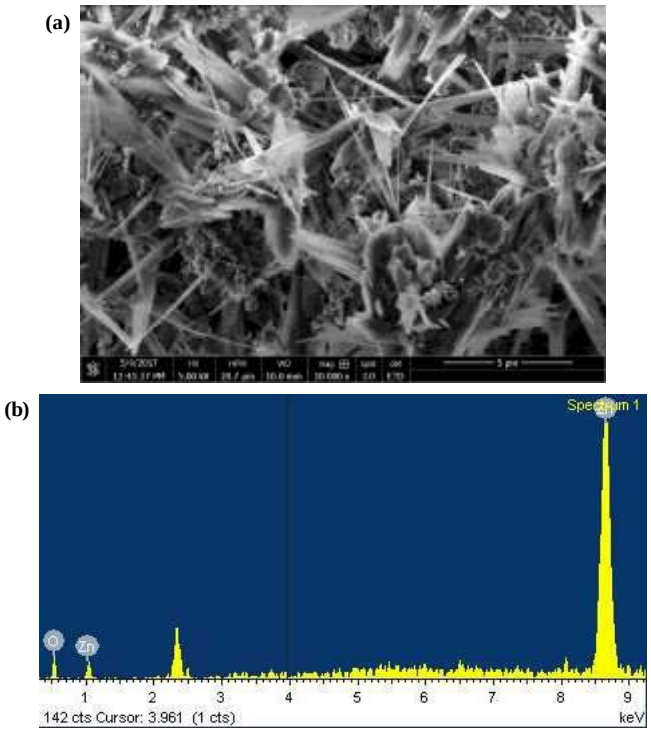

Figure 4:5: (a)Scanning Electron Micrograph of Green Synthesized ZnO-NPs Showing Clear Needle Like Structure; (b) Energy dispersive (x-ray) spectra of ZnO-NPs Showing Elemental Composition

4.2. Toxic effects of ZnO-NPs on physiological parameters of *T. aestivum*

Plants have to face environmental situations that can effect their growth and development during whole life cycle. When these conditions are harsh, growth dynamics of plants are influenced. Plants's metabolism is responsible for physiological regulation, defence responses and signaling. As a feedback to abiotic stress, biosynthesis, storage, transport and concentration of plant metabolities (both primary and secondary) get altered (Fraire-Velázquez & Balderas-Hernández, 2013). Food security in terms of nutritional deficiency due to abiotic stresses has become a major concern all over the world. In present study, attempt has been made to estimate the nutritional damage to *Triticum aestivum* (major cereal crop on earth) by ZnO-NPs stress (Zhang *et al.*, 2018).

4.2.1 Germination Index (GI)

Seed germination is the 1st indicator of the seed health, future plant vigor, and environmental conditions. It gives a measure of percentage and speed of seed germination (Javaid *et al.*, 2018). Environmental stress whether biotic or abiotic can affect rate of germination largely. In case of chemically synthesized ZnO-NPs GI was decreased upto 15% when concentration of ZnO-NPs was elevated from 0 to 400 mg/L (Figure 4.6 (a)). Sharp decrease in GI was observed when ZnO-NPs concentration was increased from 400 – 600 mg/L. There was a further decline in GI at ZnO-NPs concentration of 800 mg/L followed by a sharp drop to 45% of GI at ZnO-NPs concentration of 1000 mg/L. Statistically, GI was significantly effected by the ZnO-NPs at the $p<0.05$ level of condition [$F(5,12)= 570.05$, $p=0.000$]. Tukey's test (post hoc analysis) showed that mean (M) and standard daviation (SD) of GI of control experiment ($M=94.41, SD=0.532$) was significantly different from all other experimental concentrations.

Green synthesized ZnO-NPs have also influenced germination of *Triticum aestivum* seeds as determined on 5th day. Results have shown that germination rate has decreased from 96 % to 69 %. Which is yet an acceptable rate of germination. Decrease in toxicity is more pronounced from 800 mg/L to 1000 mg/L. One way ANOVA was applied to the conditions [$F(5,12)= 228$, $p=0.000$]. Whereas, post hoc analysis showed that GI of control experiment [(Mean=94, SD=1)] was significantly different from GI of all other experimental concentration. Although Lin and Xing has suggested the IC50 value of ZnO-NPs in some plant species. However, IC50 value for *Triticum aestivum* has not yet been reported (Lin & Xing, 2007).

Seed germination is a gauge of overall crop yield. In this study ZnO-NPs have shown an obvious negative impact on germination of *Triticum aestivum* seeds. However, there can be found a number of contradictory studies which states negative, neutral or even positive impact of different metal oxide NPs on seed germination of different plants. Zafar and coworkers studied the impact the ZnO-NPs on germination of *Brassica nigra* at a concentration range of 500-1500 mg/L and reported the adverse impact on seed germination and seedling growth. Afrayeem and Chaurasia investigated the seed germination response of *Capsicum annuum L* to ZnO-NPs. The two scientists showed that

seed germination was favored at lower concentration of NPs however germination was suppressed at higher concentrations (Afrayeem & Chaurasia, 2017).

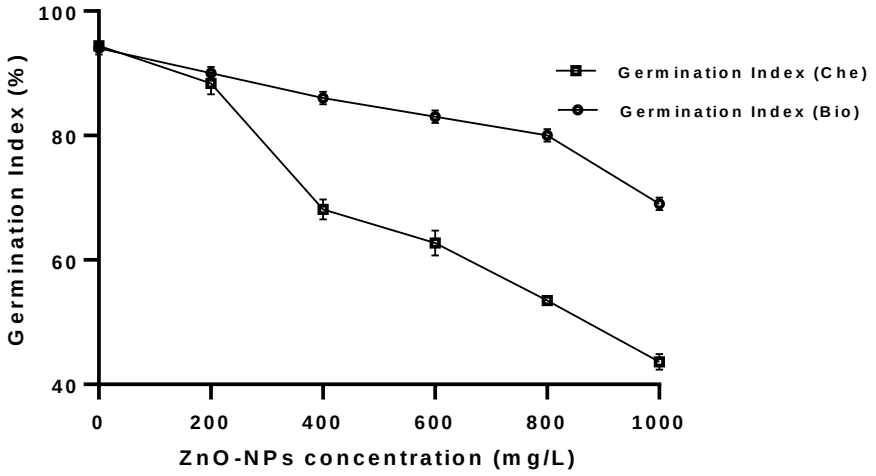

Figure 4:6: Germination Index as Influenced by the Chemically synthesized (Che) and Green/Biologically Synthesized (Bio) ZnO-NPs

4.2.2 Toxic effects of ZnO-NPs on Index of Tolerance (IT) and Stress Tolerance Index (STI)

Effect of ZnO-NPs was also evident from shoot and root length and biomass of the *Triticum aestivum.* Impact on root and shoot length was determined in terms of IT. While STI demonstrated variation in biomass as result of applied stress when compared to the control seedlings. There was a signification reduction in roots and shoots length of seedlings grown under ZnO-NPs stress as compared to the control ones as shown in Figure 4.7(a). IT was reduced from 100 to 37 and 42 for roots and shoots respectively. Stress tolerance index was dropped to 53 % and 52 % for shoots and roots respectively showing drastic damage to seedlings's biomass both in terms of length and weight. Statistical analysis used was one-way ANOVA at conditions [$F(5,12)= 1421.02$, $p=0.000$], [$F(5,12)= 1555.4$, $p=0.000$] for shoots and roots respectively. Post hoc results depicted that IT of all the experimental concentration was significantly reduced from the control group (Mean=100, SD=0, both for roots and shoots). For STI one way ANOVA was applied at the condition [$F(5,12)= 426.4$, $p=0.000$], [$F(5,12)= 1167.21$, $p=0.000$] for shoots and roots

respectively. Post hoc results depicted that stress applied by all the five concentration groups were considerably reduced as compare to control groups.

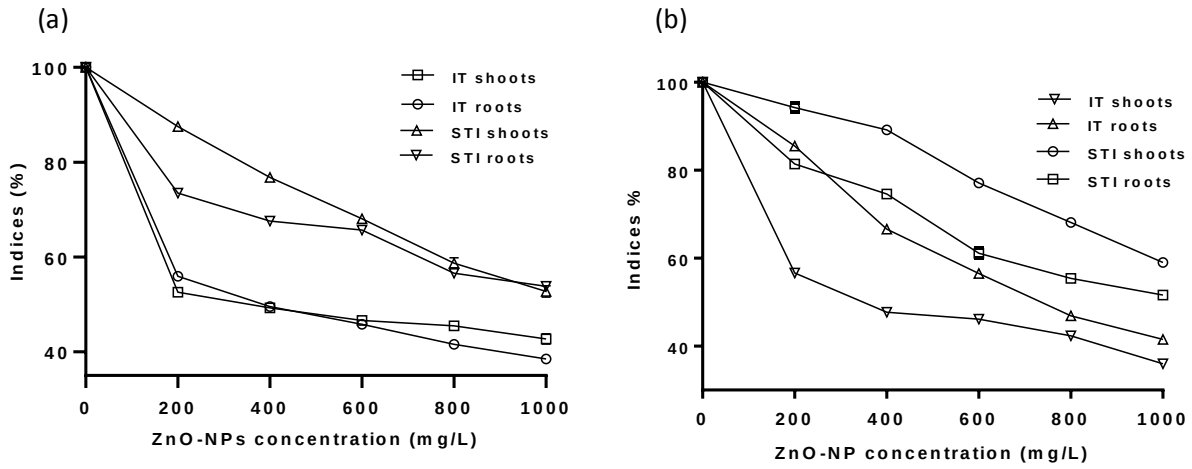

Figure 4:7: Index of Tolerance (IT) and Stress Tolerance Index (STI) as effected by (a) Chemically (b) Green Synthesized ZnO-NPs

Biologically synthesized ZnO-NPs also followed the same trend but at much drastic level as shown in figure 4.7(b). Index of tolerance for shoots drops to 36% and of roots deprived to 42 % as ZnO-NPs concentration was elevated from 0 to 1000 mg/L. One way ANOVA was applied to the conditions [F(5,12)=1338, p=0.000], [F(5,12)= 1554.6, p=0.000] for shoots and roots respectively and found to be lower than control group (Mean=100, SD=0, for both shoots and roots).

Stress tolerance index was decreased to 59 % and 51 % for shoots and roots as we moved along the concentration gradient (0-1000 mg/L). Statistcal analysis was applied to the conditions [F(5,12)= 759.48, p=0.000], [F(5,12)= 1608.79, p=0.000] for shoots and roots respectively. Whereas, post hoc analysis showed that values of control group (Mean=100, SD=0) was far greater than all applied concentrations.

4.2.3 Membrane Stability Index (MSI) & Electrolyte Leakage

Fluctuations in MSI with increase in concentration of ZnO-NPs has shown in figure 4.8 . It is clearly evident from the figure that MSI was increased when concentration of

ZnO-NPs was elevated from 0 mg/L to 600 mg/L. Then, there was a gradual decrease in MSI while increasing concentration from 600 mg/L to maximum (1000 mg/L). Trends of ion leakage from roots of *Triticum aestivum* seedling by increasing concentration of ZnO-NPs is shown in figure 4.8. Results are given in comparison to the control samples. Ion leakage kept on increasing with increasing concentration of the ZnO-NPs. As far as green synthesized ZnO-NPs were concerned pattern was a little different. It is clearly evident from the figure that MSI was increased when ZnO-NPs concentration was elevated from 0 mg/L to 800 mg/L. Then, there was a sharp dip in MSI while increasing concentration from maximum (1000 mg/L). Ion leakage from roots of *Triticum aestivum* seedling by increasing concentration of ZnO-NPs is shown in figure 4.7 as compared to the control plants.

Abiotic stresses cause modifications in cellular membrane. As a results its semipermiability is effected which leads to either perturbed function or total dysfunctionality. Exact mechanism of these modifications is not known but this aberration is easily determined as MSI and roots ion leakage. In most of plants cell membrane remains 1st target of abiotic stresses and their stability and integrity is major point of concern (Farooq & Azam, 2006).

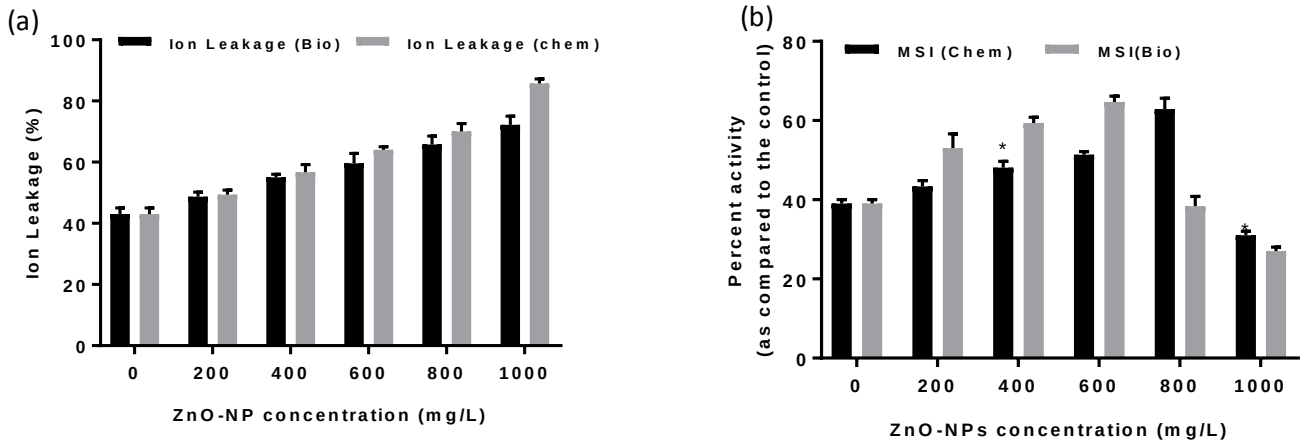

Figure 4:8: Effect of Chemically (Chem) and Biologically (Bio) Synthesized NP on Membrane Stability Index and Ions Leakage: Effect of Chemically (Chem) and Biologically (Bio) Synthesized NP on Membrane Stability Index and Ions Leakage

4.3. Quantitative analyses of Photosynthetic Pigment (Chlorophyll a, b, total chlorophyll and Carotenoids)

Figure 4.9 (a), (b) showed the impact of different concentration of ZnO-NPs stress on photosynthetic pigments (Chll a, b, total chll and carotenoids) of *Triticum aestivum*. As per experimental result (Figure 4.9(a)) photosynthetic pigments showed an increase when NP concentration was elevated from zero to 400 mg/L. From where there was a sharp decrease in amount of all four pigments. This decrease is more evident when ZnO-NPs concentration was elevated from 800 mg/L to 1000 mg/L. Thus, concentration of ZnO-NPs is inversely proportional to amount of photosynthetic pigments at higher concentrations of ZnO-NPs. Effect of green synthesized ZnO-NPs was also examined by varying concentration on photosynthetic pigments. Amount of chll a,b, total and carotenoids was even much lower than the control plants. Which exhibits an overall damage to plant health and vigor. Data was represented as a mean of three replicates standard daviation values (n=3). One was ANOVA was applied to the conditions [$F(5,12)= 984.4$, $p=0.000$]. [$F(5,12)=1090.87$, $p=0.000$]. [$F(5,12)= 3390$, $p=0.000$] and [$F(5,12)=464.26$, $p=0.000$] for chlorophyll a,b, total chlorophyll and carotenoids. Post hoc comparisons using Tukey's HSD showed that means of control groups [((Mean=2.12, SD=.047), (Mean=.5967, SD=.0220), (Mean=2.5, SD=.086) and (Mean=2.3, SD=.063) for chlorophyll a, b, total chlorophyll and carotenoids respectively] were significantly different from all experiment groups for chlorophyll a, b, total chlorophyll and carotenoids. Except the Chlorophyll b and carotenoids amount which was found to be insignificant at NP concentration 1000 mg/L ($p=.207$) and 800 mg/L ($p= 0.883$) respectively.

As far as green synthesized ZnO-NPs are concerned results (Figure 4.9 (b)) have shown that amount of all photosynthetic pigments. A gradual increase in concentration of chlorophyll b was observed from 0.74 - 2.68 mg/g of FW shoots, when NP conc. was elevated from 0 to 800 mg/L. then concentration was decreased to 1.78 mg/g of tissue weight which is still significantly higher than the control experiment (0.742 mg/g of tissue weight). Chlorophyll a concentration was increased from 2.30 to 4.10 mg/g FW with increment of ZnO-NPs stress from 0 to 400 mg/L. Which was dropped to 2.77 mg/g at 1000 mg/L ZnO-NPs, same trend was followed by total chlorophyll. Carotenoids followed

a different trend where carotenoids concentration kept on increasing with NP concentration 0-800 mg/L (2.58-4.63 mg/g of tissue FW). Then, it was dropped to 2.87 mg/g of tissue FW at 1000 mg/L of NP. Thus, NP stress has overall positive effect on the photosynthetic pigments. However, trend suggests that if concentration was further elevated beyond 1000 mg/L it will harm the pigments.

Abiotic stresses from environment can cause alteration in amount of chlorophyll a, b and carotenoids. A decrease in concentration of these phyto-chemical can cause serious damage to plant health and vigor (Sriprapat *et al.*, 2011, Shen *et al.*, 2017). It can be argued that changes in photosynthetic pigments were due to changes mostly depression in physiological parameters such as damage to roots (Zhu *et al.*, 2019). Chlorophyll a and b in harmony with carotenoids facilitates the transfer of electrons during photosystem I. When concentration of ZnO-NPs stress increases the threshold tolerance level of plant system, it may have disrupted the thylakoid membrane and disrupted the chloroplast envelop. Strong biotransformation of ZnO-NPs has earlier been reported in plants. Which can cause serious damage to photosynthetic pigments (Jin *et al.*, 2008, Ma *et al.*, 2015). Zhu and co-scientists have also documented the toxicity of ZnO-NPs in Hill's reactions (Zhu *et al.*, 2019). They may impose dysfunctionality to photosystem II as well as electron transfer. Elevated concentrations of metal ions can interrupt electron flow in PS II as a result free oxy radicals and excited chlorophyll is generated (Kato & Shimizu, 1985). One was ANOVA was applied to condition [$F(5,12)=32.54$, $p=0.000$]. [$F(5,12)=39.74$, $p=0.000$]. [$F(5,12)=121.69$, $p=0.000$], [$F(5,12)=23.97$, $p=0.000$] for chlorophyll a,b, total chlorophyll and carotenoids respectively. Amount of all photosynthetic pigments kept on increasing till 600 mg/L and then decreased exponentially. Tukey's HSD post hoc test results revealed that mean of control experiments [((Mean=2.3, SD=.33), Mean=.747, SD=.21), (Mean=2.8, SD=.159) and (Mean=2.5, SD=.366)] for chlorophyll a, b total chlorophyll and carotenoids respectively). However, there were few exceptions. Decrease in amount of chlorophyll a was found to be insignificant at NP concentration of 1000 mg/L. Also, effect of NP stress on carotenoid amount was found to be insignificant at ZnO-NPs concentration of 600,800 and 1000 mg/L ($p=.328,.979,1$ respectively) was significantly different from experimental groups.

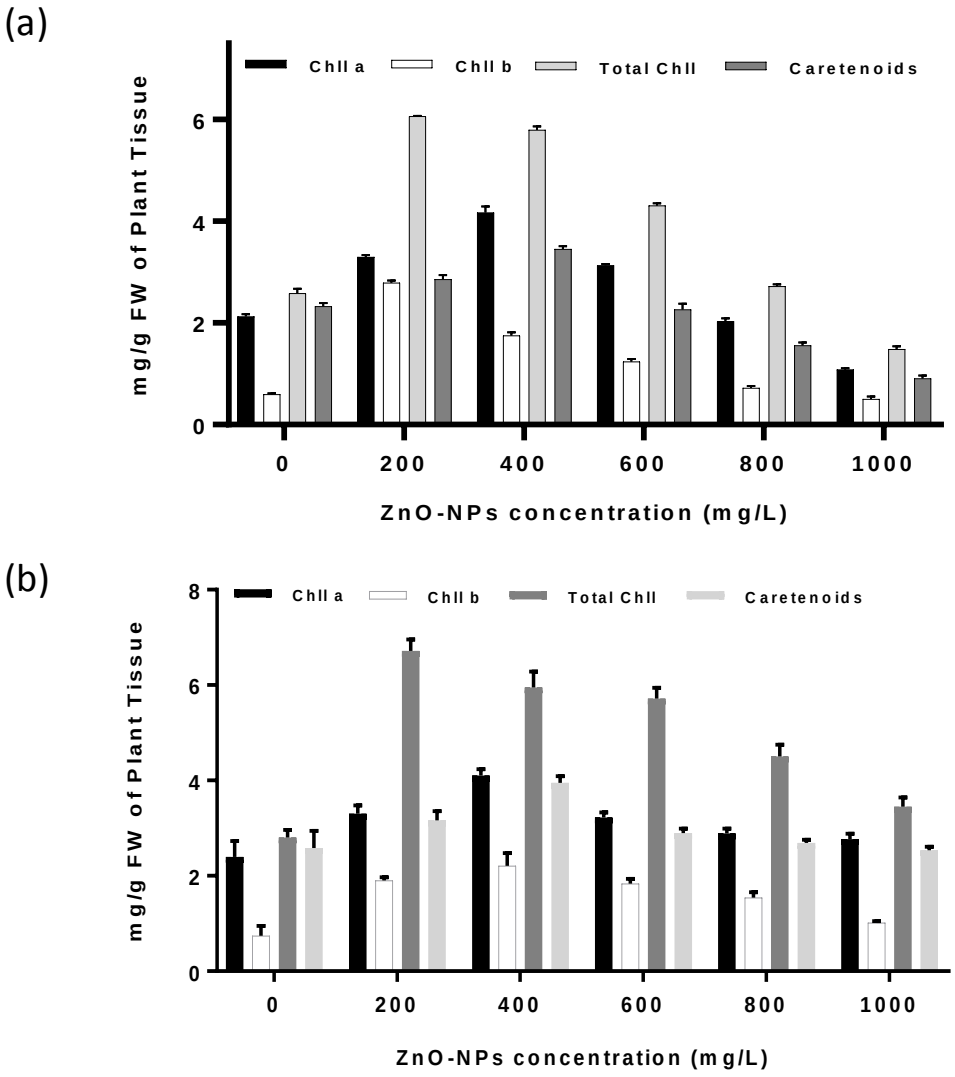

Figure 4:9: Photosynthetic Pigments as effect by (a) Chemically Synthesized NPs, (b) Green Synthesized NPs.

4.4. Estimation of Plant Stress Markers

Proline and lipid peroxidation was choosen as indicators of stress

4.4.1 Quantitative analyses of Proline

Proline is an important stress marker and an indicator of disturbed physiological functions. Proline content showed a steady increase as the concentration of ZnO-NPs was increased from zero to maximum as shown in figure 4.10.

In order to compare effect of different concentrations of ZnO-NPs stress on proline content of wheat. one way ANOVA was applied to the conditions [F(5,12)=3134.28, p=0.000], [F(5,12)=506.7, p=0.000] for shoots and roots respectively. Tukey's HSD test was used for comparison and indicated that mean score of the control group [((Mean=83.32, SD=.618), (Mean=72.02, SD=.47)] was significantly different from all the proline concentrations of all experimental groups.

Effect of biologically synthesized ZnO-NPs on Proline conc. was estimated in both roots and shoots. As depicted by the results (figure 4.10) proline concentration kept on increasing from 83.32 to 139 µmoles/g tissue, 72.02 to 106.7 µmoles/g tissue for roots and shoots respectively for all concentrations (0 - 1000 mg/L). Statistical analysis showed that there was a significant effect of green synthesized ZnO-NPs stress on amount of proline at condition [F(5,12)=3134.28, p=0.000] and [F(5,12)=506.7, p=0.000] for shoots and roots respectively at p=0.05. Post hoc comparison using Tukey's HSD test showed that mean score of control groups [((Mean = 83.32, SD = .618) and (Mean = 72.02, SD = .47)] were significantly different from all test concentrations of green synthesized ZnO-NPs.

ROS generated by the ZnO-NPs stress imparts oxidative injury to cellular structures and components, translating into metabolic disorders and ultimately to cell death (Mittler, 2002, Ahmad *et al.*, 2010, Gill & Tuteja, 2010, Hossain & Fujita, 2010). Plants have developed specified defence mechanism against these stresses. It produces water soluble non-toxic and lower molecular weight osmolytes (having conc. in millimoles). Proline is an important member of this family (Verslues & Sharma, 2010, Hayat *et al.*, 2012). Proline is a powerful antioxidant as well as an osmolyte. It efficiently scavenges the $OH^{\bullet}$ and $^1O_2$ and prevents the damage due to lipid peroxidation (Manivannan *et al.*, 2008, Verbruggen & Hermans, 2008, Martínez-Fernández *et al.*, 2016). Increased amount of proline can be accounted either for increased production or less degradation (Verbruggen & Hermans, 2008, Das & Roychoudhury, 2014).

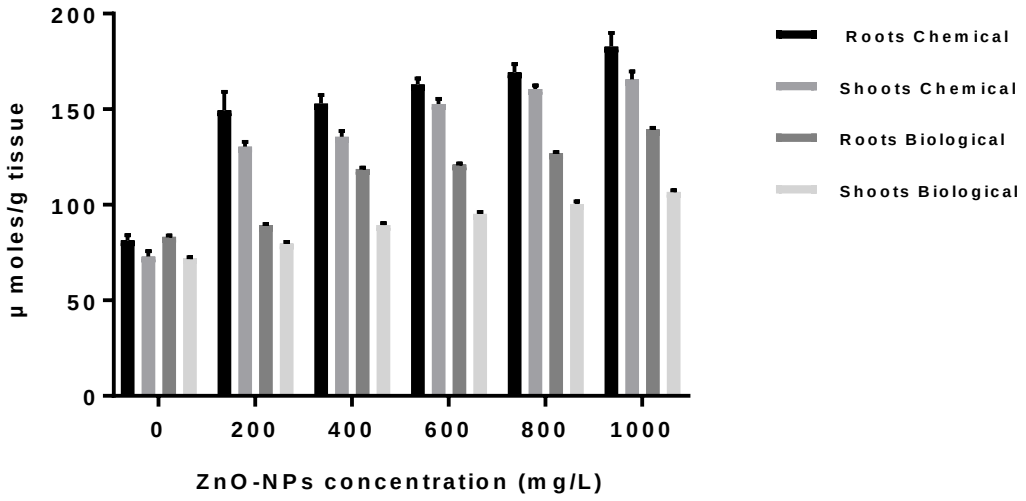

Figure 4:10: Elevated Amount of Proline(Plant Stress Marker) by Chemically and Green Synthesized NPs

4.4.2 Quantitative analyses of Lipid Peroxidase

Amount of Malondialdehyde (MDA) was estimated to measure extent of lipid peroxidation in both roots and shoots of the plants. Results had shown that there is a gradual increase in amount of MDA concentration as concentration of NP stress increases. 98% increase in amount of MDA was observed as NP concentration was raised from 0 to 1000 mg/L (Figure 4.11). Effect of chemically synthesized ZnO-NPs on lipid peroxidation were compared by one way ANOVA at condition of [F(5,12)=121, p=0.000], [F(5,12)=251, p=0.000] for roots and shoots respectively at significance level $p \leq 0.05$. Tukey's HSD post hoc comparison exhibited that means of all control groups with mean score of (Mean=9.5, SD=.703) and (Mean=8.8, SD=.3905) for shoots and roots respectively, were found to be significantly varied from lipid peroxidation values of all other experimental groups.

When oxidative stress go above plants threshold capacity, biological system undergoes dysfunctionality at normal cellular level as well as lipid-derived radicals are produced (Montillet *et al.*, 2005). These radicals can hurt DNA and protein (Sharma *et al.*, 2012). This phenomenon has most deleterious results in biological systems and membrane impairment acts as an indicator of the stress. Cell membranes are composed of poly

unsaturated fatty acids. Which becomes primary target of lipid peroxidation and damages the cell membrane oxidative outbrusts caused by reactive oxygen species are considered to be primary cause of membrane destruction via lipid peroxidation. This theoretical basis were confirmed by many Studies in past (Wang *et al.*, 2012, Cao & Rui, 2017, Spengler *et al.*, 2017). Results obtained in our experiment verified the above given narrative. A number of authors have investigated and reported elevated MDA levels in various plants by different metal oxide NPs (Ghosh *et al.*, 2010, Dimkpa *et al.*, 2012, Mohammadi *et al.*, 2013, Siddiqui *et al.*, 2014, Rao & Shekhawat, 2016, Mosa *et al.*, 2018). Present study has also investigated the effect of green synthesized NP on *Triticum aestivum* seedlings figure 4.11. MDA levels were found to be increasing gradually from 8.7011 nmol to 28.71 and from 8.8716-25.017 in shoots and roots respectively when NP concentration was increased from 0 to 1000 mg/L. Only one study was found that has reported the effect of biologically synthesized ZnO-NPs on Lathyrus *sativus* L . Root.

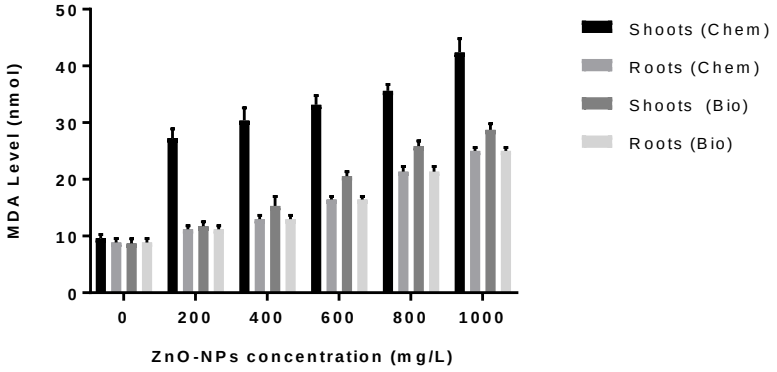

Figure 4:11: Enhanced MDA Level due to ZnO-NPs Stress

4.5. Quantitative analyses of Proteins

Protein content was analyzed in control samples and plants stressed by ZnO-NPs (200-1000mg/L). Protein content of seedling remains unaffected through all the ZnO-NPs concentrations (Figure 4.12). Results were confirmed by the statistical analysis using one way ANOVA applied to the conditions at [F(5,12)=000, p=.322], [F(5,12)= 6.054, p=.005] for shoots and roots respectively. Results showed that protein content remained unaltered by the ZnO-NPs stress at all experimental concentrations. Post hoc comparisons using

Tukay's HSD test showed that mean (Mean=0.0874, SD=0.00326) of control group were insignificantly different from all experimental groups.

Total soluble proteins were estimated to comprehend the impact of green synthesized ZnO-NPs on biochemical parameters of *Triticum aestivum*. Results of this estimation is shown in figure 4.12. It can be clearly seen that total amount of soluble proteins remains more or less same when NP concentration was increased from 0 to 1000 mg/l with an addition of 200 mg/L at each step. One way ANOVA was applied to conditions [F(5,12)= 20.301, p=000], [F(5,12)=6.054, p=0.005] for roots and shoots respectively. Post hoc comparison using Tukey HSD test established that mean (Mean=0.0875, SD=0.00060), (Mean=0.0744, SD=0.00085) for roots and shoots respectively were indifferent from test concentartions except at 200 mg/L (mean=0.085, SD=0.00030) and showed elevated amount as compared to control group.

By-products of oxidative stresses and ROS generates covalent modifications, this phenomenon is called protein oxidation. ROS above threshold levels can cause site-specific modifications of amino acids, peptide chain fragmentation, altered electric charges, aggregation of cross-linked products and hence chances of proteolysis increases. In such conditions, amount of carbonylated proteins increases and is considered as protein oxidation marker. Thiol and sulfur groups are highly susceptible to ROS attack. Thus, overall amount of the proteins remains almost same but large amount of proteins denatures and fails to perform their normal function. Some scientists have worked with plant proteomics and found out that Ag^{+2} modified 28 proteins important to various biological and physiological parameters like signaling, Ca^{+2} regulations, damages to DNA, RNA, and stress tolerance etc., which finally lead to cell death and apoptosis (Møller & Kristensen, 2004, Hancock *et al.*, 2006, Sharma *et al.*, 2012, Mirzajani *et al.*, 2014, Hossain *et al.*, 2016). Protein composition and concentration is a detrimental factor that measures the quality of the crop. Different types of abiotic stresses such as drought, heat, CO_2, salt etc have different impact on protein content of *Triticum aestivum* (Blumenthal *et al.*, 1996, Wardlaw *et al.*, 2002, Gooding *et al.*, 2003, Halford *et al.*, 2015). Same is the case with NP stress. Although data is incomplete as far as NP stress in plants is considered. However,

available studies have shown variable and in some cases contradictory results in different plants models (Hajra & Mondal, 2017)

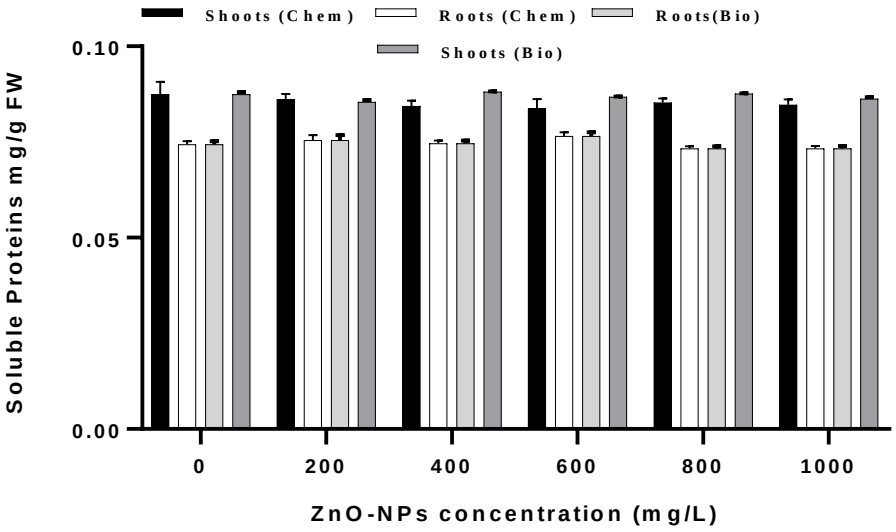

Figure 4:12: Effect of Chemically and Biologically synthesized ZnO-NPs on Protein Content of *Triticum aestivum*

4.6. Quantitative Analyses of Carbohydrates (Soluble Sugars, Reducing and Non-Reducing Sugars)

In this experiment, effect of ZnO-NPs (chemical and biological) stress was estimated on sugar conten of (total sugars, non-reducing and reducing) wheat. According to our results, total suguar content remain statistically unaltered till the NP concentration was upraised from 0 to 400 mg/L (figure 4.13). For comparison of ZnO-NPs effect on total sugar one way ANOVA was applied to the condition [F(5,12)=283.017, p=.000], [F(5,12)=121.386, p=.000] for shots and roots respectively. Total sugar content remained unaffected also, Tukey's HSD test was used for post hoc comparison. Which showed that mean of control group (Mean=48.53, SD=0.6178), (Mean= 30.080, SD= 0.7921) remained unchanged from test concentrations of ZnO-NPs. Same pattern was followed by the *T. aestivum* stressed by the green synthesized ZnO-NPs. Where one way ANOVA was applied to the condition [F(5,12)= 47.05, p=.000], [F(5,12)=156.089, p=.000] for roots

and shoots respectively to compare effect of green synthesized ZnO-NPs on *T. aestivum*. Where, according to post hoc comparison using Tukey's test of mean score of control [(Mean=48.18, SD=0.4084), (Mean=30.83, SD=0.7921) for shoots and roots respectively) remained unchanged from all other test concentrations

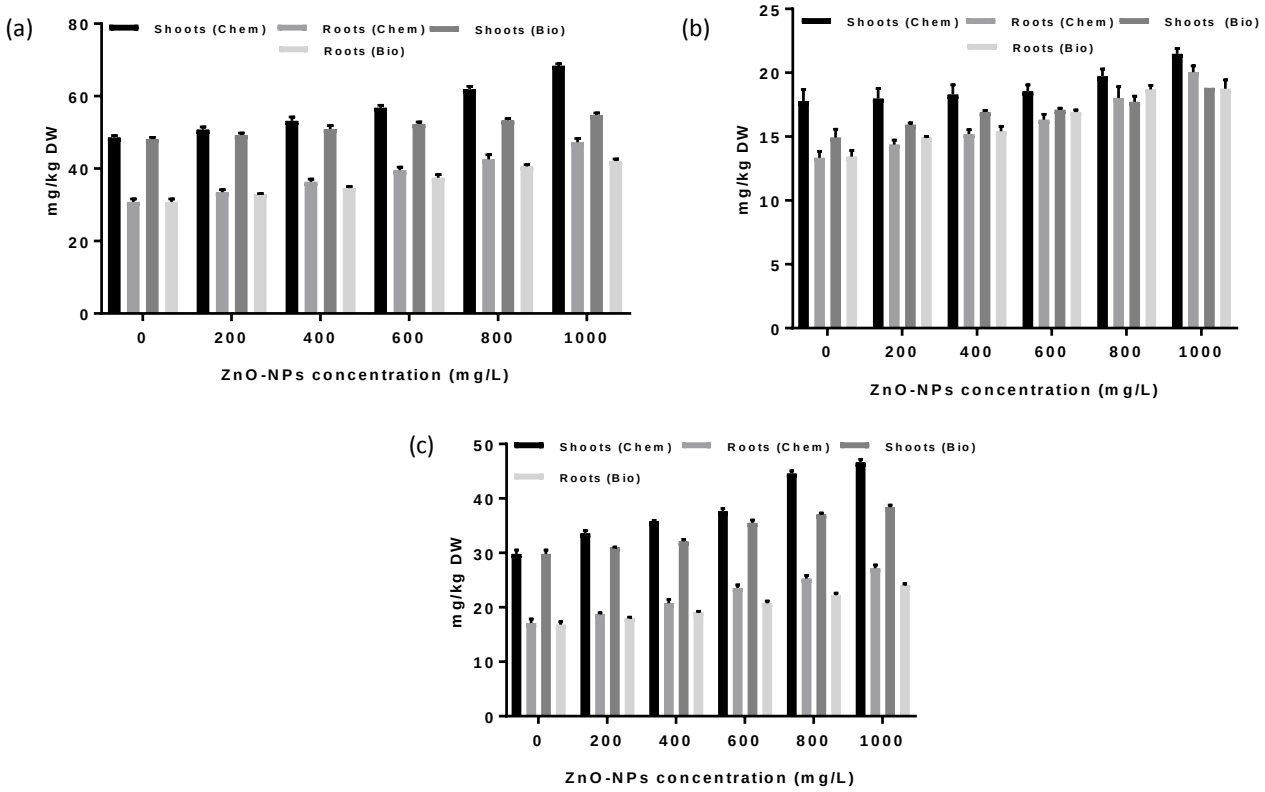

Figure 4.13: Effect of Chemically and Biologically synthesized NPs on (a)Total Sugar, (b) Non-Reducing, (c)reducing sugar Content of *Triticum aestivum*

Same pattern was followed in case reducing and non-reducing sugars as stressed by chemically and biologically synthesized NPs i.e there was a steady incease in amount of non reducing (figure 4.13 (b)) and reducing sugars (figure 4:13(c)) as moved along increasing concentration gradient. Similar results were observed and reported by the Mukharjee and co-workers. Who testified the toxicity of ZnO-NPs in green peas and pea plants (Mukherjee *et al.*, 2016). For reducing sugars stressed by the chemically synthesized NP one way ANOVA was applied to the conditions [F(5,12)=12.41, p=.000], [F(5,12)= 64.22, p=.000] to comprehend the toxic effect. For green synthesized ZnO-NPs ANOVA

conditions applied were [F(5,12)=83.74, p=.000] and [F(5,12) = 83.74, p = .000] for shoots and roots respectively. For post hoc comparison mean ± SD of control groups (Mean=14.91, SD=0.657) and (Mean=13.43, SD=0.470) shoots and roors was found to be significantly different from all other experimental concentrations. As far as green synthesized ZnO-NPs are concerned ANOVA conditions used were [F(5,12)=196.91, p= .000] and [F(5,12)=180.045, p=.000] for shootsand roots respectively. Also, (Mean=29.82, SD=0.706) and (Mean=16.83, SD=0.516) were used for post hoc comparison and found to be significantly different from experimental concentrations.

Tukey's test using post hoc experiment showed that mean scores of control groups [(Mean=17.77, SD= 0.9326) and (Mean=13.33, SD=0.506)] were not varied significantly from test concentrations of ZnO-NPs.

Majorly, there are three types of water soluble sugars named as; disaccharides (trehalose and sugars), fructans and oligosaccharides (raffinose family). All these three types are involved in plant stressed management (Keunen *et al.*, 2013). They serve as building blocks and energy providers in plants. When plant growth is inhibited by he mild abiotic stress, production of above three mention sugars along with photosynthesis still take place. During stress conditions, increased proline content along with higher levels of sugar maintain antoxident protection in many plants. Even in case of extreme conditions such as complete dehydration, plants resurrection occurs through sugar accumulation. Polysaccrides and glucose protect the cell membrane which is pre-requisite to sustain life (Camejo *et al.*, 2012). Its also worthwhile to mention that relationship of ROS and sugars is already been well-established. Magnitude of ROS production can be influenced by the sugar levels in mitochondria, chloroplast and peroxisomes. In initial stage of oxidative stress, lower molecular weight antioxidents play a vital role and sugars like galactinol, RFOs, disaccharides, sugar alcohols and fructans are verified members of anti-oxidant defence army (Nishizawa *et al.*, 2008).

4.7. Quantitative Analyses of Phenols and Flavnoids

Amount of phenols was increased when ZnO-NPs stress was increased up to 400 mg/L (Figure 4.14 and 4.15 respectively) following a sharp dip which was significantly

lower than control ones. While in case of green synthesized NPs phenolic content kept on increasing till NP concentration of 400 mg/L and then started decreasing. However, this depreciation is much less pronounced than the chemically synthesized NPs and phenolic content at maximum concentration of ZnO-NPs was still higher than the control plants. This decrease is phenolic content in both types of experiment (Chemically and green synthesized ZnO-NPs) may be due to disruption in cell signalizing pathway or damage at molecular levels. One way ANOVA was applied as statistical test to compare effect of experimental concentrations of chemically synthesized ZnO-NPs on phenolic content of *Triticum aestivum* at conditions [F(5,12)=569.14, p=.000] and [F(5,12)=189.06, p=.000] for roots and shoots respectively. Mean scores of control group [(Mean=.3475, SD=0.007) and (Mean=.2284, SD=0.0084) for roots and shoots respectively] were significantly different from experimental concentrations of ZnO-NPs. One-way ANOVA conditions applied to the green synthesized ZnO-NPs were [F(5,12)=186.28, p=.000] and [F(5,12)= 73.73, p=.000] for shoots and roots respectively. Post hoc comparison using Tukey's HSD test showed that mean±SD [(Mean=.3398, SD=0.0054) and (Mean=.2043, SD=0.0039)] were significantly different from experimental concentrations.

In case of flavonoids one way ANOVA conditions utilized were [F(5,12)=18.64, p=.03] and [F(5,12)=18.64, p=.000] for roots and shoots respectively. In Tukey's test mean score (Mean=25.79, SD=1.25) of control experiment of shoots showed that amount of flavonoid was significantly increased at test concentration of 400 mg/L with mean score of (mean=28.53, SD=.6353) (p=0.002) and was significantly reduced at ZnO-NPs concentration of 1000 mg/L with mean score of (mean=21.81, SD=1.280) (p=0.047).

Penolic content showed a varied trend as its amount kept on increasing when amount of NPs stress was elevated from 200 to 800 mg/L and then a slight deacrease was observed on further increment of ZnO-NPs stress from 800 to 1000 mg/L. This pattern was followed by both chemical and green synthesized NPs in both plant parts i.e shoots and roots. For chemically synthesized ZnO-NPs ANOVA conditions were [F(5,12)=18.64, p=.000], [F(5,12)=1.69, p=.211] and for biologically synthesized NPs there were [F(5,12)=124.98, p=.000], [F(5,12)=1.69, p=.211] for shoots and roots respectively. Mean±SD for post comparison were (Mean=25.79, SD=1.25) and (Mean=25.16,

SD=.18037) for shoots and roots respectively for both chemically and biologically synthesized NPs.

Carotenoids, phenols, flavonoids and proline are components of non-enzymatic defense system of plants (Gill & Tuteja, 2010, Miller *et al.*, 2010, Gill *et al.*, 2011). . Phenols and flavonoids both have antioxidant properties by hydrogen atoms or electrons or by scavenging ROS directly (Arora *et al.*, 2000). These are aromatics compounds that holds atleast one aromatic ring. Flavonoids and phenolics compunds are generally known as the largest group of phytochemical having antioxidant properties from plants origion (Wang *et al.*, 2016, Meng *et al.*, 2017, Andreu *et al.*, 2018, Zahoor *et al.*, 2018). These chemicals perform a variety of functions such as phytoalexins (Fawe *et al.*, 1998, BAGGA & STRANEY, 2000), detoxify agents (Yamasaki *et al.*, 1997, Jansen *et al.*, 2001, Michalak, 2006), signaling molecules (Peer & Murphy, 2006), germination stimulant (Morandi *et al.*, 1992, BAGGA & STRANEY, 2000), UV filters (Delgado-Vargas & Paredes-López, 2002, Lanot & Morris, 2005), offer resistance during drought (Hernández *et al.*, 2004), attract the pollinators (Iwashina, 2003) etc. It can scavenge different ROS in chloroplast. Phenolic compounds can inactivate the heavy metal stress through Fenton like reaction by chelating it. However, antioxidant activity of both flavonoids and phenols depends upon their chemical structure (Shimoji & Yamasaki, 2005).

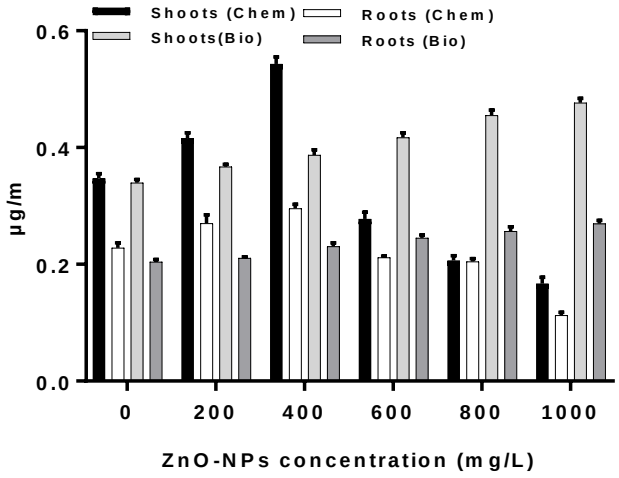

Figure 4.14: Phenolic Content as Effected by Biologically and Chemically synthesized ZnO-NPs

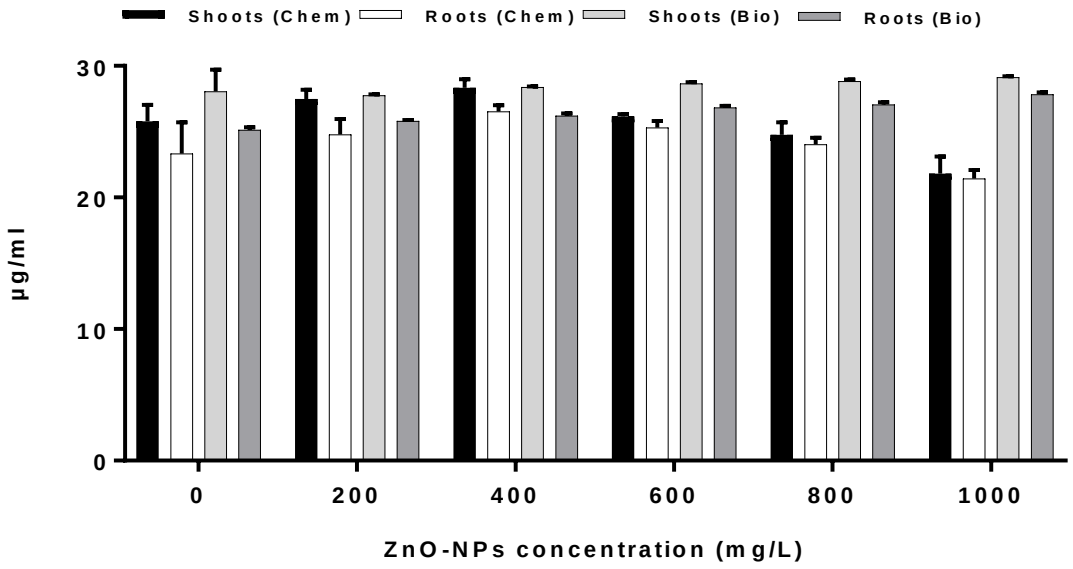

Figure 4.15: Flavonoid Content in *Triticum aestivum* as Effected by Biologically and chemically synthesized ZnO-NPs

4.8. Quantitative Analyses of Antioxidant Enzymes – As Effected by Chemically Synthesized ZnO-NPs

Antioxidant enzymes are 2nd line of defense of plants against toxic species. These offer resistance to injurious substances which are responsible for the production of ROS (Choudhury *et al.*, 2013). When plants are exposed to toxic substances level of antioxidants elevates. However, when concentration of pollutants increases than threshold levels this defense mechanism may also collapse. In order to discover the defense mechanisms of *Triticum aestivum* seedlings, activities of catalase (CAT), superoxide dismutase (SOD) and ascorbate peroxidase (APX) were estimated in roots and seedlings. SOD activities were raised as compare to control when plants were exposed to NPs and its concentration was increased from 200-1000 mg/L (Figure 4:16). One way ANOVA was used as statistical analysis to understand the effect of different concentrations of chemically synthesized ZnO-NPs on SOD acticity of Tritium *Aestivum.* Conditions used for the test were [F(5,12)=507.25, p=.000] and [F(5,12)=6072, p=.000] for shoots and roots respectively was used. Post hoc test for comparing means was used Tukey HSD test and it established that mean score of control groups [(Mean=1.02, SD=0.00513) and (Mean=.9950,

SD=0.0030) for shoots and roots respectively] were significantly varied from SOD activity of all test concentrations of ZnO-NPs.

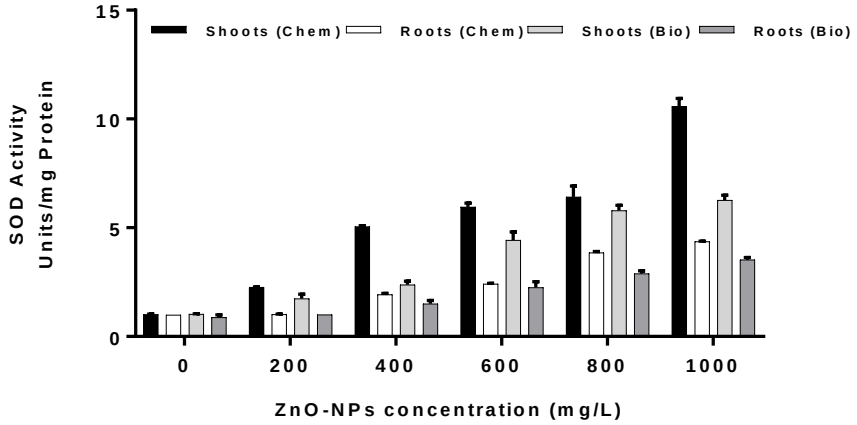

Figure 4.16 : SOD activity as Effected by Chemically and Green Synthesized ZnO-NPs

CAT (Figure 4.17) and APX (Figure 4.18) scavenge H_2O_2 as produced by the superoxide dismutase. Activities of both CAT and APX were elevated when NP concentration was increased to 600 mg/L and then collapsed drastically moving up to 1000 mg/L (Figure 4.16 & 4.17 respectively). One way ANOVA was applied to the conditions [F(5,12)= 8.759, p=.001] and [F(5,12)= 8.759, p=.001] for shoots and roots. Results showed that CAT activity was significantly reduced at 200 mg/L and 400 mg/L and then CAT activity was significantly reduced at 600 mg/L, 800 mg/L and 1000 mg/L. Means of control groups [(Mean=.0058, SD=0.00076) and (Mean=.0058, SD=0.00076) for shoots and roots] were significantly different from all calculated CAT activities of different ZnO-NPs concentrations.

For chemically synthesized ZnO-NPs statistical analysis applied was one way ANOVA at conditions [F(5,12)=1140.63, p=.000] and [F(5,12)=150.7, p=.000] for shoots and roots respectively. Tukey's test was used as post hoc comparison of mean±SD [(Mean=.1197, SD=0.00153) and (Mean=.0987, SD=0.00153)] of control groups to the experimentenal concentrations and significant increase was onserved.

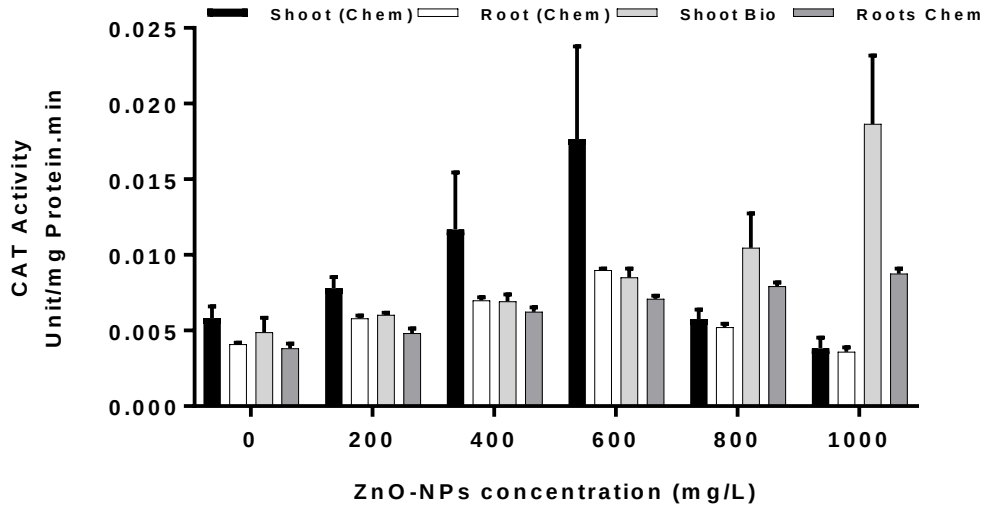

Figure 4:17 CAT activity as Effected by Chemically and Green Synthesized ZnO-NPs

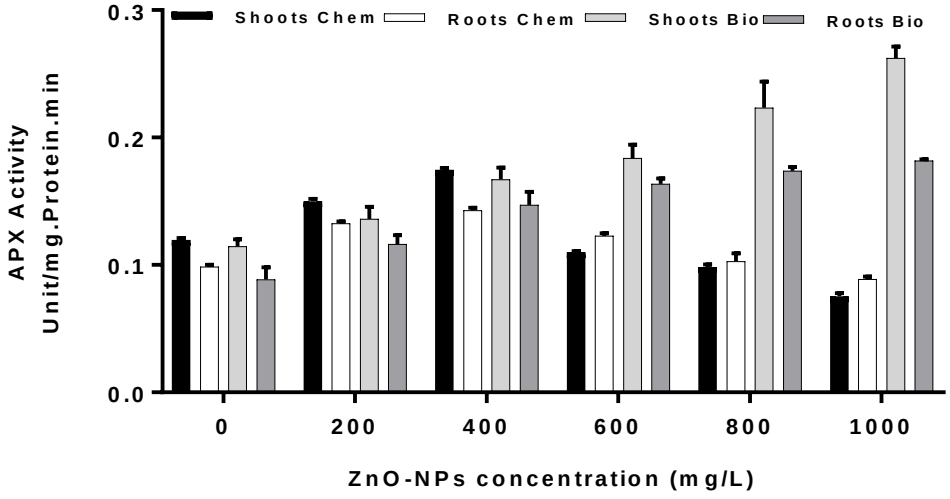

Figure 4:18 APX activity as Effected by Chemically and Green Synthesized ZnO-NPs

SOD is a metallo enzyme present in all aerobic organisms. It stands as first line of security against ROS stress forced by biotic stress. SOD dismutase $O_2^{\bullet -}$ into H_2O_2 and O_2. Absence of $OH^{\bullet}$ is assured by Haber-Weiss reaction (Mittler, Boguszewska *et al.*, 2010, Das & Roychoudhury, 2014). They are present in mitochondria (Mn-SOD), chloroplast

(Fe-SOD), cytosol, chloroplast and peroxisomes (Cu/Zn SOD). SOD is upregulated in case of abiotic stress. In plants, SOD genes are controlled by tissue-specific and environmental signals. However, when stress increases the threshold level, SOD mechanism may disrupt and SOD level decreases as observed in present study (Menezes-Benavente *et al.*, 2004, Kumar *et al.*, 2013).

H_2O_2 produced by SOD is scavenged by the catalase (CAT). Concentration of CAT increases as the amount of H_2O_2 increases by the ZnO-NPs stress as evident by the results. But CAT activity ceases at higher concentration in presence of supersaturated H_2O_2. Plant defense mechanism by antioxidant enzymes can damaged or even collapsed when abiotic stress surpasses the plant endurance. In present experiment decreased activities of APX and CAT at higher concentration of NP stress (Figure 3.6 b & c) depicts the sub-cellular damages to the plant cell. Presented results are in accordance with the interpretation of Zho and his coworkers (Sun *et al.*, 2018, Zhu *et al.*, 2019). For CAT activity two tailed coefficient of correlation found was 0.004 and -0.056. APX performs the same function as CAT but at different location (cytosol and chloroplast) and is an integral part of ascorbate-glutathione (ASC-GSH) cycle.

$$H2O2 + AA \rightarrow 2H2O + DHA$$

4.9. Quantitative Analyses of Antioxidant Enzymes – As Effected by Biologically Synthesized ZnO-NPs

In normal conditions, ROS are important constituents of cell signaling pathways. However, under special circumstances amount of ROS increases tolerance levels of plant system. And it causes oxidative burst which eventually leads to cell death. In plants, antioxidant enzymes serve as 2^{nd} line of defense after non-enzymatic shield. In case of ZnO-NPs superoxide dismutase (SOD, catalase (CAT), and ascorbate peroxidase (APX) are most important ones (Tripathi *et al.*, 2017).

SOD has two iso-forms Mn SOD and Cu-Zn SOD. These isoforms are located in cytosol and mitochondria respectively (Scandalios, 2005). SOD serves as 1^{st} line of protection against ROS stress and neutralizes $O_2^{\bullet -}$ into H_2O_2 and O_2 (Mittler, Boguszewska *et al.*, 2010). In present investigation, results have shown a steady increase

in SOD activity with increasing NP conc. from 0 to 1000 mg/L in both roots and shoots (figure 4.16). One way ANOVA was used as statistical tool to compare effect of different ZnO-NPs concentrations on SOD activity in shoots and roots of wheat at conditions [$F(5,12)=273.28$, $p=.000$] and [$F(5,12)=158.047$ $p=.000$]. Tukey's HSD test was used to compare means of control groups [(Mean=1.03, SD=0.0086) and (Mean=.8850, SD=0.1037) for shoots and roots] with experimental groups and found to be significantly different from test groups.

CAT is widely distributed enzymes in cell with high concentrations found in mitochondria and peroxisomes. It produced H_2O from H_2O_2. Which is produced by the SOD (Boguszewska *et al.,* 2010). As amount of SOD increase to deal with increasing concentration of ROS, more H_2O_2 is produced. Which is responded with increased concentration of CAT until there is a supersaturated environment of H_2O_2. CAT followed the same trend as of SOD but increase in activity was more prominent when green ZnO-NPs concentration was elevated from 800 to 1000 mg/L (Figure 4.17). Statistical conditions were same for CAT and APX activity of green synthesized ZnO-NPs both in shoots and roots as were employed in case of chemically synthesized ZnO-NPs and significant increase in CAT and APX activities were noted.

APX is involved in complex ascorbate-glutathione cycle (AsA-GSH cycle) i.e a complicated system of redox homeostasis to control the over production of ROS. Like CAT it also neutralizes the H_2O_2 generated by SOD but at a much different scale (Rico *et al.,* 2015).

4.10. Cytotoxicity Study - Chromosomal Aberration

Plants serve as a 1st tier analysis system to detect the chemical mutagens in the environment. Utilizing plant material – most often pollen cells and primary root tips is one of the most reliable, inexpensive or oldest method available for detection of abiotic pollutants in environment. These chromosomal aberration can directly be correlated to taxonomical and morphological changes, mutations, fertility-sterility relation and other characteristics. Chromosomal aberrations serves as the primary objective to confirm wether a substance is clastogen (able to break chromosome). At the same time it identifies

as turbagens (chemicals that causes mitotic disturbances, not necessarily damage DNA). Thus, cytotoxic study serves as an excellent monitoring system and also confirm the presence of hazardous materials in environment (Olorunfemi *et al.*, 2012). A detailed cytotoxic study was carried out. In which experimental concentration gradient was tested on primary root tips of *T. aestivum* for mitotic index and chromosomal aberrations. Results obtained are discussed as follows:

4.10.1 Mitotic Index

In plant cells, growth takes place by two dynamic yet strictly control processes – i. cell proliferation, ii. Followed by cell expension. Light microscopic inspection of the *T. aestivum* root squehses showed that ZnO-NP stress reduced the mitotic index to great extent as compared to control experiment. *T. aestivum* grains from all the ZnO-NPs concentration groups showed germination percentages. No. of total cells observed ranged from 1793 ± 198 to 1903 ± 106. No. of dividing cells in control experiment were 1098 ± 54. Which kept on decreasing as chemically synthesized ZnO nano-flower's concentration was elevated from 200 mg/L to 1000 mg/L and had values of 1010 ± 35, 925 ± 42, 875 ± 59,702 ± 32, 534 ± 28, respectively as shown in table 4.1.

Genotoxicity of biologically prepared ZnO-NPs was also assessed in root tips of *T. Avesticum* in terms of mitotic index and chromosomal aberrations. Normal structural and morphological parameters were shown by the chromosomes of root tips belonging to control group. However, as concentration of ZnO-NP stress was increased from 0 to 1000 mg/L mitotic index was gradually decreased with $r = -0.987$ at $p<0.01$ significance level. Highest Mitotic index was found for the control group i.e. 62 % and was decreased upto 20 % and dropped down to 43 %. Statistical analysis showed a strong direct relationship between ZnO-NPs concentration and occurrence of abnormal cells. Number of cells at different stages of cell division were also counted and given in table:4.2 and results showed that with increase in ZnO-NPs concentration, cells in different mitotic stages kept on decreasing as given in table number table:4.2.

However, when we compared the genotoxicity of chemically and green synthesized ZnO-NPs. Genotoxic effect of chemically synthesized NPs were found more strong and

pronounced. Mitotic index found at 200 mg/L was 52 % and 56 % for chemically and biologically synthesized NPs. Which kept on depreciating for ZnO-NPs synthesized by two techniques and ultimately fell on 28% and 43% respectively atZnO-NPs concentration of 1000 mg/L. Percent aberration for chemically synthesized ZnO-NPs was 13.26 % at 200 mg/L which ended up to 81.83 % at NP concentration of 1000 mg/L.

As far as, green synthesized ZnO-NPs were concerned percent aberration at 200 mg/L was 10.6 % and elevated upto 54.60 % at 1000 mg/L, significantly lower than the chemically synthesized ZnO-NPs. Scientists have reported that rate of cell division is a key aspect in defining the rate of plant growth. Studies have proved that mitotic index changes significantly when environmental conditions changes particularly in case of oxidative brust (Doonan, 1996). Similar outcomes were conveyed by Hajra and Mondal (2017) , who stated drastic decline in mitotic index. Mitotic index in pycnotic cells was decreased as stressed by ZnO-NPs (Kumari *et al.*, 2011, Hajra & Mondal, 2017)

Table 4.1: (a) Effect of ZnO Nano-flowers synthesized by co-precipitation on Mitotic Index of *Triticum aestivum*

ZnO-NPs Conc. mg/mL	No. of cell Observed	No. of Dividing Cells	Phases of Cell Division				Mitotic Index (MI)	No. of Abnormal Cells	Percent Aberration
			Prophase	Metaphase	Anaphase	Telophase			
0	1850±120	1098± 54	595±12	250±25	187±32	105±14	59.35	-	
200	1793±198	1010±35	482±15	217±13	167±23	109±9	56.33	134	13.26
400	1898±106	925±42	427±31	186±27	127±17	96±42	48.73	295	31.89
600	1853±153	875±59	396±29	169±21	110±10	87±16	47.22	456	52.11
800	1903±106	702±32	327±26	145±24	97±10	62±19	36.88	545	77.63
1000	1867±145	534±28	277±10	124±13	91±23	52±12	28.60	437	81.83

Table 4.2: Mitotic Index of *Triticum aestivum* as Effect by Green Synthesized ZnO-NPs

ZnO-NPs Conc. mg/mL	No. of cell Observed	No. of Dividing cell	Phases of Cell Division				Mitotic Index (MI)	No. of Abnormal Cells	Percent Aberration
			Prophase	Metaphase	Anaphase	Telopjase			
0	1843±127	1104±50	650±75	250±23	136±15	110±34	62%	____	____
200	1779±290	1056±34	595±62	237±21	120±8	98±26	59%	110±42	10.4%
400	1889±111	1025±25	478±57	198±19	101±11	86±23	54%	157±36	15.3%
600	1850±120	970±16	417±43	157±16	89±7	72±17	52%	258±27	26%
800	1929±76	919±42	376±36	117±13	71±9	59±9	49%	376±19	40.9%
1000	1790±210	782±23	319±26	98±9	60±10	48±14	43%	427±15	54.60%

4.10.2 Chromosomal Aberrations as Induced by ZnO-NPs Stress

A lot of research has shown that nanotechnology has ability to revolutionize the agriculture – ranging from nano-fertilizers to nano-pesticide and nano-material based packaging materials. Inspite of potential benefits, a lot of issues have been over looked. Public concerns are raising about the nano-pollutants in the environment as multiple studies have described the occurrence of NPs in soil, water and even in food materials (Nagaonkar *et al.*, 2015). Effect of ZnO nano-flowers and green synthesized ZnO-NPs was studied and reported in the form of table and figures:

Cells were studied in root tip squeshes of wheat. No abnormal cells were found in control group and normal stages of mitosis are shown in figure 4.18. However, remaining all concentrations had abnormal cell ranging from 134±14, 295±26, 456±16, 545±21, 637±19 as concentration was elevated from 200 to 1000 mg/L. Percent aberration were calculated for and found to be 13.26 (200 mg/L), 31.89 (400 mg/L), 52.11 (600 mg/L), 77.63 (800 mg/L), 81.83 (1000 mg/L). Chromosomes showed aberrations at all stages of cell division for all concentrations.

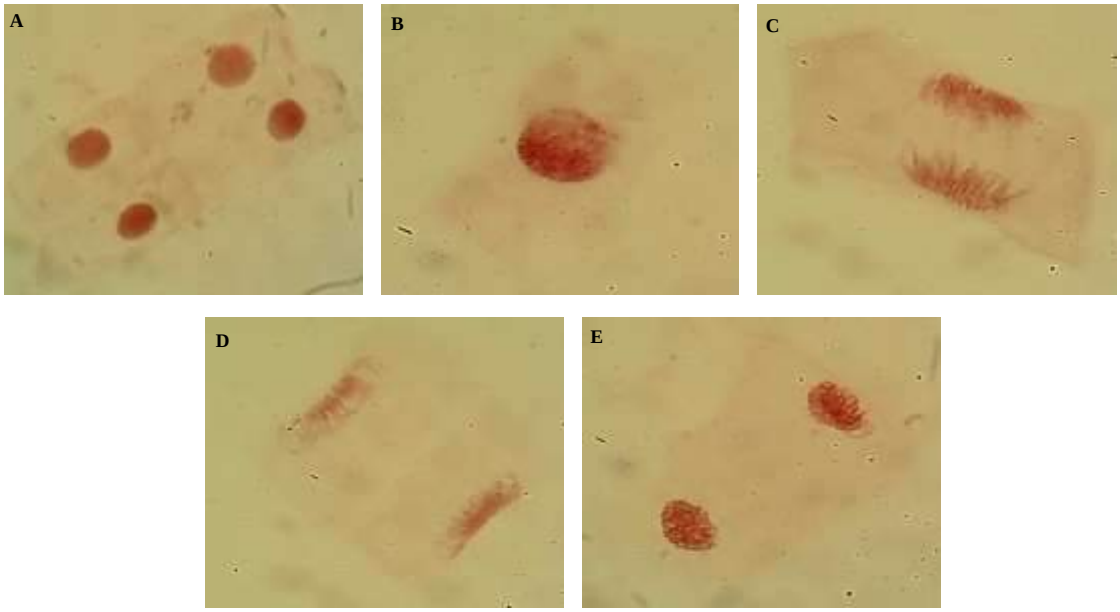

Figure 4.19: Stages of cell Division in Control Group (A – Resting cell Phase, B-Prophase, C-Metaphase, D-Anaphase, E-Telophase)

Cells were scored for chromosomal aberrations like vaculated nucleus or irregular prophase, chromosomal stickiness, distorted metaphase, anaphase with polar division,

chromosomal bridging with lags, vagrant chromosomes and multipolar anaphase. Highest number of aberrations were observed and reported at the highest concentration of the NPs applied i.e. 1000 mg/L. Number of cases showing disturbed anaphase were 3.5±0.82, 3.8±1.6, 4.1±2.5, 4.7±1.9, 5.8±3.2 and of irregular metaphase were 2.98±1.2, 3.1±1.7, 3.6±.91, 4.24±2.1, 4.75±1.9 at a concentration gradient of 200, 400, 600, 800, 1000 mg/L respectively. Highest incidents were recorded of multiple nuclei and damaged cell wall. Multiple nuclei followed an altered pattern as highest number (84±15) was observed at lowest concentration i.e 200 mg/L and vice versa 46±13 at 1000 mg/L. Events of damaged cell walls recorded were 94±17 (200mg/L), 100±25 (400mg/L), 127±15 (600 mg/L), 186±26 (800 mg/L) and 224±10 (800 mg/L).

Table 4.3: Chromosomal Aberration as Observed and Scored in the Wheat root tips due to ZnO nano-flowers synthesized by co-precipitation

ZnO-NPs Con. mg/L	0	200	400	600	800	1000
DA	-	3.5	3.8	4.1	4.7	5.8
IM		2.98	3.1	3.6	4.25	4.75
DC	-	1.2	1.6	2.4	3.1	3.7
M. nuc.	-	84	72	61	53	46
C-M.	-					
F	-	5.21	5.78	6.01	6.84	7.36
Uni.	-	4.54	4.97	5.45	5.98	6.23
Stic.	-	3.2	3.98	4.45	5.26	6.5
Bridging	-	2.89	3.15	4.21	5.08	5.97
ND	-	-	-	2.54	3.57	4.01
RC	-	-	4.5	0	5.32	5.56
M-nu	-	6.17	6.86	7.25	8.01	8.98
Elon	-	7.24	7.98	8.42	9.09	9.98
GC	-	-	4.54	4.75	5.14	5.76
MAP	-	2.31	2.67	3.56	4.76	5.25
LC	-	-	-	7.24	7.87	8.01
GC	-	45	51	65	87	98

Abbreviations : DA - Disturbed Anaphase; IM - Irregular Metaphase; DC - Disturbed Chromosome; M. nuc. Multiple Nuclei; C-M - C-Metaphase; **F –** Fragmentation; Uni.- Uncoiling; Stic. - Stickiness; B – Bridging; ND - Nucleotide deletion; RC - Ring Chromosome; M-nu - Multiple nuclei; Elon – Elongation; GC - GAP Chromosome; MAP - Multiple Anaphase; LC - Legging chromosomes;

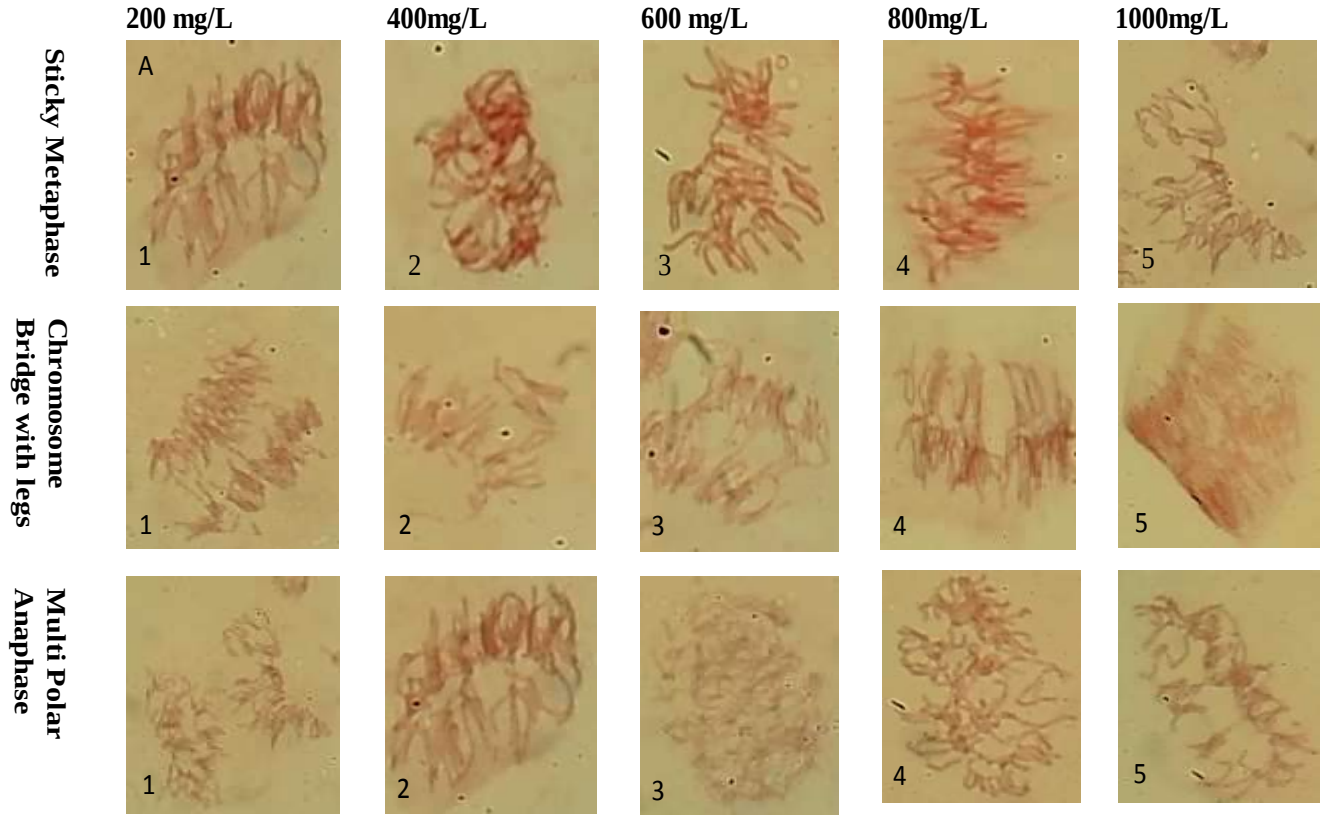

Figure 4:130: (a) Chromosomal Aberration Imparted by ZnO Nano-Flowers in Wheat Root Tips

Number of abnormal cell/chromosomes observed were 110 at NP concentration of 200 mg/L which kept on increasing to 157, 258, 376, 427 corresponding to 400, 600, 800 and 1000 mg/L NP concentration gradient with an average increase of 25% in number of abnormal cells. Coefficient of correlation was 0.921 at $p<0.01$ showing a strong direct relationship between NP concentration and occurrence of abnormal cells.

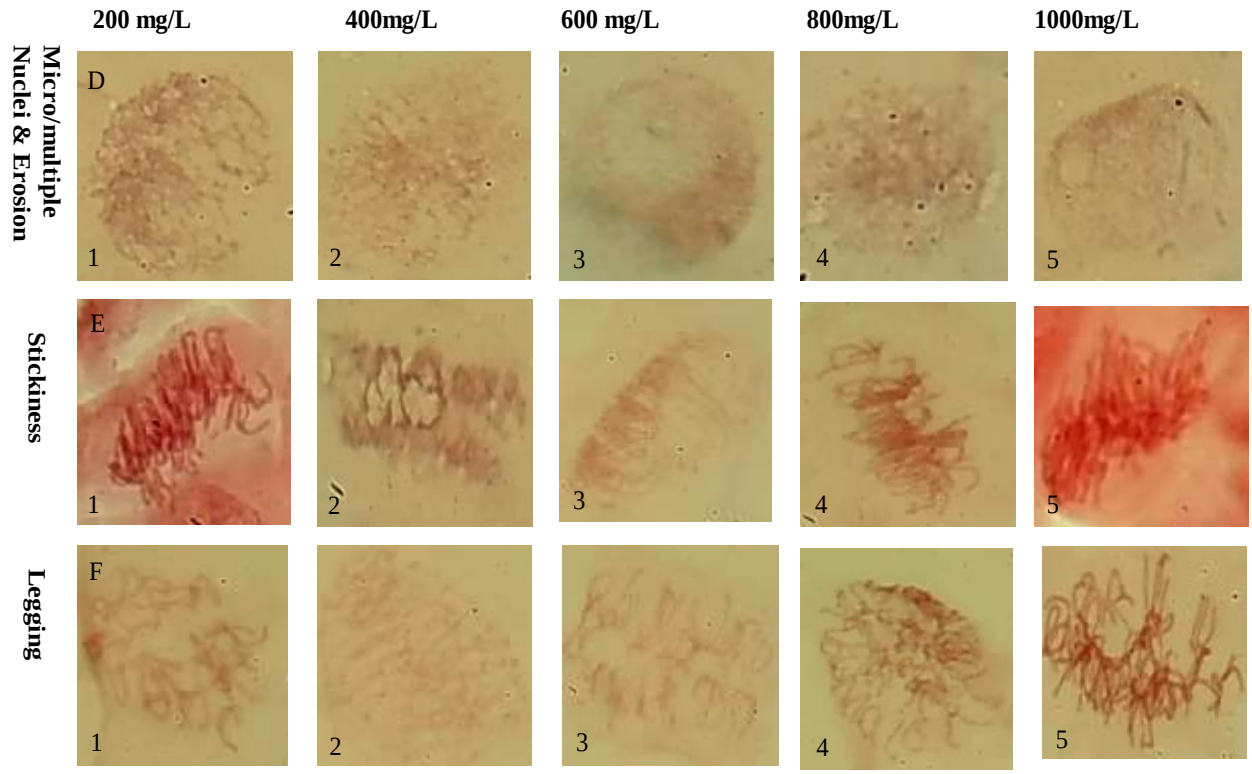

Figure 4.21: (b) Chromosomal Aberration Imparted by ZnO Nano-Flowers in Wheat Root Tips

Number of cells at different stages of cell division were also counted and given in table: . and results showed that with increase in NP concentration cells in different mitotic stages kept on decreasing as given in table number 4.3.

Incidents of chromosomal disorders such as chromosome bridges, breaks, disorders, stickiness, spindle breakage, micro nuclei and abnormalities in cell division. Incidents of chromosomal aberrations were increased along with concentration gradient. Event of chromosomal breakages, stickiness and spindle breakage were observed more frequently than others given in table 4.4.

Table 4.4: Scored Chromosomal Aberrations in Wheat Root Tips by Effected by Green Synthesized NPs

ZnO-NPs Con. mg/L	0	200	400	600	800	1000
SM	____	____	1	2.2	2.8	3.1
SA	____	_____	_____	1.5	1.9	2.3
GC	____	1.6	___	2.1	3.4	4
Bgs	____	___	___	1.2	2.6	2.9
Lag	____	___	0.98	___	1.1	2.4
CB	____	____	1.1	___	2.3	3.6
SB	____	___	___	___	1.7	2.4
CS	____	0.78	___	1.4	___	3.3
CL	____	___	___	0.68	1.56	2.54
MN	____	1.4	___	2.5	3.2	3.9

Abbreviations: SM – Sticky Metaphase; SA – Sticky Anaphase; GC – Ghost Cells; Bgs – Bridges; Lag – Laggards; CB – Chromosomal Breakage; SB – Spindle Breakage; CS – Chromosomal Stickiness; CL – Chromosomal Loops; MN – Micro-Nuclei Micro – graphs of these aberrations is given below:

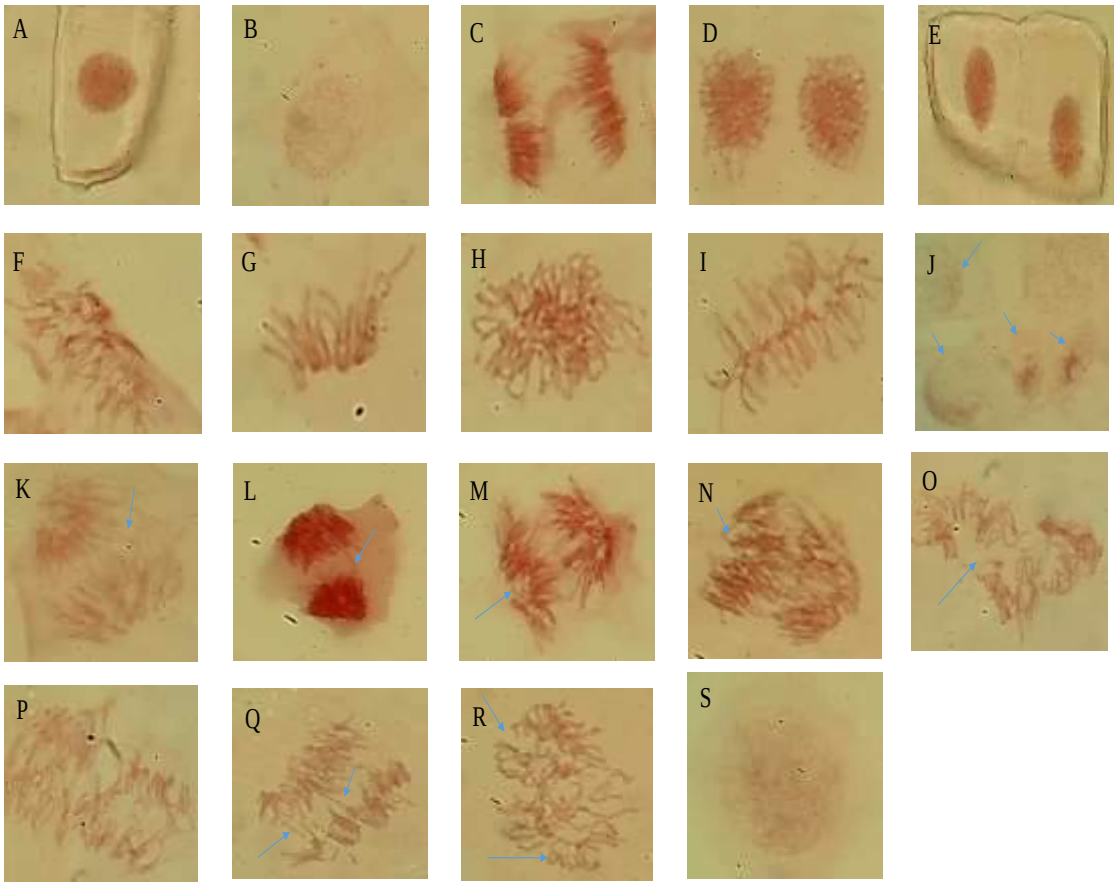

Figure 4:22: Chromosomal Aberration as Imparted by Green Synthesized NPs to Wheat Root Tips.

[(A-E) normal phases of Cell Division, (F-H) Sticky Metaphase, (I)Sticky Metaphase, (J)Ghost Cells, (K-L) Bridges, (M-N) Laggards, (O) Chromosomal Breakage, (P) Spindle Breakage, (Q) Chromosomal Stickiness, (R) Chromosomal Loops, (S) Micro - Nuclei]

However, when we compared the genotoxicity of chemically and green synthesized ZnO-NPs. Genotoxic effect of chemically synthesized NPs was found more strong and pronounced. Mitotic index found at 200 mg/L was 56% and 52% for chemically and biologically synthesized NPs. Which kept on depreciating for ZnO-NPs synthesized by two techniques and ultimately fell on 28% and 43% respectively. Percent aberration for chemically synthesized ZnO-NPs was 13.26% at 200 mg/L which ended up to 81.83% at NP concentration of 1000mg/L. As far as, green synthesized ZnO-NPs were concerned percent aberration at 200 mg/L was 10.6 and elevated upto 54.60 at 1000 mg/L, significantly lower than the chemically synthesized ZnO-NPs. Similar, trends

were observed in types of chromosomal aberration. More diverse aberrations with more frequents were observed in case of ZnO-NPs prepared through co-precipitation method as compared to the ZnO-NPs synthesized by the orange peels with minimum number of chemicals. The results narrated above shows that ZnO-NPs prepared by both ways impart toxicity to primary roots of the wheat. Above given data implies that when ZnO-NPs come in contact with root cells, may enter into it through cell wall and membrane. Once got access to cell organelles, these chemicals cause extensive damage to the DNA, thus inhibiting the synthesis of DNA in S phase of interphase. Similar results were reported by the Abdelsalam and co-worker who had studied the genotoxicity of Ag NP on roots of wheat (Abdelsalam *et al.,* 2018). Abiotic stress to wheat roots in forms of ZnO-NPs caused altered chromosomal orientations at different stages of cell division. Most expectedly intermixing of chromatin material or more correctly chromatin fiber resulted in chromosomal stickiness in almost all phases of cell division. Incidents of chromosomal breaks, laggards and events of multiple nuclei were indications of induced mutagenicity. Such type of toxicities imposed by ZnO-NPs in a amount dependent way have already been testified by Ahmad and Sun (Ahmed *et al.*, 2017, Sun *et al.,* 2019). ZnO-NPs have proven its excellent anti-microbial properties attributable to its greater surface area to volume proportion. Thus its capacity to bind a large number of ligands inside the cell. A number of scientific evidences are present that argues that antimicrobial properties of ZnO-NPs governs through destroying the DNA (Tiwari *et al.,* 2018). As far as, plants are concerned, data regarding genotoxicity in limited and results are contradictory. There is a dire need for more scientific investigation in this regard.

4.11. Quantitative Real Time – Polymerase Chain Reaction (qRT-PCR)

Stability (both in terms of quality and quantity) of messenger-RNA is an important factor for studying gene expression. There are several reasons behind this most important being:

- Stability level of mRNA is measured by balance between its rate of synthesis and degradation.
- Stability of mRNA can be altered by numerous environmental factors.
- An efficient system of mRNA degradation is required to remove deadly errors in mRNA synthesis (Liu *et al.,* 2014).

Thus, it is a critical step. mRNA was quantified by using nano-drop method. A nano-drop is common lab fluoro-spectrophotometer that reads a 2 µL of sample on a pedestal. In present study Skanlt RE 4.1, Thermoscientific nano-drop plate was used. Absorbance was taken at 260, 280 and 320 nm. The 260/280 ratio ranged from 1.6 to 2.3 confirming high quality RNA whereas RNA quantity was nearly 800 to 1200 ng/µL. Following table is showing 260/280 ratio and RNA concentration of each sample:

Table 4.5: Representing mRNA Quantity and Quality in all Sample and Control Groups

Sr. No	Samples coding	260/280 ratio	Quantity (ng/µL)
1	a shoot	1.93	843
2	a root	2.01	1191
3	b shoot	1.89	961
4	b root	2.21	820
5	c shoot	2.10	1267
6	c root	2.00	897
7	d shoot	1.93	1001
8	d root	1.89	934
9	e shoot	2.19	1139
10	e root	2.2	969
11	Ct shoot	2.34	1245
12	Ct root	2.07	1304
13	1 shoot	1.99	890
14	1 root	1.79	931
15	2 shoot	1.92	869
16	2 root	2.04	1067

17	3 shoot	2.19	1123
18	3 root	1.972	1390
19	4 shoot	2.0	1119
20	4 root	1.59	1038
21	5 shoot	1.98	839
22	5 root	2.11	1059

Where a,b,c,d,e corresponds to concentration gradient of 1000, 800,600,400,200 mg/L of chemically synthesized NPs. Also, 1,2,3,4,5 represents 1000, 800,600,400,200 mg/L of green synthesized NPs, Ct stands for control groups.

Nucleic acid captivates UV/Vis light around 260 nm owing to aromatic bases (purines and pyrimidines) in its structures. Hence, forming a reliable standard for nucleic acid quantification. Also, proteins and phenols shows strong absorbance at 280nm. As a matter of fact A260/280 ratio gives us a measure of protein impurities. For pure RNA with ratio falls within a range of 1.8-2.3. A lower ratio presents protein contamination in RNA samples, which may harm the downstream applications.

4.11.1 Primer Optimization and Gel Analysis

Gradient 1:

2 % agarose gel was analyzed with temperature of 45°C-60°C. Beta Actin was presenting bands on multiplicity of temperatures where as GAPDH primer was displaying multiple bands. In this case different dilutions of cDNA were optimized. 1-7 well (original cDNA), 8-14 (1:10), 15-21 (1:100), 21-28 (1:1000) with Beta Actin. 28 well plate with identical dilutions was used for GAPDH primer. Concentrated CDNA couldn’t amplify whereas its dilutions produced acceptable results.

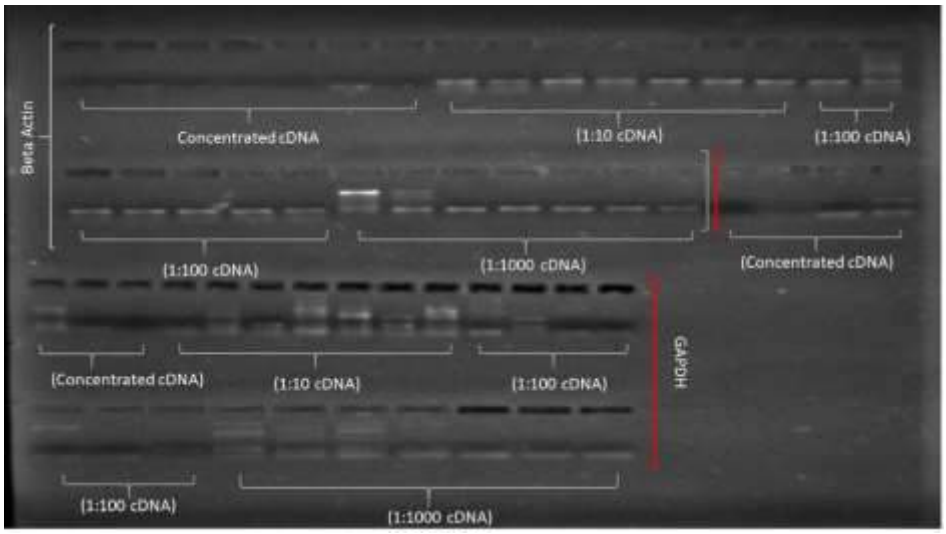

Figure 4:23: Agrose Gel Analysis of House Keeping Genes (Beta Actin and GAPDH)

Beta Actin and GAPDH Primer: 28 wells were used for Beta Actin where as in last 28 wells GAPDH primer was used. Different dilutions were optimized. 10 times diluted cDNA has good bands compared to other dilutions.

Gradient 2:

Different dilutions of complementary DNA were optimized for *TaHMA2* and Ta*WRKY10* primer. Temperature range was 50°C to 60.9°C. 18 wells for *TaHMA2* whereas 19- 36 were used against Ta*WRKY10* Primer. 1-6 and 19-24 wells with (1:10 of cDNA), wells 7-12 and 25-30 (1:100 of cDNA), 13-18 and 31-36 wells having (1:1000 of cDNA).

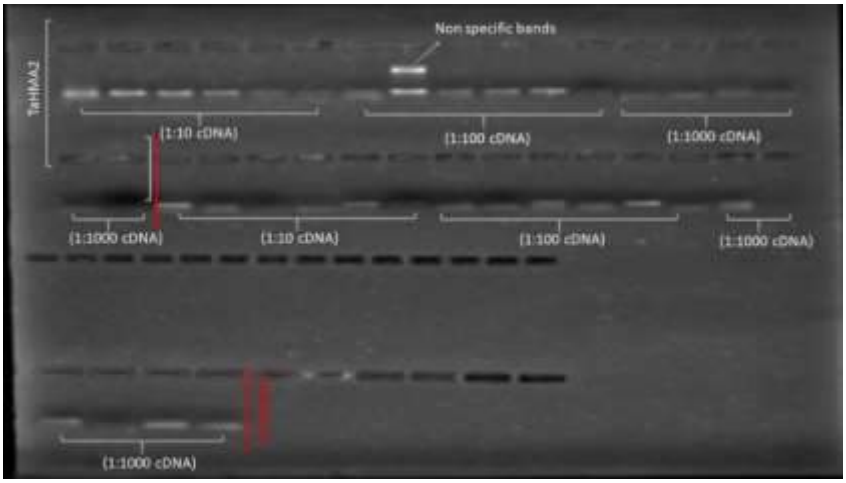

Figure 4:24: Agrose gell Analysis of Test Genes *TaHMA2* and Ta*WRKY10*)

***TaHMA2* and Ta*WRKY10* Primer:** wells 1-18 with *TaHMA2* primer whereas 19-36 with Ta*WRKY10* primers. Different concentration of cDNA was used.

4.11.2 Expression Profile of Ta*WRKY10* Gene in Wheat by ZnO-NPs Stress

Plants have a number of stress responding genes families. Among these families *WRKY* family is largest one that serves a key role in stress reaction, defense directives and plant growth. In present investigation, Ta*WRKY10* gene was choosen to study the effect of oxidative stress posed by the ZnO-NPs and resulting damage to wheat seedlings at very intial growth stage. Expression levels of *WRKY10* genes appeared to be more abundant at lower concentration of ZnO-NPs (both Chemically and biologically synthesized) and expressed a lower level as amount of NP stress was elevated when expression levels were quantified both with house keeping genes β-actin and GAPDH.

WRKY family consist of highly conserved sixty amino acid stretched *WRKY* domain which contain a conserved heptapeptide motif *WRKY*GQK at the N-terminus and a novel zinc-finger-like motif at the C-terminus. Both heptapeptide sequence and zinc-finger-like motif are required for the high binding affinity of *WRKY* TFs to the consensus *cis*-acting elements termed W box (TTGACT/C) (Bakshi & Oelmüller, 2014). 1st *WRKY* transcription factor was characerised from swee potato, number of *WRKY* factors have been identified in rice, arabidopsis, soybean, poplar, pinus, physcomitrella patens and barley. Scientists have found that *WRKY* factors take part in many physiological funtions such as germination, seed development and embryogenesis. It play a crucial role in biosynthetic pathways, hormone signaling and trichome development. *WRKY* factors responsive to abiotic stress with particular emphasis on oxidative brust out have been identified (Lagacé & Matton, 2004, Eulgem & Somssich, 2007, Ueda *et al.*, 2011) (Lagacé & Matton, 2004, Xie *et al.*, 2007). It is well established fact, that in plants, lipid peroxidation occurs due to abiotic stress (Kong *et al.*, 2011). Amount of MDA content serves to guage the extent of oxidative demage caused to the plant by abiotic stress. Its been reported previously that Ta*WRKY10* decreases the amount of MDA thus protecting the plant by oxidative damage (Wang *et al.*, 2013). Our results confirmed these previous studies. As MDA content kept on increasing along with the concentration gradient (from 0 to 1000 mg/L). However the increase was not significant (as depicted by one way anova and Tukey's test) till NP concentration of 600 mg/L (for both biologically and chemically Synthesized NPs). Over-expression of Ta*WRKY10* genes kept

the MDA concentration within the sustainabile limit. But as long as long the abiotic stress was raised above threshold level, cellular defence mechanism of the plant was shatter as can be seen by the minimum expression levels of Ta*WRKY10* genes. MDA level was very high (as expressed by one way anova values and Tukey's test) as compared to controlled plants (both for biologically and chemically synthesized NP). Growth parameters analysed earlier in the same documents also strengthen the results being discussed here. Plant's growth parameters are discussed as germination index, stress tolerance index (STI) (amount of biomass) and Index of tolerance (IT)(length of shoots and Roots) in section 4.2. Where it can be clearly observed that physiological growth parameters were adversely effeced at NP concentration (for both chemically and biologically synthesized NP) above 600 mg/L. ROS consist of highly reactive oxygen species that are toxic to plants at cellular and sub-cellular levels. Plants have to develop a mechanism to control levels of ROS to combat with oxidative damages. Our results have clearly depicted that over-expression of Ta*WRKY10* genes plays a role to control sub-cellular level injuries by reducing amount of ROS in wheat seedlings. Also, it played a significant role in plant development at seedling stage by reducing amount of ROS accumulation.

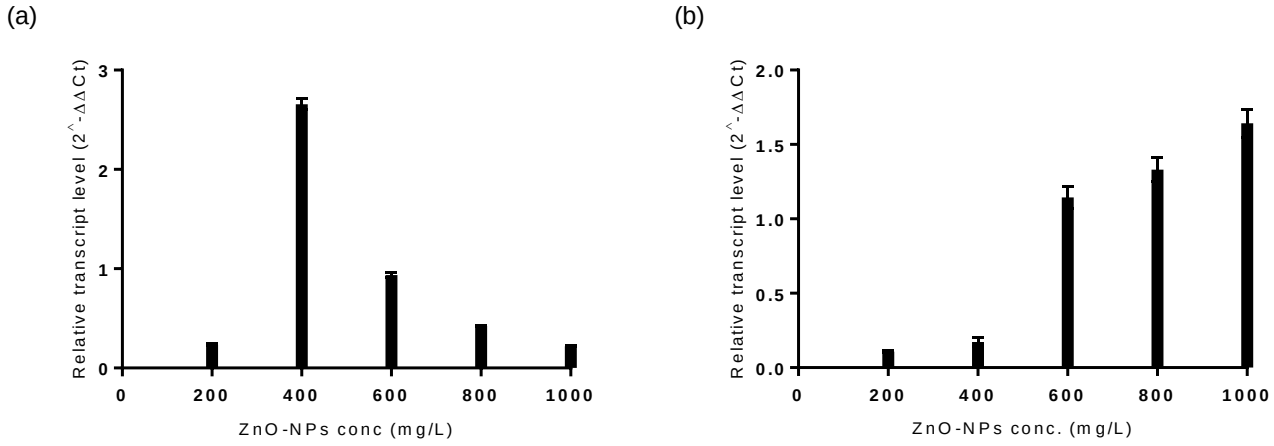

Figure 4:25: Expression profiles of TaWRKY10 in wheat. The expression levels of TaWRKY10 in seedlings (a), stressed by different con. of chemically synthesized ZnO-NPs (b), stressed by different con. of green synthesized ZnO-NPs were detected using real-time PCR. The data are normalized with GAPDH and Beta actin as a standard and are presented as the means ± SD (n = 3).

To determine the effect of ZnO toxicity on *HMA2* genes, mRNA was reverse transcribed to cDNA. Which was quantified using qRT-PCR with house keeping gene (β-actin and GAPDH) as internal control. It was previously confirmed that amount of Zn^{2+} ions is decreased concentration gradient of ZnO-NPs (both chemically and green synthesized NPs) was elevated from 0 to 1000 mg/L. Tanslocation of Zn^{2+} ions from roots to leave lead to the over expression of the *TaHMA2* genes expression. Minimum expression level was observed for concentration 200 mg/L and maximum was observed for 1000 mg/L both in case of green and chemically synthesized NPs. (Figure 4.21 (a) & (b)).

Metals ions like Zn2+, Cu2+, Cu+, Co2+ are transported crossways the cell membrane by P1B-ATPases. Many family members of this sub-family have been recognized in plants that holds a vital role in plants such as DNA-binding proteins, elementary components of vital enzymes (alcohol dehydrogenase, RNA plymerase, Cu-Zn superoxide dismutase) (Eren & Argüello, 2004). Aluminium (Al) and Magneses (Mn) are known as natural phytotxoic and used to present abundently in highly acidic soils. After these two elements Zn phytotosicty is most widespread due to anthopogenic activities.

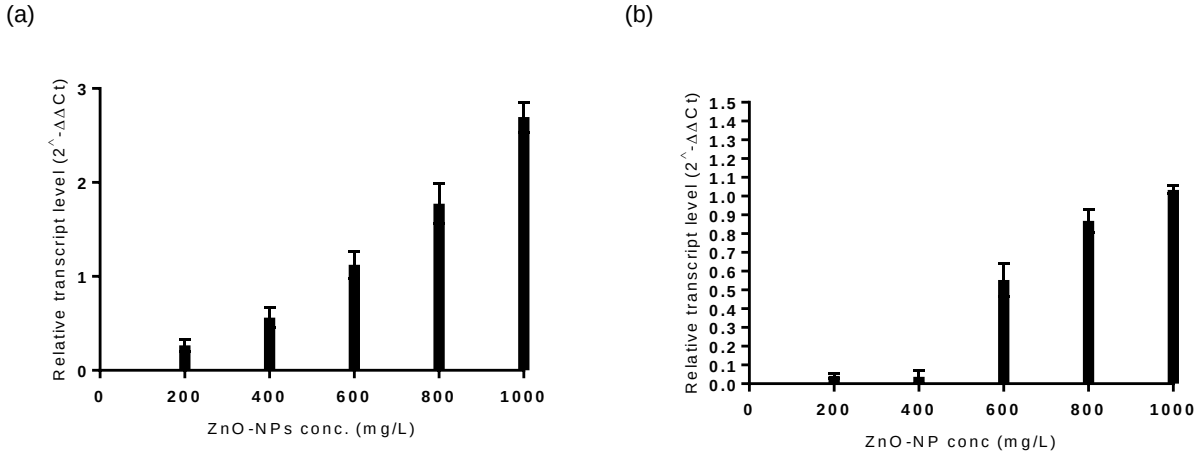

Figure 4:26: Expression profiles of *TaWRKY10* in wheat. The expression levels of TaHMA2 in seedlings (a), stressed by different con. of chemically synthesized ZnO-NPs (b), stressed by different con. of green synthesized ZnO-NPs were detected using real-time PCR. The

data are normalized with GAPDH and Beta actin as a standard and are presented as the means ± SD (n = 3).

Major sources remains fertilizers, manures, pesticides, sludges, incinirators, galvanized products and mines. Now-a-days, new source of Zn^{2+} is being added. That belongs to exhaust form nano-industry due to extensive utilities of ZnO in marketable products and as nano-fertilizers. These nano-Zn^{2+} is expectedly more phytotoxic than its bulk counterpart due its size, greater solubiliy and readily availability (Chaney, 1993). Young leaves may become a victim of chlorosis via competiion with Mg^{2+} and Fe^{2+} (Marschner, 1995). Thus, plants have developed specified mechanism against metal ion stress which consist of, chelators, chaperones, membrane transporters. These mechanism functions either to distribute metal ions through out the organism or avoid high levels of free metal ions in cytoplasm. For his whole process, metal ion pumps are required which may transport these ions agains electrochemical gradient and are key player to maintain matel homeostasis. P_{IB}-ATPases is a sub-family of P-type ATPases – major metal transport and *TaHMA2* belongs to this sub-family. A number of auhors have isolated, characterize and confirmed the role of *TaHMA2* in wheat (Mills *et al.*, 2012, Tan *et al.*, 2013). However, it is 1st time that over expression of *TaHMA2* was examined as quantified by ZnO-NPs stress.

4.12. Conclusion and Recommendation.

In this research endeavor it is clearly ascertained that *Triticum aestivum* can act as a bio-indicator of NP toxicity particularly for higher concentrations of ZnO-NPs in natural environment. In order to evaluate and compare the phyto-toxicities of the metal oxide NPs, ZnO-NPs were synthesized successfully by two methods. First, ZnO nano-flowers were manufactured by co-precipitation process and secondly ZnO-NPs were crafted through green route by using minimum amount of chemicals and with aqueous solution of orange peel extract. Experimental data has revealed that both types of NPs penetrates into plant body through the roots and caused toxicity majorly through ROS generation and shape of the NPs. Other causes of toxicity remained solubility release of toxic ions by dissolution and aggregation. Physiological analysis of *Triticum aestivum* seedlings showed that biotic stress by ZnO (both green and chemically synthesized) damaged growth and development of *Tritium aestivum*. Photosynthetic pigments (carotenoids, chlorophyll a,b and total) were dropped down significantly showing an over damage to plant's health. Our

results confirmed that membrane stability was severely injured by the stress applied. Plant stress markers (proline and MDA) showed significantly higher concentration as compared to the controlled experiment confirming the strength and stringency of stress posed by ZnO-NPs. However, overall protein content remained unaffected as compared to the control plants. Sugar content was found to be elevated slightly by the stress applied. Plant's non-enzymatic (phenols and flavonoids) and enzymatic (SOD,CAT and APX) defense mechanism were shattered at higher concentration of chemically synthesized NP defense. However, in case of green synthesized ZnO-NPs considerable increase in all the parameter mentioned was observed. Both kinds of NPs have proven to be mitotic-depressive and cytotoxic to wheat root tips and both of these effects were more pronounced with increase in concentration. *TaHMA2* gene was chosen to study the metal stress experienced by the plants in roots. Whereas, Ta*WRKY10* gene was selected to understand the impression of metal trauma on growth and development of seedlings.

Technological advances are inevitable and man-kind is in dire need to produce much more with limited resources without destroying natural assets – the only raw material provider on earth. Thus, with scientific advancements, new methodologies and ways and means are being devised on almost daily basis. It not only provides better solutions of problems we are facing today, but also those are cost effect and using less raw materials. Nanotechnology prognosticators used to predict that the dream of nano-age will come true within two decades. And the life on earth – as it is known today - will be changed forever. In America, (NSF) "The National Science Foundation" is massively funding the research in all area of nanotechnology and has declared it as a science most likely capable of breakthroughs of near future. The word "Nano" is derived from Greek word meaning "dwarf" and expresses the billionth part of the measurement. The substantial difference between NPs and bulk material is that NPs have maximum number of atoms present on their surfaces. Therefore, NPs have completely different exterior composition than their bulk counterpart. Thus, NPs shows entirely different physical and chemical properties as compared to bulk material.. Scientists have manipulated these properties for manufacturing countless products that would otherwise were just a dream. Some of these engineered commodities includes battery storage and renewable energy captures, agricultural products (fertilizers and pesticides), food packaging materials, water purification systems, smart clothing, a whole new branch of medicine known as nano-medicine and a lot more.

However, there is a mounting concern regarding nano-pollutants in environment and their possible toxicities in the living systems. NPs can easily be internalized by humans, animals and plants. They can enter in cells and can cause damages at sub-cellular levels. Toxicities of engineered NP have proven toxicities in animals and plants and associated with number of disorders extending from respiratory disorders to neurological diseases and cardiovascular problems. In such a scenario plants have become primary victims of nano-pollutants. Plants plays crucial role in keeping ecological balance by converting the solar energy to raw materials. Due to scientific investigations and industrial utilization, NPs are released in to air, soil and water. NPs are also exhausted to environment as waste materials and resides into landfills, rives or air as smoke. These NPs interact directly with the plants and there are non-deniable proofs that they are causing toxicities to the "only producers" of this universe. Reports have shown that due to their novel properties carbon and metal based NPs are capable to impart/alter genetic and physiological constituents of the plants. There are five challenges associated with the estimation and combating the nano-pollutants as follows:

i. Toxicity of NPs depends upon a lot of factors like shape, size, surface chemistry, solubility, and nature of environment (air, water, soil) and living system it is interacting with. Therefore, toxicity of an engineered NP say ZnO will entirely be different with change in its size, shape or environment. Biggest challenge in front of nano-scientists these days is to develop an instrument that can gauge the toxicity of these particles in coming 3 to 10 years.
ii. There are many contradictory reports about the toxicities of nanomaterials. The second biggest challenge is to develop and authenticate the methodologies evaluating the toxicity of NPs. That are globally accepted and effective.
iii. There is a dire need to develop models and simulations for the life cycle assessment of the NPs in the environment.
iv. Similar to the above mentioned point exposures, fate of the NPs in living systems should be well documented.
v. There is need of a strategic program that focuses solely on risks of engineered NPs.
vi. There should be a check on all source of NP exhaust and a threshold level should have defined for all kind of NP exhaust in the environment.

REFERENCES

Abdelsalam NR, Abdel-Megeed A, Ali HM, Salem MZ, Al-Hayali MF & Elshikh MS (2018). Genotoxicity effects of silver nanoparticles on wheat (Triticum aestivum L.) root tip cells. Ecotoxicology and environmental safety 155: 76-85.

Abdolmaleki A, Mallakpour S & Borandeh S (2011). Preparation, characterization and surface morphology of novel optically active poly (ester-amide)/functionalized ZnO bionanocomposites via ultrasonication assisted process. Applied Surface Science 257: 6725-6733.

Afrayeem SM & Chaurasia A (2017). Effect of zinc oxide nanoparticles on seed germination and seed vigour in chilli (Capsicum annuum L.). Journal of Pharmacognosy and Phytochemistry 6: 1564-1566.

Ahmad P, Jaleel CA, Salem MA, Nabi G & Sharma S (2010). Roles of enzymatic and nonenzymatic antioxidants in plants during abiotic stress. Critical reviews in biotechnology 30: 161-175.

Ahmed B, Dwivedi S, Abdin MZ, Azam A, Al-Shaeri M, Khan MS, Saquib Q, Al-Khedhairy AA & Musarrat J (2017). Mitochondrial and chromosomal damage induced by oxidative stress in Zn 2+ ions, ZnO-bulk and ZnO-NPs treated Allium cepa roots. Scientific reports 7: 40685.

Ainsworth EA & Gillespie KM (2007). Estimation of total phenolic content and other oxidation substrates in plant tissues using Folin–Ciocalteu reagent. Nature protocols 2: 875.

Andreu L, Nuncio-Jáuregui N, Carbonell-Barrachina ÁA, Legua P & Hernández F (2018). Antioxidant properties and chemical characterization of Spanish Opuntia ficus-indica Mill. cladodes and fruits. Journal of the science of food and agriculture 98: 1566-1573.

Apel K & Hirt H (2004). Reactive oxygen species: metabolism, oxidative stress, and signal transduction. Annu. Rev. Plant Biol. 55: 373-399.

Aravantinou AF, Tsarpali V, Dailianis S & Manariotis ID (2015). Effect of cultivation media on the toxicity of ZnO nanoparticles to freshwater and marine microalgae. Ecotoxicology and environmental safety 114: 109-116.

Arora A, Byrem TM, Nair MG & Strasburg GM (2000). Modulation of Liposomal Membrane Fluidity by Flavonoids and Isoflavonoids. Archives of Biochemistry and Biophysics 373: 102-109.

Aslani F, Bagheri S, Muhd Julkapli N, Juraimi AS, Hashemi FSG & Baghdadi A (2014). Effects of engineered nanomaterials on plants growth: an overview. The Scientific World Journal 2014.

Au - Kaur I, Au - Ellis L-J, Au - Romer I, Au - Tantra R, Au - Carriere M, Au - Allard S, Au - Mayne-L'Hermite M, Au - Minelli C, Au - Unger W, Au - Potthoff A, Au - Rades S & Au - Valsami-Jones E (2017). Dispersion of Nanomaterials in Aqueous Media: Towards Protocol Optimization. JoVE e56074.

Auffan M, Rose J, Bottero J-Y, Lowry GV, Jolivet J-P & Wiesner MR (2009). Towards a definition of inorganic nanoparticles from an environmental, health and safety perspective. Nature nanotechnology 4: 634.

Awad MA, Hendi AA, Ortashi KM, Elradi DF, Eisa NE, Al-lahieb LA, Al-Otiby SM, Merghani NM & Awad AA (2014). Silver nanoparticles biogenic synthesized using an orange peel extract and their use as an anti-bacterial agent. International journal of physical sciences 9: 34-40.

Azizi S, Ahmad MB, Namvar F & Mohamad R (2014). Green biosynthesis and characterization of zinc oxide nanoparticles using brown marine macroalga Sargassum muticum aqueous extract. Materials Letters 116: 275-277.

Babu KS, Reddy AR, Sujatha C, Reddy KV & Mallika A (2013). Synthesis and optical characterization of porous ZnO. Journal of Advanced Ceramics 2: 260-265.

BAGGA S & STRANEY D (2000). Modulation of cAMP and phosphodiesterase activity by flavonoids which induce spore germination of Nectria haematococca MP VI (Fusarium solani). Physiological and molecular plant pathology 56: 51-61.

Bai Y, Sunarti S, Kissoudis C, Visser RGF & van der Linden CG (2018). The Role of Tomato WRKY Genes in Plant Responses to Combined Abiotic and Biotic Stresses. Frontiers in plant science 9: 801-801.

Bakshi M & Oelmüller R (2014). WRKY transcription factors: Jack of many trades in plants. Plant signaling & behavior 9: e27700-e27700.

Bala N, Saha S, Chakraborty M, Maiti M, Das S, Basu R & Nandy P (2015). Green synthesis of zinc oxide nanoparticles using Hibiscus subdariffa leaf extract: effect of temperature on synthesis, anti-bacterial activity and anti-diabetic activity. RSC Advances 5: 4993-5003.

Balashanmugam P, Nandhini R, Vijayapriyadharshini V & Kalaichelvan P (2013). Biosynthesis of silver nanoparticle from orange peel extract and its antibacterial activity against fruit and vegetable pathogens. Int. J. Inn. Res. Eng.

Balážová Ľ, Babula P, Baláž M, Bačkorová M, Bujňáková Z, Briančin J, Kurmanbayeva A & Sagi M (2018). Zinc oxide nanoparticles phytotoxicity on halophyte from genus Salicornia. Plant Physiology and Biochemistry.

Bandyopadhyay S, Plascencia-Villa G, Mukherjee A, Rico CM, José-Yacamán M, Peralta-Videa JR & Gardea-Torresdey JL (2015). Comparative phytotoxicity of ZnO NPs, bulk ZnO, and ionic zinc onto the alfalfa plants symbiotically associated with Sinorhizobium meliloti in soil. Science of the Total Environment 515: 60-69.

Barillet S, Jugan M-L, Laye M, Leconte Y, Herlin-Boime N, Reynaud C & Carrière M (2010). In vitro evaluation of SiC nanoparticles impact on A549 pulmonary cells: cyto-, genotoxicity and oxidative stress. Toxicology letters 198: 324-330.

Baskar G, Chandhuru J, Fahad KS & Praveen A (2013). Mycological synthesis, characterization and antifungal activity of zinc oxide nanoparticles. Asian Journal of Pharmacy and Technology 3: 142-146.

Bates L, Waldren R & Teare I (1973). Rapid determination of free proline for water-stress studies. Plant and soil 39: 205-207.

Berk Z (2016). Chapter 1 Introduction: history, production, trade, and utilization. Citrus Fruit Processing 1-8.

Bhushan B (2017). Springer handbook of nanotechnology. Springer.

Bhuvaneshwari M, Iswarya V, Nagarajan R, Chandrasekaran N & Mukherjee A (2016). Acute toxicity and accumulation of ZnO NPs in Ceriodaphnia dubia: Relative contributions of dissolved ions and particles. Aquatic Toxicology 177: 494-502.

Bhuyan T, Mishra K, Khanuja M, Prasad R & Varma A (2015). Biosynthesis of zinc oxide nanoparticles from Azadirachta indica for antibacterial and photocatalytic applications. Materials Science in Semiconductor Processing 32: 55-61.

Bienert GP, Møller AL, Kristiansen KA, Schulz A, Møller IM, Schjoerring JK & Jahn TP (2007). Specific aquaporins facilitate the diffusion of hydrogen peroxide across membranes. Journal of Biological Chemistry 282: 1183-1192.

Billinge SJ & Levin I (2007). The problem with determining atomic structure at the nanoscale. Science 316: 561-565.

Blumenthal C, Rawson H & McKenzie E (1996). Changes in Wheat Grain Quality Due to Doubling the Level of Atmospheric CO (2). Cereal Chemistry 73: 762-766.

Boguszewska D, Grudkowska M & Zagdańska B (2010). Drought-responsive antioxidant enzymes in potato (Solanum tuberosum L.). Potato research 53: 373-382.

Boonyanitipong P, Kositsup B, Kumar P, Baruah S & Dutta J (2011). Toxicity of ZnO and TiO2 nanoparticles on germinating rice seed Oryza sativa L. International Journal of Bioscience, Biochemistry and Bioinformatics 1: 282.

Bradfield SJ, Kumar P, White JC & Ebbs SD (2017). Zinc, copper, or cerium accumulation from metal oxide nanoparticles or ions in sweet potato: Yield effects and projected dietary intake from consumption. Plant Physiology and Biochemistry 110: 128-137.

Braydich-Stolle LK, Schaeublin NM, Murdock RC, Jiang J, Biswas P, Schlager JJ & Hussain SM (2009). Crystal structure mediates mode of cell death in TiO 2 nanotoxicity. Journal of Nanoparticle Research 11: 1361-1374.

Brayner R (2008). The toxicological impact of nanoparticles. Nano Today 3: 48-55.

Brunner TJ, Wick P, Manser P, Spohn P, Grass RN, Limbach LK, Bruinink A & Stark WJ (2006). In vitro cytotoxicity of oxide nanoparticles: comparison to asbestos, silica, and the effect of particle solubility. Environmental science & technology 40: 4374-4381.

Camejo D, Martí M, Olmos E, Torres W, Sevilla F & Jiménez A (2012). Oligogalacturonides stimulate antioxidant system in alfalfa roots. Biologia plantarum 56: 537-544.

Cao G (2004). Nanostructures & nanomaterials: synthesis, properties & applications. Imperial college press.

Cao W & Rui Y (2017). Interactions between nanoparticles and plants: phytotoxicity and defense mechanisms AU - Yang, Jie. Journal of Plant Interactions 12: 158-169.

Castro L, Blázquez ML, González F, Muñoz JÁ & Ballester A (2015). Biosynthesis of silver and platinum nanoparticles using orange peel extract: characterisation and applications. IET nanobiotechnology 9: 252-258.

Chakra C, Rao KV, Pavani T & Kollu NV (2015). Microbial Synthesis of ZnO Nano Particles by Lactobacillus Sporogenes and Effect of Size of Nano Particles by Temperature Variation and Antibacterial Studies. Nanomedicine and Nanobiology 2: 1-9.

Chaney R (1993). Zinc phytotoxicity. Zinc in soils and plants,ed.^eds.), p.^pp. 135-150. Springer.

Chauhan R, Kumar A, Chaudhary RP & Education T (2010). Synthesis and characterization of silver doped ZnO nanoparticles. Arch. Appl. Sci. Res 2: 378-385.

Chen J, Dou R, Yang Z, You T, Gao X & Wang L (2018). Phytotoxicity and bioaccumulation of zinc oxide nanoparticles in rice (Oryza sativa L.). Plant Physiology and Biochemistry 130: 604-612.

Chen W, Hu C, Yang Y, Cui J & Liu Y (2016). Rapid synthesis of carbon dots by hydrothermal treatment of lignin. Materials 9: 184.

Chernyshev A (2009). Effect of nanoparticle size on the onset temperature of surface melting. Materials Letters 63: 1525-1527.

Choudhury S, Panda P, Sahoo L & Panda SK (2013). Reactive oxygen species signaling in plants under abiotic stress. Plant signaling & behavior 8: e23681.

Ciarmiello LF, Woodrow P, Fuggi A, Pontecorvo G & Carillo P (2011). Plant genes for abiotic stress. Abiotic Stress in Plants–Mechanisms and Adaptations 283-308.

Ciolkowski I, Wanke D, Birkenbihl RP & Somssich IE (2008). Studies on DNA-binding selectivity of WRKY transcription factors lend structural clues into WRKY-domain function. Plant molecular biology 68: 81-92.

Cona A, Rea G, Angelini R, Federico R & Tavladoraki P (2006). Functions of amine oxidases in plant development and defence. Trends in plant science 11: 80-88.

Congress E (2016). International Journal of Infection Control.

Coomber D (2012). Radiochemical methods in analysis. Springer Science & Business Media.

da Cruz TN, Savassa SM, Gomes MH, Rodrigues ES, Duran NM, de Almeida E, Martinelli AP & de Carvalho HW (2017). Shedding light on the mechanisms of absorption and transport of ZnO nanoparticles by plants via in vivo X-ray spectroscopy. Environmental Science: Nano 4: 2367-2376.

Das K & Roychoudhury A (2014). Reactive oxygen species (ROS) and response of antioxidants as ROS-scavengers during environmental stress in plants. Frontiers in Environmental Science 2: 53.

Davar F, Majedi A & Mirzaei A (2015). Green synthesis of ZnO nanoparticles and its application in the degradation of some dyes. Journal of the American Ceramic Society 98: 1739-1746.

de Barros CHN, Cruz GCF, Mayrink W & Tasic L (2018). Bio-based synthesis of silver nanoparticles from orange waste: effects of distinct biomolecule coatings on size, morphology, and antimicrobial activity. Nanotechnology, science and applications 11: 1.

de la Rosa G, López-Moreno ML, de Haro D, Botez CE, Peralta-Videa JR & Gardea-Torresdey JL (2013). Effects of ZnO nanoparticles in alfalfa, tomato, and cucumber at the germination stage: root development and X-ray absorption spectroscopy studies. Pure and Applied Chemistry 85: 2161-2174.

Delgado-Vargas F & Paredes-López O (2002). Natural colorants for food and nutraceutical uses. CRC press.

DEMİR E, Kaya N & KAYA B (2014). Genotoxic effects of zinc oxide and titanium dioxide nanoparticles on root meristem cells of Allium cepa by comet assay. Turkish Journal of Biology 38: 31-39.

Denno RF, Douglass LW & Jacobs D (1986). Effects of Crowding and Host Plant Nutrition on a Wing-Dimorphic Planthopper. Ecology 67: 116-123.

Deshpande P, Dapkekar A, Oak M, Paknikar K & Rajwade J (2018). Nanocarrier-mediated foliar zinc fertilization influences expression of metal homeostasis related genes in flag leaves and enhances gluten content in durum wheat. PLOS ONE 13: e0191035.

Dhas NL, Raval NJ, Kudarha RR, Acharya NS & Acharya SR (2018). Core–shell nanoparticles as a drug delivery platform for tumor targeting. Inorganic Frameworks as Smart Nanomedicines,ed.^eds.), p.^pp. 387-448. Elsevier.

Dimapilis EAS, Hsu C-S, Mendoza RMO & Lu M-C (2018). Zinc oxide nanoparticles for water disinfection. Sustainable Environment Research 28: 47-56.

Dimkpa CO, McLean JE, Latta DE, Manangón E, Britt DW, Johnson WP, Boyanov MI & Anderson AJ (2012). CuO and ZnO nanoparticles: phytotoxicity, metal speciation, and induction of oxidative stress in sand-grown wheat. Journal of Nanoparticle Research 14: 1125.

Dinesh V, Biji P, Ashok A, Dhara S, Kamruddin M, Tyagi A & Raj B (2014). Plasmon-mediated, highly enhanced photocatalytic degradation of industrial textile dyes using hybrid ZnO@ Ag core–shell nanorods. RSC Advances 4: 58930-58940.

Dobrucka R & Długaszewska J (2016). Biosynthesis and antibacterial activity of ZnO nanoparticles using Trifolium pratense flower extract. Saudi Journal of Biological Sciences 23: 517-523.

Doğaroğlu ZG & Köleli N (2017). TiO2 and ZnO nanoparticles toxicity in barley (Hordeum vulgare L.). CLEAN–Soil, Air, Water 45: 1700096.

Doonan J (1996). Plant growth: Roots in the cell cycle. Current Biology 6: 788-789.

Dormann J-L, Fiorani D & Tronc E (2007). Magnetic relaxation in fine-particle systems. Advances in Chemical Physics, Volume 98 283-494.

Du W, Sun Y, Ji R, Zhu J, Wu J & Guo H (2011). TiO 2 and ZnO nanoparticles negatively affect wheat growth and soil enzyme activities in agricultural soil. Journal of Environmental Monitoring 13: 822-828.

Du Z & Bramlage WJ (1992). Modified thiobarbituric acid assay for measuring lipid oxidation in sugar-rich plant tissue extracts. Journal of Agricultural and Food Chemistry 40: 1566-1570.

Ebadi M, Zolfaghari MR, Aghaei SS, Zargar M, Shafiei M, Zahiri HS & Noghabi KA (2019). A bio-inspired strategy for the synthesis of zinc oxide nanoparticles (ZnO NPs) using the cell extract of cyanobacterium Nostoc sp. EA03: from biological function to toxicity evaluation. RSC advances 9: 23508-23525.

Elmer WH & White JC (2016). The use of metallic oxide nanoparticles to enhance growth of tomatoes and eggplants in disease infested soil or soilless medium. Environmental Science: Nano 3: 1072-1079.

Elstner E (1991). Mechanisms of oxygen activation in different compartments of plant cells. Active Oxygen/Oxidative Stress and Plant Metabolism. 6: 13-26.

Eren E & Argüello JM (2004). Arabidopsis HMA2, a Divalent Heavy Metal-Transporting P_{IB}-Type ATPase, Is Involved in Cytoplasmic Zn²⁺ Homeostasis. Plant Physiology 136: 3712.

Espina L, Somolinos M, Lorán S, Conchello P, García D & Pagán R (2011). Chemical composition of commercial citrus fruit essential oils and evaluation of their antimicrobial activity acting alone or in combined processes. Food control 22: 896-902.

Espitia PJP, Soares NdFF, dos Reis Coimbra JS, de Andrade NJ, Cruz RS & Medeiros EAA (2012). Zinc oxide nanoparticles: synthesis, antimicrobial activity and food packaging applications. Food and bioprocess technology 5: 1447-1464.

Espitia PJP, Soares NdFF, Coimbra JSdR, de Andrade NJ, Cruz RS & Medeiros EAA (2012). Zinc Oxide Nanoparticles: Synthesis, Antimicrobial Activity and Food Packaging Applications. Food and Bioprocess Technology 5: 1447-1464.

Eulgem T & Somssich IE (2007). Networks of WRKY transcription factors in defense signaling. Current opinion in plant biology 10: 366-371.

Farooq S & Azam F (2006). The use of cell membrane stability (CMS) technique to screen for salt tolerant wheat varieties. Journal of plant physiology 163: 629-637.

Farouk A, Fikry R & Mohsen M (2016). Chemical composition and antioxidant activity of Ocimum basilicum L. essential oil cultivated in Madinah Monawara, Saudi Arabia and its comparison to the Egyptian chemotype. Journal of Essential Oil Bearing Plants 19: 1119-1128.

Fawe A, Abou-Zaid M, Menzies J & Bélanger R (1998). Silicon-mediated accumulation of flavonoid phytoalexins in cucumber. Phytopathology 88: 396-401.

Feng Y, Cui X, He S, Dong G, Chen M, Wang J & Lin X (2013). The role of metal nanoparticles in influencing arbuscular mycorrhizal fungi effects on plant growth. Environmental science & technology 47: 9496-9504.

Fonash SJ & Van de Voorde M (2018). Engineering, medicine and science at the nano-scale. John Wiley & Sons.

Fraire-Velázquez S & Balderas-Hernández VE (2013). Abiotic stress in plants and metabolic responses. Abiotic stress—plant responses and applications in agriculture. Rijeka, Croatia: InTech 25-48.

Gao L, Nie L, Wang T, Qin Y, Guo Z, Yang D & Yan X (2006). Carbon nanotube delivery of the GFP gene into mammalian cells. ChemBioChem 7: 239-242.

García-Gómez C, Obrador A, González D, Babín M & Fernández MD (2017). Comparative effect of ZnO NPs, ZnO bulk and ZnSO4 in the antioxidant defences of two plant species growing in two agricultural soils under greenhouse conditions. Science of the Total Environment 589: 11-24.

Gersten B (2005). Solvothermal synthesis of nanoparticles. Chemfiles 5: 11-12.

Ghodake G, Seo YD & Lee DS (2011). Hazardous phytotoxic nature of cobalt and zinc oxide nanoparticles assessed using Allium cepa. Journal of hazardous materials 186: 952-955.

Ghosh M, Bandyopadhyay M & Mukherjee A (2010). Genotoxicity of titanium dioxide (TiO2) nanoparticles at two trophic levels: plant and human lymphocytes. Chemosphere 81: 1253-1262.

Ghosh M, Jana A, Sinha S, Jothiramajayam M, Nag A, Chakraborty A, Mukherjee A & Mukherjee A (2016). Effects of ZnO nanoparticles in plants: cytotoxicity, genotoxicity, deregulation of antioxidant defenses, and cell-cycle arrest. Mutation Research/Genetic Toxicology and Environmental Mutagenesis 807: 25-32.

Gill SS & Tuteja N (2010). Reactive oxygen species and antioxidant machinery in abiotic stress tolerance in crop plants. Plant physiology and biochemistry 48: 909-930.

Gill SS, Khan NA, Anjum NA & Tuteja N (2011). Amelioration of cadmium stress in crop plants by nutrients management: morphological, physiological and biochemical aspects. Plant Stress 5: 1-23.

Gooding M, Ellis R, Shewry P & Schofield J (2003). Effects of restricted water availability and increased temperature on the grain filling, drying and quality of winter wheat. Journal of Cereal Science 37: 295-309.

Gupta J & Bahadur D (2018). Defect-Mediated Reactive Oxygen Species Generation in Mg-Substituted ZnO Nanoparticles: Efficient Nanomaterials for Bacterial Inhibition and Cancer Therapy. ACS Omega 3: 2956-2965.

Hackbarth S, Schlothauer J, Preuß A & Röder B (2010). New insights to primary photodynamic effects–Singlet oxygen kinetics in living cells. Journal of Photochemistry and Photobiology B: Biology 98: 173-179.

Hajra A & Mondal NK (2017). Effects of ZnO and TiO2 nanoparticles on germination, biochemical and morphoanatomical attributes of Cicer arietinum L. Energy, Ecology and Environment 2: 277-288.

Halford NG, Curtis TY, Chen Z & Huang J (2015). Effects of abiotic stress and crop management on cereal grain composition: implications for food quality and safety. Journal of experimental botany 66: 1145-1156.

Halliwell B & Gutteridge J (1984). Oxygen toxicity, oxygen radicals, transition metals and disease. Biochemical journal 219: 1.

Halliwell B & Gutteridge JM (2015). Free radicals in biology and medicine. Oxford University Press, USA.

Hancock J, Desikan R, Harrison J, Bright J, Hooley R & Neill S (2006). Doing the unexpected: proteins involved in hydrogen peroxide perception. Journal of Experimental Botany 57: 1711-1718.

Harvey D (2000). Modern analytical chemistry. McGraw-Hill New York.

Hayat S, Hayat Q, Alyemeni MN, Wani AS, Pichtel J & Ahmad A (2012). Role of proline under changing environments: a review. Plant signaling & behavior 7: 1456-1466.

Heath RL & Packer L (1968). Photoperoxidation in isolated chloroplasts: I. Kinetics and stoichiometry of fatty acid peroxidation. Archives of biochemistry and biophysics 125: 189-198.

Heiligtag FJ & Niederberger M (2013). The fascinating world of nanoparticle research. Materials Today 16: 262-271.

Hernandez-Viezcas J, Castillo-Michel H, Servin A, Peralta-Videa J & Gardea-Torresdey J (2011). Spectroscopic verification of zinc absorption and distribution in the desert plant Prosopis juliflora-velutina (velvet mesquite) treated with ZnO nanoparticles. Chemical engineering journal 170: 346-352.

Hernandez-Viezcas JA, Castillo-Michel H, Andrews JC, Cotte M, Rico C, Peralta-Videa JR, Ge Y, Priester JH, Holden PA & Gardea-Torresdey JL (2013). In situ synchrotron X-ray fluorescence mapping and speciation of CeO2 and ZnO nanoparticles in soil cultivated soybean (Glycine max). ACS nano 7: 1415-1423.

Hernández I, Alegre L & Munné-Bosch S (2004). Drought-induced changes in flavonoids and other low molecular weight antioxidants in Cistus clusii grown under Mediterranean field conditions. Tree physiology 24: 1303-1311.

Ho C-L, Teo S-S, Rahim RA & Phang S-M (2010). Transcripts of Gracilaria changii that improve copper tolerance of Escherichia coli. Asia-Pacific Journal of Molecular Biology and Biotechnology 18: 315-319.

Hossain MA & Fujita M (2010). Evidence for a role of exogenous glycinebetaine and proline in antioxidant defense and methylglyoxal detoxification systems in mung bean seedlings under salt stress. Physiology and Molecular Biology of Plants 16: 19-29.

Hossain Z, Mustafa G, Sakata K & Komatsu S (2016). Insights into the proteomic response of soybean towards Al2O3, ZnO, and Ag nanoparticles stress. Journal of hazardous materials 304: 291-305.

Hu C, Liu X, Li X & Zhao Y (2014). Evaluation of growth and biochemical indicators of Salvinia natans exposed to zinc oxide nanoparticles and zinc accumulation in plants. Environmental Science and Pollution Research 21: 732-739.

Huang S, Van Aken O, Schwarzländer M, Belt K & Millar AH (2016). The Roles of Mitochondrial Reactive Oxygen Species in Cellular Signaling and Stress Response in Plants. Plant physiology 171: 1551-1559.

Hussein MZ, Azmin WHWN, Mustafa M & Yahaya AH (2009). Bacillus cereus as a biotemplating agent for the synthesis of zinc oxide with raspberry-and plate-like structures. Journal of inorganic biochemistry 103: 1145-1150.

Huttel Y, Martínez L, Mayoral A & Fernández I (2018). Gas-phase synthesis of nanoparticles: present status and perspectives. MRS Communications 8: 947-954.

Ibrahim NA, El-Sakhawy FS, Mohammed MM, Farid MA, Abdel-Wahed NA & Deabes DA (2015). Chemical composition, antimicrobial and antifungal activities of essential oils of the leaves of Aegle marmelos (L.) Correa growing in Egypt. Journal of Applied Pharmaceutical Science 5: 001-005.

Ingale AG & Chaudhari A (2013). Biogenic synthesis of nanoparticles and potential applications: An eco-friendly approach. Journal of Nanomedicine & Nanotechnology 2013.

Iskandar F (2009). Nanoparticle processing for optical applications–A review. Advanced Powder Technology 20: 283-292.

Ismail RA, Ali AK, Ismail MM & Hassoon KI (2011). Preparation and characterization of colloidal ZnO nanoparticles using nanosecond laser ablation in water. Applied Nanoscience 1: 45-49.

Iwashina T (2003). Flavonoid function and activity to plants and other organisms. Biological Sciences in Space 17: 24-44.

Jacob S, Bharathkumar R & Ashwathram G (2014). Aspergillus niger mediated synthesis of ZnO nanoparticles and their antimicrobial and in vitro anticancerous activity. World J. Pharm. Res 3: 3044-3054.

Jain AK, Singh D, Dubey K, Maurya R & Pandey AK (2018). Chapter Four - Chromosomal Aberrations. Mutagenicity: Assays and Applications,(Kumar A, Dobrovolsky VN, Dhawan A & Shanker R, ed.^eds.), p.^pp. 69-92. Academic Press.

Jain N, Bhargava A, Tarafdar JC, Singh SK & Panwar J (2013). A biomimetic approach towards synthesis of zinc oxide nanoparticles. Appl Microbiol Biotechnol 97: 859-869.

Jain S & Mehata MS (2017). Medicinal Plant Leaf Extract and Pure Flavonoid Mediated Green Synthesis of Silver Nanoparticles and their Enhanced Antibacterial Property. Scientific Reports 7: 15867.

Jaiswal L, Shankar S & Rhim J-W (2019). Chapter 3 - Applications of nanotechnology in food microbiology. Methods in Microbiology, Vol. 46 (Gurtler V, Ball AS & Soni S, ed.^eds.), p.^pp. 43-60. Academic Press.

Jansen MA, van den Noort RE, Tan MA, Prinsen E, Lagrimini LM & Thorneley RN (2001). Phenol-oxidizing peroxidases contribute to the protection of plants from ultraviolet radiation stress. Plant Physiology 126: 1012-1023.

Javaid MM, Florentine S, Ali HH & Weller S (2018). Effect of environmental factors on the germination and emergence of Salvia verbenaca L. cultivars (verbenaca and vernalis): An invasive species in semi-arid and arid rangeland regions. PLoS One 13: e0194319.

Javed R, Usman M, Yücesan B, Zia M & Gürel E (2017). Effect of zinc oxide (ZnO) nanoparticles on physiology and steviol glycosides production in micropropagated shoots of Stevia rebaudiana Bertoni. Plant Physiology and Biochemistry 110: 94-99.

Jayaseelan C, Rahuman AA, Kirthi AV, Marimuthu S, Santhoshkumar T, Bagavan A, Gaurav K, Karthik L & Rao KVB (2012). Novel microbial route to synthesize ZnO nanoparticles using Aeromonas hydrophila and their activity against pathogenic bacteria and fungi. Spectrochimica Acta Part A: Molecular and Biomolecular Spectroscopy 90: 78-84.

Jha AK & Prasad K (2016). Synthesis of ZnO Nanoparticles from Goat Slaughter waste for Environmental Protection.

Jiang J, Pi J & Cai J (2018). The Advancing of Zinc Oxide Nanoparticles for Biomedical Applications. Bioinorg Chem Appl 2018: 1062562.

Jiang J, Pi J & Cai J (2018). The advancing of zinc oxide nanoparticles for biomedical applications. Bioinorg Chem Appl 2018.

Jin XF, Yang XE, Islam E, Liu D, Mahmood Q, Li H & Li J (2008). Ultrastructural changes, zinc hyperaccumulation and its relation with antioxidants in two ecotypes of Sedum alfredii Hance. Plant Physiology and Biochemistry 46: 997-1006.

Jones CG, Hare JD & Compton SJ (1989). Measuring plant protein with the Bradford assay. Journal of chemical ecology 15: 979-992.

Judy JD (2013). Bioavailability of manufactured nanomaterials in terrestrial ecosystems.

Kahrilas GA, Wally LM, Fredrick SJ, Hiskey M, Prieto AL & Owens JE (2014). Microwave-Assisted Green Synthesis of Silver Nanoparticles Using Orange Peel Extract. ACS Sustainable Chemistry & Engineering 2: 367-376.

Karatutlu A, Barhoum A & Sapelkin A (2018). Chapter 1 - Liquid-phase synthesis of nanoparticles and nanostructured materials. Emerging Applications of Nanoparticles and Architecture Nanostructures,(Barhoum A & Makhlouf ASH, ed.^eds.), p.^pp. 1-28. Elsevier.

Kato M & Shimizu S (1985). Chlorophyll metabolism in higher plants VI. Involvement of peroxidase in chlorophyll degradation. Plant and cell physiology 26: 1291-1301.

Kaviya S, Santhanalakshmi J, Viswanathan B, Muthumary J & Srinivasan K (2011). Biosynthesis of silver nanoparticles using Citrus sinensis peel extract and its antibacterial activity. Spectrochimica Acta Part A: Molecular and Biomolecular Spectroscopy 79: 594-598.

Kazeminezhad I, Sadollahkhani A & Farbod M (2013). Synthesis of ZnO nanoparticles and flower-like nanostructures using nonsono- and sono-electrooxidation methods. Materials Letters 92: 29-32.

Keunen E, Peshev D, Vangronsveld J, Van Den Ende W & Cuypers A (2013). Plant sugars are crucial players in the oxidative challenge during abiotic stress: extending the traditional concept. Plant, cell & environment 36: 1242-1255.

Khan MA, Khan T & Nadhman A (2016). Applications of plant terpenoids in the synthesis of colloidal silver nanoparticles. Advances in colloid and interface science.

Khan MF, Ansari AH, Hameedullah M, Ahmad E, Husain FM, Zia Q, Baig U, Zaheer MR, Alam MM & Khan AM (2016). Sol-gel synthesis of thorn-like ZnO nanoparticles endorsing mechanical stirring effect and their antimicrobial activities: Potential role as nano-antibiotics. Scientific Reports 6.

Khan MF, Ansari AH, Hameedullah M, Ahmad E, Husain FM, Zia Q, Baig U, Zaheer MR, Alam MM & Khan AM (2016). Sol-gel synthesis of thorn-like ZnO nanoparticles endorsing mechanical stirring effect and their antimicrobial activities: Potential role as nano-antibiotics. Scientific reports 6: 27689.

Khan T, Khan MA & Nadhman A (2015). Synthesis in plants and plant extracts of silver nanoparticles with potent antimicrobial properties: current status and future prospects. Applied microbiology and biotechnology 99: 9923-9934.

Khot LR, Sankaran S, Maja JM, Ehsani R & Schuster EW (2012). Applications of nanomaterials in agricultural production and crop protection: a review. Crop protection 35: 64-70.

Kim HW, Kwon YJ, Mirzaei A, Kang SY, Choi MS, Bang JH & Kim SS (2017). Synthesis of zinc oxide semiconductors-graphene nanocomposites by microwave irradiation for application to gas sensors. Sensors and Actuators B: Chemical 249: 590-601.

Kim MJ, Ciani S & Schachtman DP (2010). A peroxidase contributes to ROS production during Arabidopsis root response to potassium deficiency. Molecular Plant 3: 420-427.

Kim S, Kim J & Lee I (2011). Effects of Zn and ZnO nanoparticles and Zn2+ on soil enzyme activity and bioaccumulation of Zn in Cucumis sativus. Chemistry and Ecology 27: 49-55.

Klaus T, Joergere R, Olsson E & Granqvist C (2001). Trends Biotechnol. 19: 15. doi: 10.1016. S0167-7799 (00) 01514-01516.

Kolthoff I (1932). Theory of coprecipitation. The formation and properties of crystalline precipitates. The Journal of Physical Chemistry 36: 860-881.

Kon K, Kratosova G, Duran N, Ingle A & Rai M (2015). Fungi as an efficient mycosystem for the synthesis of metal nanoparticles: Progress and key aspects of research.

Kong X, Pan J, Zhang M, Xing X, Zhou Y, Liu Y, Li D & Li D (2011). ZmMKK4, a novel group C mitogen-activated protein kinase kinase in maize (Zea mays), confers salt and cold tolerance in transgenic Arabidopsis. Plant, cell & environment 34: 1291-1303.

Konwarh R, Gogoi B, Philip R, Laskar M & Karak N (2011). Biomimetic preparation of polymer-supported free radical scavenging, cytocompatible and antimicrobial "green" silver nanoparticles using aqueous extract of Citrus sinensis peel. Colloids and Surfaces B: Biointerfaces 84: 338-345.

Kou H, Jia L & Wang C (2012). Electrochemical deposition of flower-like ZnO nanoparticles on a silver-modified carbon nanotube/polyimide membrane to improve its photoelectric activity and photocatalytic performance. Carbon 50: 3522-3529.

Koupaei MH, Shareghi B, Saboury AA, Davar F, Semnani A & Evini M (2016). Green synthesis of zinc oxide nanoparticles and their effect on the stability and activity of proteinase K. RSC Advances 6: 42313-42323.

Krieger-Liszkay A, Fufezan C & Trebst A (2008). Singlet oxygen production in photosystem II and related protection mechanism. Photosynthesis Research 98: 551-564.

Kruszewski M, Brzoska K, Brunborg G, Asare N, Dobrzyńska M, Dušinská M, Fjellsbø LM, Georgantzopoulou A, Gromadzka-Ostrowska J & Gutleb AC (2011). Toxicity of silver nanomaterials in higher eukaryotes. Advances in molecular toxicology, Vol. 5 ed.^eds.), p.^pp. 179-218. Elsevier.

Kumar RR, Sharma SK, Goswami S, Singh K, Gadpayle KA, Singh GP, Pathak H & Rai RD (2013). Transcript profiling and biochemical characterization of mitochondrial superoxide dismutase (mtSOD) in wheat (Triticum aestivum) under different exogenous stresses. Australian Journal of Crop Science 7: 414.

Kumari M, Khan SS, Pakrashi S, Mukherjee A & Chandrasekaran N (2011). Cytogenetic and genotoxic effects of zinc oxide nanoparticles on root cells of Allium cepa. Journal of hazardous materials 190: 613-621.

Kumari R, Sahai A & Goswami N (2015). Effect of nitrogen doping on structural and optical properties of ZnO nanoparticles. Progress in Natural Science: Materials International 25: 300-309.

Lagacé M & Matton DP (2004). Characterization of a WRKY transcription factor expressed in late torpedo-stage embryos of Solanum chacoense. Planta 219: 185-189.

Lagha-Benamrouche S & Madani K (2013). Phenolic contents and antioxidant activity of orange varieties (Citrus sinensis L. and Citrus aurantium L.) cultivated in Algeria: Peels and leaves. Industrial Crops and Products 50: 723-730.

Landa P, Vankova R, Andrlova J, Hodek J, Marsik P, Storchova H, White JC & Vanek T (2012). Nanoparticle-specific changes in Arabidopsis thaliana gene expression after exposure to ZnO, TiO2, and fullerene soot. Journal of hazardous materials 241: 55-62.

Lanot A & Morris P (2005). Elicitation of isoflavan phytoalexins. Lotus japonicus handbook,ed.^eds.), p.^pp. 355-361. Springer.

Latha PP & Kumari RS (2016). Toxicity and Environmental Risks of Nanomaterials: Challenges and Future Needs. Indian Journal of Research in Pharmacy and Biotechnology 4: 247.

Lee S, Chung H, Kim S & Lee I (2013). The genotoxic effect of ZnO and CuO nanoparticles on early growth of buckwheat, Fagopyrum esculentum. Water, Air, & Soil Pollution 224: 1668.

Lin D & Xing B (2007). Phytotoxicity of nanoparticles: inhibition of seed germination and root growth. Environmental Pollution 150: 243-250.

Lin D & Xing B (2008). Root uptake and phytotoxicity of ZnO nanoparticles. Environmental science & technology 42: 5580-5585.

Liu H, Luo M & Wen J-k (2014). mRNA stability in the nucleus. Journal of Zhejiang University SCIENCE B 15: 444-454.

Liu N, Wang Y, Ge F, Liu S & Xiao H (2018). Antagonistic effect of nano-ZnO and cetyltrimethyl ammonium chloride on the growth of Chlorella vulgaris: Dissolution and accumulation of nano-ZnO. Chemosphere 196: 566-574.

Liu R & Lal R (2015). Potentials of engineered nanoparticles as fertilizers for increasing agronomic productions. Science of the total environment 514: 131-139.

Liu R, Zhang H & Lal R (2016). Effects of stabilized nanoparticles of copper, zinc, manganese, and iron oxides in low concentrations on lettuce (Lactuca sativa) seed germination: nanotoxicants or nanonutrients? Water, Air, & Soil Pollution 227: 42.

López-Moreno ML, de la Rosa G, Cruz-Jiménez G, Castellano L, Peralta-Videa JR & Gardea-Torresdey JL (2017). Effect of ZnO nanoparticles on corn seedlings at different temperatures; X-ray absorption spectroscopy and ICP/OES studies. Microchemical Journal 134: 54-61.

Lu AH, Salabas EeL & Schüth F (2007). Magnetic nanoparticles: synthesis, protection, functionalization, and application. Angewandte Chemie International Edition 46: 1222-1244.

Lv J, Zhang S, Luo L, Zhang J, Yang K & Christie P (2015). Accumulation, speciation and uptake pathway of ZnO nanoparticles in maize. Environmental Science: Nano 2: 68-77.

Ma C, Rui Y, Liu S, Li X, Xing B & Liu L (2015). Phytotoxic mechanism of nanoparticles: destruction of chloroplasts and vascular bundles and alteration of nutrient absorption. Scientific reports 5: 11618.

Ma H, Williams PL & Diamond SA (2013). Ecotoxicity of manufactured ZnO nanoparticles–a review. Environmental Pollution 172: 76-85.

Mahajan P, Dhoke S & Khanna A (2011). Effect of nano-ZnO particle suspension on growth of mung (Vigna radiata) and gram (Cicer arietinum) seedlings using plant agar method. Journal of Nanotechnology 2011.

Makarov V, Love A, Sinitsyna O, Makarova S, Yaminsky I, Taliansky M & Kalinina N (2014). “Green” nanotechnologies: synthesis of metal nanoparticles using plants. Acta Naturae (англоязычная версия) 6.

Manivannan P, Jaleel CA, Somasundaram R & Panneerselvam R (2008). Osmoregulation and antioxidant metabolism in drought-stressed Helianthus annuus under triadimefon drenching. Comptes Rendus Biologies 331: 418-425.

Manmathan H & Lapitan N (2013). Measuring Germination Percentage in Wheat. Bio-protocol 3: e866.

Mantzaris NV (2005). Liquid-phase synthesis of nanoparticles: Particle size distribution dynamics and control. Chemical Engineering Science 60: 4749-4770.

Marcovich A & Shinn T (2014). Toward a new dimension: Exploring the nanoscale. Oxford University Press, USA.

Marschner H (1995). Mineral nutrition of higher plants. 2nd. Edn. Academic Pres.

Martínez-Fernández D, Barroso D & Komárek M (2016). Root water transport of Helianthus annuus L. under iron oxide nanoparticle exposure. Environmental Science and Pollution Research 23: 1732-1741.

Mayo DW, Miller FA & Hannah RW (2004). Course notes on the interpretation of infrared and Raman spectra. John Wiley & Sons.

McNear Jr D (2015). The rhizosphere–roots, soil and everything in between. Nat Educ Knowl 4 (3): 1. ed.^eds.), p.^pp.

Medina-Velo IA, Dominguez OE, Ochoa L, Barrios AC, Hernández-Viezcas JA, White JC, Peralta-Videa JR & Gardea-Torresdey JL (2017). Nutritional quality of bean seeds harvested from plants grown in different soils amended with coated and uncoated zinc oxide nanomaterials. Environmental Science: Nano 4: 2336-2347.

Menezes-Benavente L, Teixeira FK, Kamei CLA & Margis-Pinheiro M (2004). Salt stress induces altered expression of genes encoding antioxidant enzymes in seedlings of a Brazilian indica rice (Oryza sativa L.). Plant Science 166: 323-331.

Meng X-H, Liu C, Fan R, Zhu L-F, Yang S-X, Zhu H-T, Wang D, Yang C-R & Zhang Y-J (2017). Antioxidative Flavan-3-ol Dimers from the Leaves of Camellia fangchengensis. Journal of agricultural and food chemistry 66: 247-254.

Michalak A (2006). Phenolic compounds and their antioxidant activity in plants growing under heavy metal stress. Polish Journal of Environmental Studies 15.

Milani N, McLaughlin MJ, Stacey SP, Kirby JK, Hettiarachchi GM, Beak DG & Cornelis G (2012). Dissolution kinetics of macronutrient fertilizers coated with manufactured zinc oxide nanoparticles. Journal of agricultural and food chemistry 60: 3991-3998.

Miller G, Suzuki N, Ciftci-Yilmaz S & Mittler R (2010). Reactive oxygen species homeostasis and signalling during drought and salinity stresses. Plant, cell & environment 33: 453-467.

Mills RF, Peaston KA, Runions J & Williams LE (2012). HvHMA2, a P1B-ATPase from Barley, Is Highly Conserved among Cereals and Functions in Zn and Cd Transport. PLOS ONE 7: e42640.

Mirzajani F, Askari H, Hamzelou S, Schober Y, Römpp A, Ghassempour A & Spengler B (2014). Proteomics study of silver nanoparticles toxicity on Oryza sativa L. Ecotoxicology and environmental safety 108: 335-339.

Mittler R Oxidative stress, antioxidants and stress tolerance Trends Plant Sci 2002 7. ed.^eds.), p.^pp. N.

Mittler R (2002). Oxidative stress, antioxidants and stress tolerance. Trends in plant science 7: 405-410.

Mohamad NAN, Arham NA, Jai J & Hadi A (2014). Plant extract as reducing agent in synthesis of metallic nanoparticles: a review. Vol. 832 ed.^eds.), p.^pp. 350-355. Trans Tech Publ.

Mohammadi R, Maali-Amiri R & Abbasi A (2013). Effect of TiO 2 nanoparticles on chickpea response to cold stress. Biological trace element research 152: 403-410.

Møller IM & Kristensen BK (2004). Protein oxidation in plant mitochondria as a stress indicator. Photochemical & photobiological sciences 3: 730-735.

Montillet J-L, Chamnongpol S, Rustérucci C, Dat J, Van De Cotte B, Agnel J-P, Battesti C, Inzé D, Van Breusegem F & Triantaphylides C (2005). Fatty acid hydroperoxides and H2O2 in the execution of hypersensitive cell death in tobacco leaves. Plant physiology 138: 1516-1526.

Morandi D, Branzanti B & Gianinazzi-Pearson V (1992). Effect of some plant flavonoids on in vitro behaviour of an arbuscular mycorrhizal fungus. Agronomie 12: 811-816.

Mosa KA, El-Naggar M, Ramamoorthy K, Alawadhi H, Elnaggar A, Wartanian S, Ibrahim E & Hani H (2018). Copper Nanoparticles Induced Genotoxicty, Oxidative Stress, and Changes in Superoxide Dismutase (SOD) Gene Expression in Cucumber (Cucumis sativus) Plants. Frontiers in Plant Science 9.

Mousavi Kouhi SM, Lahouti M, Ganjeali A & Entezari MH (2014). Comparative phytotoxicity of ZnO nanoparticles, ZnO microparticles, and Zn2+ on rapeseed (Brassica napus L.): investigating a wide range of concentrations. Toxicological & Environmental Chemistry 96: 861-868.

Mukherjee A, Sun Y, Morelius E, Tamez C, Bandyopadhyay S, Niu G, White JC, Peralta-Videa JR & Gardea-Torresdey JL (2016). Differential toxicity of bare and hybrid ZnO nanoparticles in green pea (Pisum sativum L.): A life cycle study. Frontiers in Plant Science 6: 1242.

Munzuroglu O & Geckil H (2002). Effects of metals on seed germination, root elongation, and coleoptile and hypocotyl growth in Triticum aestivum and Cucumis sativus. Archives of Environmental Contamination and Toxicology 43: 203-213.

Murdock RC, Braydich-Stolle L, Schrand AM, Schlager JJ & Hussain SM (2008). Characterization of nanomaterial dispersion in solution prior to in vitro exposure using dynamic light scattering technique. Toxicological sciences 101: 239-253.

Nagaonkar D, Shende S & Rai M (2015). Biosynthesis of copper nanoparticles and its effect on actively dividing cells of mitosis in Allium cepa. Biotechnology progress 31: 557-565.

Natarajan AT (2002). Chromosome aberrations: past, present and future. Mutation Research/Fundamental and Molecular Mechanisms of Mutagenesis 504: 3-16.

Nava OJ, Soto-Robles CA, Gómez-Gutiérrez CM, Vilchis-Nestor AR, Castro-Beltrán A, Olivas A & Luque PA (2017). Fruit peel extract mediated green synthesis of zinc oxide nanoparticles. Journal of Molecular Structure 1147: 1-6.

Naveed Ul Haq A, Nadhman A, Ullah I, Mustafa G, Yasinzai M & Khan I (2017). Synthesis Approaches of Zinc Oxide Nanoparticles: The Dilemma of Ecotoxicity. Journal of Nanomaterials 2017: 8510342.

Nayantara & Kaur P (2018). Biosynthesis of nanoparticles using eco-friendly factories and their role in plant pathogenicity: a review. Biotechnology Research and Innovation 2: 63-73.

Nishizawa A, Yabuta Y & Shigeoka S (2008). Galactinol and raffinose constitute a novel function to protect plants from oxidative damage. Plant physiology 147: 1251-1263.

NIU CF, Wei W, ZHOU QY, TIAN AG, HAO YJ, ZHANG WK, Ma B, Lin Q, ZHANG ZB & ZHANG JS (2012). Wheat WRKY genes TaWRKY2 and TaWRKY19 regulate abiotic stress tolerance in transgenic Arabidopsis plants. Plant, cell & environment 35: 1156-1170.

Noctor G, Veljovic-Jovanovic S, Driscoll S, Novitskaya L & Foyer CH (2002). Drought and oxidative load in the leaves of C3 plants: a predominant role for photorespiration? Annals of Botany 89: 841-850.

Olorunfemi D, Duru E & Okieimen F (2012). Induction of chromosome aberrations in Allium cepa L. root tips on exposure to ballast water. Caryologia 65: 147-151.

Omran BA, Nassar HN, Fatthallah NA, Hamdy A, El-Shatoury EH & El-Gendy NS (2018). Waste upcycling of Citrus sinensis peels as a green route for the synthesis of silver nanoparticles. Energy Sources, Part A: Recovery, Utilization, and Environmental Effects 40: 227-236.

Ordonez A, Gomez J & Vattuone M (2006). Antioxidant activities of Sechium edule (Jacq.) Swartz extracts. Food chemistry 97: 452-458.

Paino IMM, J. Gonçalves F, Souza FL & Zucolotto V (2016). Zinc Oxide Flower-Like Nanostructures That Exhibit Enhanced Toxicology Effects in Cancer Cells. ACS Applied Materials & Interfaces 8: 32699-32705.

Patnaik P (2004). Dean's analytical chemistry handbook. McGraw-Hill New York.

Peer W & Murphy AS (2006). Flavonoids as signal molecules: targets of flavonoid action. The science of flavonoids,ed.^eds.), p.^pp. 239-268. Springer.

Peralta-Videa JR, Hernandez-Viezcas JA, Zhao L, Diaz BC, Ge Y, Priester JH, Holden PA & Gardea-Torresdey JL (2014). Cerium dioxide and zinc oxide nanoparticles alter the nutritional value of soil cultivated soybean plants. Plant physiology and biochemistry 80: 128-135.

Pérez-de-Luque A (2017). Interaction of Nanomaterials with Plants: What Do We Need for Real Applications in Agriculture? Frontiers in Environmental Science 5: 12.

Pérez-de-Luque A (2017). Interaction of Nanomaterials with Plants: What Do We Need for Real Applications in Agriculture? Frontiers in Environmental Science 5.

Pokhrel LR & Dubey B (2013). Evaluation of developmental responses of two crop plants exposed to silver and zinc oxide nanoparticles. Science of the Total Environment 452: 321-332.

Prakash MG & Chung IM (2016). Determination of zinc oxide nanoparticles toxicity in root growth in wheat (Triticum aestivum L.) seedlings. Acta Biologica Hungarica 67: 286-296.

Prasannan A & Imae T (2013). One-Pot Synthesis of Fluorescent Carbon Dots from Orange Waste Peels. Industrial & Engineering Chemistry Research 52: 15673-15678.

Preston RJ (2014). Chromosome Aberrations. Encyclopedia of Toxicology (Third Edition),(Wexler P, ed.^eds.), p.^pp. 955-958. Academic Press, Oxford.

Qiao K, Gong L, Tian Y, Wang H & Chai T (2018). The metal-binding domain of wheat heavy metal ATPase 2 (TaHMA2) is involved in zinc/cadmium tolerance and translocation in Arabidopsis. Plant cell reports 37: 1343-1352.

Rai P, Kwak W-K & Yu Y-T (2013). Solvothermal synthesis of ZnO nanostructures and their morphology-dependent gas-sensing properties. ACS applied materials & interfaces 5: 3026-3032.

Raliya R, Nair R, Chavalmane S, Wang W-N & Biswas P (2015). Mechanistic evaluation of translocation and physiological impact of titanium dioxide and zinc oxide nanoparticles on the tomato (Solanum lycopersicum L.) plant. Metallomics 7: 1584-1594.

Rao KG, Ashok C, Rao KV, Chakra CS & Rajendar V (2015). Synthesis of TiO2 nanoparticles from orange fruit waste. Synthesis 2: 1.

Rao S & Shekhawat G (2014). Toxicity of ZnO engineered nanoparticles and evaluation of their effect on growth, metabolism and tissue specific accumulation in Brassica juncea. Journal of Environmental Chemical Engineering 2: 105-114.

Rao S & Shekhawat GS (2016). Phytotoxicity and oxidative stress perspective of two selected nanoparticles in Brassica juncea. 3 Biotech 6: 244-244.

Raskar S & Laware S (2014). Effect of zinc oxide nanoparticles on cytology and seed germination in onion. Int J Curr Microbiol App Sci 3: 467-473.

Rehan M, Abdel-Wahed NAM, Farouk A & El-Zawahry MM (2018). Extraction of Valuable Compounds from Orange Peel Waste for Advanced Functionalization of Cellulosic Surfaces. ACS Sustainable Chemistry & Engineering 6: 5911-5928.

Rejman J, Oberle V, Zuhorn IS & Hoekstra D (2004). Size-dependent internalization of particles via the pathways of clathrin-and caveolae-mediated endocytosis. Biochemical journal 377: 159.

Rico C, Peralta-Videa J & Gardea-Torresdey J (2015). Chemistry, biochemistry of nanoparticles, and their role in antioxidant defense system in plants. Nanotechnology and Plant Sciences,ed.^eds.), p.^pp. 1-17. Springer.

Rico CM, Majumdar S, Duarte-Gardea M, Peralta-Videa JR & Gardea-Torresdey JL (2011). Interaction of nanoparticles with edible plants and their possible implications in the food chain. Journal of agricultural and food chemistry 59: 3485-3498.

Ruus A, Schaanning M, Øxnevad S & Hylland K (2005). Experimental results on bioaccumulation of metals and organic contaminants from marine sediments. Aquatic toxicology 72: 273-292.

Sabo-Attwood T, Unrine JM, Stone JW, Murphy CJ, Ghoshroy S, Blom D, Bertsch PM & Newman LA (2012). Uptake, distribution and toxicity of gold nanoparticles in tobacco (Nicotiana xanthi) seedlings. Nanotoxicology 6: 353-360.

Salah N, Habib SS, Khan ZH, Memic A, Azam A, Alarfaj E, Zahed N & Al-Hamedi S (2011). High-energy ball milling technique for ZnO nanoparticles as antibacterial material. International journal of nanomedicine 6: 863.

Salah N, Habib SS, Khan ZH, Memic A, Azam A, Alarfaj E, Zahed N & Al-Hamedi S (2011). High-energy ball milling technique for ZnO nanoparticles as antibacterial material. International Journal of Nanomedicine 6: 863-869.

Salah SM, Yajing G, Dongdong C, Jie L, Aamir N, Qijuan H, Weimin H, Mingyu N & Jin H (2015). Seed priming with polyethylene glycol regulating the physiological and molecular mechanism in rice (Oryza sativa L.) under nano-ZnO stress. Scientific reports 5: 14278.

Scandalios J (2005). Oxidative stress: molecular perception and transduction of signals triggering antioxidant gene defenses. Brazilian Journal of Medical and Biological Research 38: 995-1014.

Schröck E, Du Manoir S, Veldman T, Schoell B, Wienberg J, Ferguson-Smith M, Ning Y, Ledbetter D, Bar-Am I & Soenksen D (1996). Multicolor spectral karyotyping of human chromosomes. Science 273: 494-497.

Sharma P, Jha AB, Dubey RS & Pessarakli M (2012). Reactive oxygen species, oxidative damage, and antioxidative defense mechanism in plants under stressful conditions. Journal of botany 2012.

Shaymurat T, Gu J, Xu C, Yang Z, Zhao Q, Liu Y & Liu Y (2012). Phytotoxic and genotoxic effects of ZnO nanoparticles on garlic (Allium sativum L.): a morphological study. Nanotoxicology 6: 241-248.

Shen C, James SA, de Jonge MD, Turney TW, Wright PF & Feltis BN (2013). Relating cytotoxicity, zinc ions, and reactive oxygen in ZnO nanoparticle–exposed human immune cells. toxicological sciences 136: 120-130.

Shen Y, Li J, Gu R, Yue L, Zhan X & Xing B (2017). Phenanthrene-triggered Chlorosis is caused by elevated Chlorophyll degradation and leaf moisture. Environmental pollution 220: 1311-1321.

Shimoji H & Yamasaki H (2005). Inhibitory effects of flavonoids on alternative respiration of plant mitochondria. Biologia plantarum 49: 117-119.

Shoeb M, Singh BR, Khan JA, Khan W, Singh BN, Singh HB & Naqvi AH (2013). ROS-dependent anticandidal activity of zinc oxide nanoparticles synthesized by using egg albumen as a biotemplate. Advances in Natural Sciences: Nanoscience and Nanotechnology 4: 035015.

Siddiqui MH, Al-Whaibi MH, Faisal M & Al Sahli AA (2014). Nano-silicon dioxide mitigates the adverse effects of salt stress on Cucurbita pepo L. Environmental toxicology and chemistry 33: 2429-2437.

Singh AK (2015). Engineered nanoparticles: structure, properties and mechanisms of toxicity. Academic Press.

Spengler A, Wanninger L & Pflugmacher S (2017). Oxidative stress mediated toxicity of TiO2 nanoparticles after a concentration and time dependent exposure of the aquatic macrophyte Hydrilla verticillata. Aquatic Toxicology 190: 32-39.

Sriprapat W, Kullavanijaya S, Techkarnjanaruk S & Thiravetyan P (2011). Diethylene glycol removal by Echinodorus cordifolius (L.): The role of plant–microbe interactions. Journal of hazardous materials 185: 1066-1072.

Subbaiah LV, Prasad TNVKV, Krishna TG, Sudhakar P, Reddy BR & Pradeep T (2016). Novel effects of nanoparticulate delivery of zinc on growth, productivity, and zinc biofortification in maize (Zea mays L.). Journal of agricultural and food chemistry 64: 3778-3788.

Sudhakar P, Latha P & Reddy P (2016). Phenotyping crop plants for physiological and biochemical traits. Academic Press.

Suman T, Rajasree SR & Kirubagaran R (2015). Evaluation of zinc oxide nanoparticles toxicity on marine algae Chlorella vulgaris through flow cytometric, cytotoxicity and oxidative stress analysis. Ecotoxicology and environmental safety 113: 23-30.

Sun J, Lin H, Zhang S, Lin Y, Wang H, Lin M, Hung Y-C & Chen Y (2018). The roles of ROS production-scavenging system in Lasiodiplodia theobromae (Pat.) Griff. & Maubl.-induced pericarp browning and disease development of harvested longan fruit. Food chemistry 247: 16-22.

Sun TY, Gottschalk F, Hungerbühler K & Nowack B (2014). Comprehensive probabilistic modelling of environmental emissions of engineered nanomaterials. Environmental pollution 185: 69-76.

Sun Z, Xiong T, Zhang T, Wang N, Chen D & Li S (2019). Influences of zinc oxide nanoparticles on Allium cepa root cells and the primary cause of phytotoxicity. Ecotoxicology 28: 175-188.

Taheri M, Qarache H, Qarache A & Yoosefi M (2015). The Effects of Zinc-Oxide Nanoparticles on Growth Parameters of Corn (SC704). STEM Fellowship Journal 1: 17-20.

Tan J, Wang J, Chai T, Zhang Y, Feng S, Li Y, Zhao H, Liu H & Chai X (2013). Functional analyses of T a HMA 2, a P 1B-type ATP ase in wheat. Plant biotechnology journal 11: 420-431.

Tanou G, Molassiotis A & Diamantidis G (2009). Induction of reactive oxygen species and necrotic death-like destruction in strawberry leaves by salinity. Environmental and experimental botany 65: 270-281.

Taylor AF, Rylott EL, Anderson CW & Bruce NC (2014). Investigating the toxicity, uptake, nanoparticle formation and genetic response of plants to gold. PLOS one 9: e93793.

Temin HM (1995). Genetics of Retroviruses a. Annals of the New York Academy of Sciences 758: 161-165.

Thi TUD, Nguyen TT, Thi YD, Thi KHT, Phan BT & Pham KN (2020). Green synthesis of ZnO nanoparticles using orange fruit peel extract for antibacterial activities. RSC Advances 10: 23899-23907.

Thrane J-E, Kyle M, Striebel M, Haande S, Grung M, Rohrlack T & Andersen T (2015). Spectrophotometric analysis of pigments: a critical assessment of a high-throughput method for analysis of algal pigment mixtures by spectral deconvolution. PloS one 10: e0137645.

Tigli O & Juhala J (2011). ZnO nanowire growth by physical vapor deposition. ed.^eds.), p.^pp. 608-611. IEEE.

Tiwari V, Mishra N, Gadani K, Solanki PS, Shah NA & Tiwari M (2018). Mechanism of Anti-bacterial Activity of Zinc Oxide Nanoparticle Against Carbapenem-Resistant Acinetobacter baumannii. Frontiers in Microbiology 9.

Tripathi DK, Singh S, Singh S, Pandey R, Singh VP, Sharma NC, Prasad SM, Dubey NK & Chauhan DK (2017). An overview on manufactured nanoparticles in plants: uptake, translocation, accumulation and phytotoxicity. Plant Physiology and Biochemistry 110: 2-12.

Tripathi DK, Shweta, Singh S, Singh S, Pandey R, Singh VP, Sharma NC, Prasad SM, Dubey NK & Chauhan DK (2017). An overview on manufactured nanoparticles in plants: Uptake, translocation, accumulation and phytotoxicity. Plant Physiology and Biochemistry 110: 2-12.

Tripathi DK, Mishra RK, Singh S, Singh S, Singh VP, Singh PK, Chauhan DK, Prasad SM, Dubey N & Pandey AC (2017). Nitric oxide ameliorates zinc oxide nanoparticles phytotoxicity in wheat seedlings: implication of the ascorbate-glutathione cycle. Frontiers in plant science 8: 1.

Tripathy N, Hong T-K, Ha K-T, Jeong H-S & Hahn Y-B (2014). Effect of ZnO nanoparticles aggregation on the toxicity in RAW 264.7 murine macrophage. Journal of hazardous materials 270: 110-117.

Tripoli E, La Guardia M, Giammanco S, Di Majo D & Giammanco M (2007). Citrus flavonoids: Molecular structure, biological activity and nutritional properties: A review. Food chemistry 104: 466-479.

Ueda M, Zhang Z & Laux T (2011). Transcriptional activation of Arabidopsis axis patterning genes WOX8/9 links zygote polarity to embryo development. Developmental cell 20: 264-270.

Uhm YR, Han BS, Lee MK, Hong SJ & Rhee CK (2007). Synthesis and characterization of nanoparticles of ZnO by levitational gas condensation. Materials Science and Engineering: A 449–451: 813-816.

Vandebriel RJ & De Jong WH (2012). A review of mammalian toxicity of ZnO nanoparticles. Nanotechnology, Science and Applications 5: 61-71.

Verbruggen N & Hermans C (2008). Proline accumulation in plants: a review. Amino acids 35: 753-759.

Verma A, Uzun O, Hu Y, Hu Y, Han H-S, Watson N, Chen S, Irvine DJ & Stellacci F (2008). Surface-structure-regulated cell-membrane penetration by monolayer-protected nanoparticles. Nature materials 7: 588.

Verslues PE & Sharma S (2010). Proline metabolism and its implications for plant-environment interaction. The Arabidopsis Book/American Society of Plant Biologists 8.

Vinay C, Goudanavar P & Acharya A (2018). Development and characterization of pomegranate and orange fruit peel extract based silver nanoparticles. Journal of Manmohan Memorial Institute of Health Sciences 4: 72-85.

Wang C, Deng P, Chen L, Wang X, Ma H, Hu W, Yao N, Feng Y, Chai R & Yang G (2013). A wheat WRKY transcription factor TaWRKY10 confers tolerance to multiple abiotic stresses in transgenic tobacco. PloS one 8: e65120.

Wang L, Tian X, Wei W, Chen G & Wu Z (2016). Fingerprint analysis and quality consistency evaluation of flavonoid compounds for fermented Guava leaf by combining high-performance liquid chromatography time-of-flight electrospray ionization mass spectrometry and chemometric methods. Journal of separation science 39: 3906-3916.

Wang N-N, Xu S-W, Sun Y-L, Liu D, Zhou L, Li Y & Li X-B (2019). The cotton WRKY transcription factor (GhWRKY33) reduces transgenic Arabidopsis resistance to drought stress. Scientific Reports 9: 724.

Wang P, Menzies NW, Lombi E, McKenna BA, Johannessen B, Glover CJ, Kappen P & Kopittke PM (2013). Fate of ZnO nanoparticles in soils and cowpea (Vigna unguiculata). Environmental science & technology 47: 13822-13830.

Wang X, Li Q, Pei Z & Wang S (2018). Effects of zinc oxide nanoparticles on the growth, photosynthetic traits, and antioxidative enzymes in tomato plants. Biologia plantarum 62: 801-808.

Wang X, Yang X, Chen S, Li Q, Wang W, Hou C, Gao X, Wang L & Wang S (2016). Zinc oxide nanoparticles affect biomass accumulation and photosynthesis in Arabidopsis. Frontiers in plant science 6: 1243.

Wang Z, Xie X, Zhao J, Liu X, Feng W, White JC & Xing B (2012). Xylem-and phloem-based transport of CuO nanoparticles in maize (Zea mays L.). Environmental science & technology 46: 4434-4441.

Wardlaw IF, Blumenthal C, Larroque O & Wrigley CW (2002). Contrasting effects of chronic heat stress and heat shock on kernel weight and flour quality in wheat. Functional Plant Biology 29: 25-34.

Watson J-L, Fang T, Dimkpa CO, Britt DW, McLean JE, Jacobson A & Anderson AJ (2015). The phytotoxicity of ZnO nanoparticles on wheat varies with soil properties. Biometals 28: 101-112.

Wiesmann N, Tremel W & Brieger J (2020). Zinc oxide nanoparticles for therapeutic purposes in cancer medicine. Journal of Materials Chemistry B 8: 4973-4989.

Woisky RG & Salatino A (1998). Analysis of propolis: some parameters and procedures for chemical quality control. Journal of apicultural research 37: 99-105.

Xia T, Kovochich M, Brant J, Hotze M, Sempf J, Oberley T, Sioutas C, Yeh JI, Wiesner MR & Nel AE (2006). Comparison of the abilities of ambient and manufactured

nanoparticles to induce cellular toxicity according to an oxidative stress paradigm. Nano letters 6: 1794-1807.

Xiang L, Zhao H-M, Li Y-W, Huang X-P, Wu X-L, Zhai T, Yuan Y, Cai Q-Y & Mo C-H (2015). Effects of the size and morphology of zinc oxide nanoparticles on the germination of Chinese cabbage seeds. Environmental Science and Pollution Research 22: 10452-10462.

Xie Z, Zhang Z-L, Hanzlik S, Cook E & Shen QJ (2007). Salicylic acid inhibits gibberellin-induced alpha-amylase expression and seed germination via a pathway involving an abscisic-acid-inducible WRKY gene. Plant molecular biology 64: 293-303.

Yadav A, Kon K, Kratosova G, Duran N, Ingle AP & Rai M (2015). Fungi as an efficient mycosystem for the synthesis of metal nanoparticles: progress and key aspects of research. Biotechnology letters 37: 2099-2120.

Yamasaki H, Sakihama Y & Ikehara N (1997). Flavonoid-peroxidase reaction as a detoxification mechanism of plant cells against H2O2. Plant Physiology 115: 1405-1412.

Yan H, Jia H, Chen X, Hao L, An H & Guo X (2014). The cotton WRKY transcription factor GhWRKY17 functions in drought and salt stress in transgenic Nicotiana benthamiana through ABA signaling and the modulation of reactive oxygen species production. Plant and Cell Physiology 55: 2060-2076.

Yang H, Liu C, Yang D, Zhang H & Xi Z (2009). Comparative study of cytotoxicity, oxidative stress and genotoxicity induced by four typical nanomaterials: the role of particle size, shape and composition. Journal of applied Toxicology 29: 69-78.

Yang Z, Chen J, Dou R, Gao X, Mao C & Wang L (2015). Assessment of the Phytotoxicity of Metal Oxide Nanoparticles on Two Crop Plants, Maize (Zea mays L.) and Rice (Oryza sativa L.). International journal of environmental research and public health 12: 15100-15109.

Yoon S-J, Kwak JI, Lee W-M, Holden PA & An Y-J (2014). Zinc oxide nanoparticles delay soybean development: a standard soil microcosm study. Ecotoxicology and environmental safety 100: 131-137.

Yoshikawa M, Inoue K, Nakagawa T, Ishida H, Hasuike N & Harima H (2008). Characterization of ZnO nanoparticles by resonant Raman scattering and cathodoluminescence spectroscopies. Applied Physics Letters 92: 113115.

Zahoor M, Shafiq S, Ullah H, Sadiq A & Ullah F (2018). Isolation of quercetin and mandelic acid from Aesculus indica fruit and their biological activities. BMC biochemistry 19: 5.

Zak AK, Razali R, Majid WHA & Darroudi M (2011). Synthesis and characterization of a narrow size distribution of zinc oxide nanoparticles. Int J Nanomedicine 6: 1399-1403.

Zapata B, Balmaseda J, Fregoso-Israel E & Torres-Garcia E (2009). Thermo-kinetics study of orange peel in air. Journal of thermal analysis and calorimetry 98: 309-315.

Zegaoui Z, Planchais S, Cabassa C, Djebbar R, Belbachir OA & Carol P (2017). Variation in relative water content, proline accumulation and stress gene expression in two cowpea landraces under drought. Journal of plant physiology 218: 26-34.

Zhang D, Hua T, Xiao F, Chen C, Gersberg RM, Liu Y, Stuckey D, Ng WJ & Tan SK (2015). Phytotoxicity and bioaccumulation of ZnO nanoparticles in Schoenoplectus tabernaemontani. Chemosphere 120: 211-219.

Zhang H, Li Y & Zhu J-K (2018). Developing naturally stress-resistant crops for a sustainable agriculture. Nature Plants 4: 989-996.

Zhang H, Ji Z, Xia T, Meng H, Low-Kam C, Liu R, Pokhrel S, Lin S, Wang X & Liao Y-P (2012). Use of metal oxide nanoparticle band gap to develop a predictive paradigm for oxidative stress and acute pulmonary inflammation. ACS nano 6: 4349-4368.

Zhang J, Zhao B, Pan Z, Gu M & Punnoose A (2015). Synthesis of ZnO Nanoparticles with Controlled Shapes, Sizes, Aggregations, and Surface Complex Compounds for Tuning or Switching the Photoluminescence. Crystal Growth & Design 15: 3144-3149.

Zhang R, Zhang H, Tu C, Hu X, Li L, Luo Y & Christie P (2015). Phytotoxicity of ZnO nanoparticles and the released Zn (II) ion to corn (Zea mays L.) and cucumber (Cucumis sativus L.) during germination. Environmental Science and Pollution Research 22: 11109-11117.

Zhao L, Peralta-Videa JR, Ren M, Varela-Ramirez A, Li C, Hernandez-Viezcas JA, Aguilera RJ & Gardea-Torresdey JL (2012). Transport of Zn in a sandy loam soil treated with ZnO NPs and uptake by corn plants: electron microprobe and confocal microscopy studies. Chemical Engineering Journal 184: 1-8.

Zhao L, Hernandez-Viezcas JA, Peralta-Videa JR, Bandyopadhyay S, Peng B, Munoz B, Keller AA & Gardea-Torresdey JL (2013). ZnO nanoparticle fate in soil and zinc bioaccumulation in corn plants (Zea mays) influenced by alginate. Environmental Science: Processes & Impacts 15: 260-266.

Zhao L, Sun Y, Hernandez-Viezcas JA, Servin AD, Hong J, Niu G, Peralta-Videa JR, Duarte-Gardea M & Gardea-Torresdey JL (2013). Influence of CeO2 and ZnO nanoparticles on cucumber physiological markers and bioaccumulation of Ce and Zn: a life cycle study. Journal of agricultural and food chemistry 61: 11945-11951.

Zhao L, Sun Y, Hernandez-Viezcas JA, Hong J, Majumdar S, Niu G, Duarte-Gardea M, Peralta-Videa JR & Gardea-Torresdey JL (2015). Monitoring the environmental effects of CeO2 and ZnO nanoparticles through the life cycle of corn (Zea mays) plants and in situ μ-XRF mapping of nutrients in kernels. Environmental science & technology 49: 2921-2928.

Zhu J, Zou Z, Shen Y, Li J, Shi S, Han S & Zhan X (2019). Increased ZnO nanoparticle toxicity to wheat upon co-exposure to phenanthrene. Environmental Pollution.

Zhu X, Zhu L, Duan Z, Qi R, Li Y & Lang Y (2008). Comparative toxicity of several metal oxide nanoparticle aqueous suspensions to Zebrafish (Danio rerio) early developmental stage. Journal of Environmental Science and Health, Part A 43: 278-284.

Zia ur R (2006). Citrus peel extract – A natural source of antioxidant. Food Chemistry 99: 450-454.